Tumor-targeted delivery of childhood vaccine recall antigens by attenuated *Listeria* reduces pancreatic cancer

Benson Chellakkan Selvanesan[1$], Dinesh Chandra[1$], Wilber Quispe-Tintaya[1$], Arthee Jahangir[1], Ankur Patel[1], Kiran Meena[1], Rodrigo Alberto Alves Da Silva[1], Steven K Libutti[2], Ziqiang Yuan[2], Jenny Li[1], Sarah Siddiqui[1], Amanda Beck[3], Lydia Tesfa[4], Wade Koba[5], Jennifer Chuy[6], John C. McAuliffe[7], Rojin Jafari[8], David Entenberg[8,9,10], Yarong Wang[8,9,10], John Condeelis[8,9,10,11], and Claudia Gravekamp[1*].

[$]These authors contributed equally to this manuscript.

Running title: Cancer treatment through childhood vaccine recall antigens

[1]*Albert Einstein College of Medicine, Department of Microbiology and Immunology, 1300 Morris Park Avenue, Bronx, NY 10461, USA*

[2]*Rutgers University, Cancer Institute of New Jersey, 195 Little Albany St, New Brunswick, New Jersey 08901, USA*

[3]*Albert Einstein College of Medicine, Michael F. Price Center, 1301 Morris Park Avenue, Room 158, Bronx, NY 10461*

[4]*Albert Einstein College of Medicine, Jack and Pearl Resnick Campus, 1300 Morris Park Avenue, Chanin Building, Room 309, Bronx, NY 10461*

[5]*Albert Einstein College of Medicine, Department of Radiology, MRRC, 1300 Morris Park Avenue, Bronx, NY 10461, USA*

[6]*Montefiore/Einstein Center for Cancer Care, Department of Medical Oncology, 1695 Eastchester Road, 2nd Floor, Bronx, NY 10461, USA*

[7]*Montefiore Medical Center, Department of Surgery, 1521 Jarrett Place, 2nd Floor, Bronx, NY 10461, USA*

[8]*Albert Einstein College of Medicine, Michael F. Price Center, Department of Anatomy and Structural Biology, 1301 Morris Park Avenue.*

[9]*Albert Einstein College of Medicine, Michael F. Price Center, Gruss-Lipper Biophotonics Center, 1301 Morris Park Avenue.*

[10]*Albert Einstein College of Medicine, Michael F. Price Center, Integrated Imaging Program, 1301 Morris Park Avenue.*

[11]*Albert Einstein College of Medicine, Michael F. Price Center, Department of Surgery, 1301 Morris Park Avenue.*

Keywords: *Listeria monocytogenes*, childhood recall antigens, pancreatic cancer, breast cancer, memory T cells

* To whom correspondence should be addressed:

Claudia Gravekamp

Albert Einstein College of Medicine

Department of Microbiology and Immunology

1300 Morris Park Avenue

Forchheimer Bldg., Room 407A

Bronx, NY 10461

Email: claudia.gravekamp@einstein.yu.edu

Phone: 718-430-4048(office)/4067 (lab)/Fax: 718-430-8711

ABSTRACT

Pancreatic ductal adenocarcinoma is poorly immunogenic, and immune suppression prevents T cell activation. We developed a microbial-based immunotherapeutic concept for selective delivery of immunogenic tetanus toxoid ($TT_{856-1313}$) antigen into tumor cells by attenuated *Listeria monocytogenes*, and reactivation of TT-specific memory T cells to kill infected tumor cells. Treatment of KPC mice with *Listeria*-TT resulted in TT accumulation inside tumor cells, and attraction of TT-specific CD4 and CD8 T cells. Lymph node-like structures were frequently observed in contact with pancreatic tumors of treated mice, and exhibited CD4 and CD8 T cells producing IFNγ. Gemcitabine combined with *Listeria*-TT significantly improved migration of CD4 T cells into tumors, and enhanced perforin and granzyme B production. The combination treatment also significantly reduced pancreatic tumors and metastases in Panc-02 and KPC mouse models, with minimal side effects, turning “cold” tumors into “hot” tumors. This study provides insight into mechanisms for improving immunotherapy for pancreatic cancer.

INTRODUCTION

Pancreatic ductal adenocarcinoma (PDAC) is extremely difficult to cure. Modern systemic therapies, such as gemcitabine, provide some survival benefits[1-4], while gemcitabine and abraxane or FOLFIRINOX further modestly improve survival[5,6]. This underscores the need for additional and innovative approaches. Cancer immunotherapy with checkpoint inhibitors has shown promising results, however, less so for PDAC[7]. PDAC is poorly immunogenic because of the low mutational load and the few effective neoantigens present[8,9], and because immune suppression, particularly by myeloid-derived suppressor cells (MDSC) and tumor-associated macrophages (TAM), prevents T cell activation in the tumor microenvironment (TME)[10-12]. Moreover, evidence suggests that naïve T cells are more prone to undergo apoptosis or are less efficiently activated than memory T cells in the TME of cancer patients and tumor-bearing mice[13,14].

To address these problems we have developed a novel treatment modality using an attenuated bacterium *Listeria monocytogenes*[15] (*Listeria*) to deliver a highly immunogenic recall antigen such as tetanus toxoid (TT)(as an alternative to neoantigens) selectively into tumor cells, and to reactivate pre-existing memory T cells against TT (generated during childhood vaccinations) **(Fig 1a)**. These TT-specific memory cells are in turn attracted to the *Listeria*-TT in the TME, where they destroy the infected now highly immunogenic tumor cells**.** These memory T cells circulate in the blood for life, and can be reactivated at any age. Such an approach overcomes the need for participation of naïve T cells during cancer treatment. To further improve T cell responses against TT, *Listeria*-TT was combined with low doses of gemcitabine (GEM) to reduce immune suppressive MDSC and TAM populations.

In previous studies we have shown that, most likely through C3bi and C1q receptors[16-18], *Listeria* attracts and infects MDSC[10]. These MDSC are present in large numbers in patients and mice with cancer[11,19]. However, the primary tumor also

selectively attracts MDSC through the production of cytokines and factors[11,20], where MDSC deliver *Listeria* to the TME as a Trojan horse[10,19]. Once at the tumor site, *Listeria* spreads from MDSC into tumor cells through a cell-to-cell mechanism unique to *Listeria*[21]. *Listeria* can also infect tumor cells directly[22]. *Listeria* would be rapidly killed in healthy tissues, but is protected from immune clearance in the TME through strong immune suppression. Because of this combination of selective attraction of MDSC by bacteria and cancer with the strong immune suppression occurring in the TME but not in normal tissues, *Listeria* can selectively enter, multiply, and survive in the TME but not in normal tissues[10,19,23,24]. Based on these results we now use *Listeria* as a platform for the selective delivery of anticancer agents to the TME[19,23,25].

In the current study, we tested the combination of *Listeria*-TT+GEM **(Fig 1b)** in two mouse models of pancreatic cancer, a syngeneic Panc-02 model[26] and a transgenic KPC model[27,28]. *Listeria*-TT was administered intraperitoneally, and the *in vivo* uptake by tumor cells was verified by intravital imaging. We demonstrate that the combination of *Listeria*-TT+GEM robustly reduced pancreatic cancer at early and advanced stages in both Panc-02 and KPC mouse models. Our results unveil new mechanisms of *Listeria* to improve immunotherapy for PDAC.

RESULTS

Development and characterization of *Listeria*-TT

The Listeria construct used to develop *Listeria*-TT includes pGG34[29], a truncated non-cytolytic Listeriolysin O (LLO) fused to a non-toxic $TT_{856\text{-}1313}$ fragment, and a myc sequence for detection as outlined in **Fig 2a.** Secretion of LLO-$TT_{856\text{-}1313}$ protein into the culture medium by the bacteria was detected by western blotting **(Fig 2b).** Infection of Panc-02 tumor cells with *Listeria*-$TT_{856\text{-}1313}$ resulted in the expression of TT protein in the tumor cells **(Fig 2c).**

Listeria-TT infection of tumor cells *in vitro* and *in vivo*

We previously showed that *Listeria* can be used as a delivery platform for anticancer agents[19,23], however TT fusion to LLO could potentially alter LLO function (LLO is required to escape the vacuole after phagocytosis[30]). To test *Listeria*-TT delivery function, we determined the infection rate of pancreatic tumor cells cultured with *Listeria*-TT in comparison to *Listeria* alone. Panc-02 tumor cells were abundantly infected in both cases **(Fig 2d).** We also determined that *Listeria*-TT effectively killed the Panc-02 cells **(Fig 2e)**.

TT is highly immunogenic, and might lead to faster elimination of *Listeria*-TT *in vivo* than *Listeria* alone, consequently preventing accumulation in the TME. To assess this, a single high dose of *Listeria*-TT was injected intraperitoneally (ip) into Panc-02 mice, and numbers of *Listeria*-TT were quantified in all tissues (tumors, metastases, and normal tissues) at different time points. As shown in **Fig 2f,** *Listeria*-TT accumulated robustly in tumors and metastases, but could hardly be detected in normal tissues. Interestingly, the same dose of *Listeria* injected intravenously was nearly undetectable in tumors and metastases **(SI Fig 1a and b).** This was true not only for metastases in the liver and pancreas, but also for metastases in the lungs **(SI Fig 1c).**

To confirm that *Listeria*-TT was taken up *in vivo* by tumor cells within the TME of live mice, we injected Alexa-680-labeled *Listeria*-TT into the peritoneal cavity of transgenic mice whose macrophages expressed cyan fluorescent protein (CFP)[31], and which had orthotopic, Dendra-2 labeled pancreatic tumors (Panc-02-Dendra). High-resolution intravital multiphoton microscopy (IVMI) of these tumors showed individual *Listeria*-TT bacteria inside tumor cells and macrophages **(Fig 2g).** Finally, presence of TT protein was demonstrated immunohistochemically inside tumor cells of the pancreatic ducts, and in the TME of KPC mice that received *Listeria*-TT or *Listeria*-TT+GEM **(Fig 2h).** Notably, detection of TT was much stronger in the tumors of *Listeria*-TT+GEM-treated

mice than of *Listeria*-TT-treated mice. While GEM kills Listeria *in vitro*, more *Listeria* bacteria were detected in the tumors of *Listeria*+GEM-treated mice compared to *Listeria*-TT alone **(Fig 2ij).** It might be possible that GEM drives the bacteria to a safer place, i.e. the TME and inside tumor cells were *Listeria* could survive and multiply, to escape the GEM and the immune system.

Listeria-TT reactivates memory T cells to TT in tumor-bearing mice

Our concept is to generate pre-existing memory T cells specific for TT prior to tumor development, to avoid the necessity of activating naïve T cells in a TME. Therefore, we generated TT-specific memory CD4 and CD8 T cells in mice through two injections of Tetanus vaccine prior to tumor development **(Fig 3a).** One week after the second immunization, Panc-02 tumor cells were injected into the mammary fat pad. When tumors were 10 mm in diameter, the *Listeria* TT+GEM treatment was initiated as in **Fig 1b.** After the complete treatment cycle, spleen cells were isolated from the Panc-02 tumor-bearing mice, restimulated with TT protein *in vitro*, and analyzed for memory T cell responses producing IFNγ **(Fig 3b)**. We found that CD4 and CD8 T cells of mice that received *Listeria* -TT or *Listeria* -TT+GEM were strongly activated by TT, but not of mice that received saline or GEM alone (Mann-Whitney $p<0.05$ and $p<0.001$), indicating the high specificity of CD4 and CD8 memory T cells responsive to the TT protein. Similar results were obtained for memory cells isolated from tumors in KPC mice **(Fig 3c)**

To evaluate whether *Listeria*-TT+GEM could overcome immune suppression in the tumor-bearing Panc-02 mice, we also analyzed "*in vivo*" T cell responses, i.e., without *in vitro* restimulation with TT. At the end of the treatment cycle, CD4 and CD8 T cell responses (CD69, Granzyme B, Perforin, and IFNγ) were strongly improved in spleen cell populations (pooled) of mice treated with *Listeria*-TT+GEM compared to all control groups **(Table 1a, SI Fig 2ab).** Both CD4 and CD8 T cells produced high levels of

Granzyme B, Perforin, and/or IFNγ. These responses were even stronger for CD4 T cells than for CD8 T cells. Moreover, *Listeria*-TT or GEM alone also increased the production of Perforin in CD4 and CD8 T cells compared to the saline treatments. Similar results were found in KPC mice, i.e., *Listeria*-TT+GEM improved T cell responses compared to all other groups **(Table 1b).** In sum, therefore, the analysis showed that T cells were activated by TT, *Listeria*, and GEM in the tumor-bearing mice.

Listeria-TT+GEM turns "cold" tumors into "hot" tumors

To confirm that *Listeria*-TT+GEM was able to overcome immune suppression in the TME, we performed RNAseq analyses of pancreatic tumors from KPC mice that had been treated with *Listeria*-TT+GEM, or untreated. As shown in **Fig 3d**, CD4 and CD8 T cells were strongly represented in the tumors of *Listeria*-TT+GEM-treated KPC mice but not in the untreated group. Moreover, multiple granzymes as well as Perforin were highly expressed in the *Listeria*-TT+GEM-treated mice, as were factors involved in tumor cell apoptotic pathways, including multiple caspases, TNF and Fas.

We also analyzed whether T cells in orthotopic Panc-02 tumors of mice treated with *Listeria*-TT, or *Listeria*-TT+GEM were specific for TT by ELISPOT **(Fig 2k)** and flow cytometry **(Fig 2l).** The numbers of TT-specific T cells producing IFNγ were 10-fold higher in the tumors of *Listeria*-TT-treated mice compared to the saline or GEM control groups, and 3 times higher than *Listeria*-TT+GEM **(Fig 2l).**

Based on the fact that *Listeria* causes TT accumulation in the TME **(Fig 2h)** and TT-specific memory T cells have been generated **(Fig 3a-c),** we expect these memory T cells to be attracted to the TME. To visualize the TME and T cells in more detail, the KPC tumors were analyzed by immunohistochemistry (IHC). As shown in **Fig 4a and e,** CD4 T cells were present in the tumors of KPC mice treated with LM-TT, but hardly at all in the tumors of saline- or GEM-treated mice. More detail about the CD4 T cells in the

KPC tumors of all four treatment groups is shown in **SI Fig 3a-d.** Most remarkable was that addition of GEM to the *Listeria*-TT treatment significantly enhanced the migration of CD4 T cells to the tumors of KPC mice compared to all other groups, even compared to the *Listeria*-TT group. These CD4 T cells were found in the tumor areas that expressed TT protein and CD31-positive vessels **(SI Fig 4a-c).** Of note is, that CD8 T cells were sparsely present in the tumor areas **(SI Fig 3e-h).**

Notably, lymph node-like structures (LNS) were frequently observed in close contact with the KPC tumors of mice treated with *Listeria*-TT or *Listeria*-TT+GEM, and less frequently in KPC mice treated with saline or GEM **(Fig 4a)**. Higher magnification images of an LNS are shown in **SI Fig 4d.** To determine whether T cells present in the LNS were functional and exhibited memory phenotype, we isolated the CD45+ lymphocytes (81.2%) from the LNS of *Listeria*-TT-treated mice, and then gated the CD4 (40.4%) or CD8 (52.0%) T cells by flow cytometry, followed by gating of the IFNγ+ CD4 (3.28%) or CD8 (2.91%) T cells **(Fig 4b).** Within these IFNγ+ CD4 and IFNγ+ CD8 T cell populations, 54% and 55%, respectively, exhibited a memory phenotype (CD44+CD62L-).

Of clinical relevance is that Perforin and Granzyme B, both involved in T cell-mediated tumor cell cytolysis, were detected in both pancreatic tumors and LNS of *Listeria*-TT+GEM-treated mice, and less abundantly in *Listeria*-TT-treated mice, but not at all in tumors or LNS of saline or GEM-treated mice **(Fig 4c,d and e, SI Fig 4e)**. Of note is, that Perforin was less abundantly produced than Granzyme B in general. Also, L-selectin as well as Cxc3 and chemokines Cxcl9 and Cxcl10 were highly upregulated in KPC tumors of mice treated with *Listeria*-TT+GEM compared to untreated mice **(SI Fig 5a)**. These genes are known to be involved in T cell trafficking[32,33]. Also, CD40 and CD40L was highly upregulated in KPC tumors by *Listeria*-TT+GEM **(SI-Fig 5a).** It has

been reported that CD40 engagement activates T cells and correlates with antitumor activity[34]. Together, the results indicated that *Listeria*-TT+GEM treatment altered "cold" tumors to "hot" tumors, promoting a strong influx of CD4 T cells into the KPC tumors, as well as production of Perforin and Granzyme B. These results are supported by the RNAseq data as discussed above, showing that immune responses in the KPC tumors were strongly activated by *Listeria*-TT+GEM **(Fig 3d).**

Listeria-TT and GEM alter the TME

In Panc-02 tumor bearing mice, GEM reduced the blood MDSC population by 80-90%, and in primary tumors by 50%, compared to the saline group **(Fig 3e),** and the TAM population by 67% in primary tumors compared to the saline group **(Fig 3e).** Moreover, for the residual MDSC and TAM cells, the production in pancreatic metastases of factors involved in immune suppression, including IL-10, IL-6 and the transcription factor MARCO, was reduced in mice treated with *Listeria*-TT+GEM **(Table 1cd, SI Fig 6ab)**, while there was increased production by these cells of TNFα, involved in tumor cell killing, and expression of CD80, involved in T cell activation. These findings indicated that *Listeria* TT+GEM altered the TME.

Listeria-TT+GEM reduces early and advanced pancreatic cancer in Panc-02 and KPC mice

Finally, we tested *Listeria*-TT+GEM therapeutically in Panc-02 mice with early and advanced pancreatic cancer. We found nearly complete elimination of early stage pancreatic cancer **(SI Fig 5b),** and a significant reduction in primary (85%; p=0.0001) and metastatic tumor burdens (89%; p=0.0001) of advanced pancreatic cancer for mice treated as outlined in **Fig 1b**, compared to the saline group **(Fig 5a and d).**

We also tested *Listeria*-TT+GEM in mice with advanced orthotopically generated Panc-02 tumors and metastases. Fourteen days after injection of Panc-02 tumor cells into the pancreas, when tumors and metastases were developed, treatment with *Listeria*-TT+GEM and control groups were started as in **Fig 1b.** Two days after the last treatment, mice were euthanized and analyzed for tumor weight and number of metastases. A significant reduction was observed in the weight of the primary tumors (68%; p=0.0238) and in the number of liver metastases (95%; p=0.0159) compared to the saline group **(Fig 5b and e).**

Most importantly, we evaluated *Listeria*-TT+GEM treatment of 3.5-5 month old KPC mice with advanced pancreatic cancer by PET scan analysis. SUVmax, a measure of the metabolic activity of tumors and metastases, provided an indicator of tumor growth. Small changes in the SUVmax of tumors and metastases in the saline and GEM control groups were not statistically significant, nor was the 50% decrease in the LM-TT group **(Fig 5c).** However, significant reductions in SUVmax for PDAC tumors from 1.9 to 0.4, and for liver metastases from 2.1 to 0.3, were observed in the mice receiving *Listeria* TT+GEM treatment **(Fig 5c and f)**. The PDAC tumors were reduced by 80% (p=0.0020) and the liver metastases by 87% (p=0.03).

Safety of *Listeria*-TT

A dose-limiting toxicity study (DLT) for *Listeria*-TT showed that the LD_{50} of *Listeria*-TT was 2×10^8 CFU **(SI Fig 5c)**. Our treatment studies used a dosage of 10^7 CFU of *Listeria*-TT, well below the LD_{50}.

We also analyzed potential toxicity by pathological examination, 2 days after treatment of C57Bl6 mice with *Listeria*-TT+GEM**.** Though a mild increase in leukocytes was observed in the spleen, liver, and lungs, no significant pathological effects of *Listeria*-TT+GEM were observed. **(SI Table 1a).** In addition, we compared liver functions

of the treated C57Bl/6 mice. A small increase in the aminotransferase (AST) level was observed in plasma from *Listeria*-TT+GEM-treated mice compared to the saline group, while alanine aminotransferase (ALT) levels were similar between the two groups **(SI Table 1b).**

DISCUSSION

The success of cancer immunotherapies such as checkpoint inhibitors and CAR T cells in PDAC has been underwhelming, due to low immunogenicity of the tumor, strong immune suppression at multiple levels, and inefficient activation of naïve T cells in the TME[8,9,11-14]. Moreover, low neoantigen expression levels, due to immunoediting or other causes, result in poor attraction of neoantigen-specific T cells[35,36]. In this study, we demonstrated the effectiveness of a tumor-targeting attenuated *Listeria*, in combination with GEM, in treating animal models of early and advanced pancreatic cancer. Our treatment strategy offers the advantages of selective delivery of immunogenic TT protein, at high concentrations, to the TME and into tumor cells, recruiting pre-existing TT-specific memory T cells (generated during childhood vaccinations), and altering the function of macrophages and MDSC in the TME in favor of immune stimulation.

We found that GEM significantly improved the migration of CD4 T cells to the KPC tumor, when added to the *Listeria*-TT treatment, which may have been the result of more *Listeria*-TT and thus more TT protein in the tumors of mice treated with *Listeria*-TT+GEM compared to *Listeria*-TT alone. Also, GEM reduced the MDSC population which down regulates L-selectin on T cells, a gene involved in T cell trafficking. L-selectin was strongly upregulated in tumors of KPC mice treated with *Listeria*-TT+GEM.

A notable finding was the appearance of well-developed LNS in close contact with the tumors in KPC mice treated with *Listeria*-TT or *Listeria*-TT+GEM. While it is unclear

whether or not these may have been the source of T cells trafficking to the tumors, Perforin and Granzyme B were detected in both LNS and tumors of *Listeria*-TT+GEM- and *Listeria*-TT-treated mice. The Cxcr3 receptor and chemokines Cxcl9 and Cxcl10 (interacts with Cxcr3) were also highly upregulated by *Listeria*-TT+GEM in KPC tumors, possibly participating in T cell trafficking to the KPC tumors. Detailed studies will be required to identify the pathways of T cell migration into these tumors.

Tertiary lymph node structures in proximity to pancreatic tumors have been correlated with increased patient survival in PDAC[37]. Conversely, tumor draining lymph nodes were found to correlate with immune suppression, a more metastatic character, and poor outcome in PDAC patients[38]. Our study showed that *Listeria*-TT+GEM overcame immune suppression in the TME, as demonstrated by functional T cells in the LNS and tumor areas producing Perforin, Granzyme, and IFNγ, and this correlated with a strong decrease in the number of metastases and tumor growth in mice.

Listeria-based immunotherapies for pancreatic cancer have also been reported by others. KPC mice in the early stage of PDAC that were immunized with *Listeria* ΔActA ΔInlB (LADD) engineered to express the Kras12GD mutation, combined with anti-CD25 Abs and cyclophosphamide, demonstrated delayed PanIN progression and moderately but significantly improved survival[39]. In another interesting study using the flank model, 4T1 and CT26 mice were immunized with LADD expressing AH1, also expressed by the tumors. This stimulated migration of tumor-specific CD8 T cells into tumors, reducing Tregs and converting M2 macrophages to M1[40]. In addition, mouse models of cervical, breast, and skin cancer have been successfully treated with *Listeria* expressing E7, Her2/neu, Flk-1, CD105, Mage-b, ISG15, and HMW-MAA[41].

Listeria has also been tested in clinical trials in patients with various cancers, including pancreatic cancer, showing safety and tumor-specific T cell responses and improved survival (for a review see Forbes et al)[42]. Of note is that the concept of *Listeria*

in these clinical trials is different from our concept. *Listeria* used in the clinical trials is based on a “classical concept”, i.e. the delivery of tumor-specific antigens into dendritic cells to stimulate naïve and memory T cells to these antigens which are naturally expressed by the tumors, while our concept is based on colonizing and changing the TME by *Listeria*, and delivery of highly immunogenic antigens into tumor cells by Listeria. This “classical concept” in clinical trials is partly the result of altering the *Listeria* (deletion of *ActA* and *InlB*) to improve safety and consequently cannot spread and/or multiply *in vivo*, and partly the result of administering *Listeria* intravenously (iv). We administer the *Listeria* in our mouse models intraperitoneally (ip). As demonstrated in this study, *Listeria* administered iv hardly reach tumors and metastases (pancreatic and breast cancer), but when administered ip *Listeria* colonizes the TME abundantly, delivers antigens in high concentration to the TME and inside tumor cells, and infects/alters MDSC and TAM. In multiple biodistribution studies in mice with pancreatic and breast cancer we found that *Listeria* was rapidly eliminated most likely by the immune system in blood[10,19,23], because the blood lacks immune suppression, while the TME is heavily immune suppressed.

We demonstrated that GEM administered ip to mice, significantly reduced the MDSC population in blood. However, in PDAC patients no direct evidence could be found that iv GEM reduced the MDSC population in blood[43,44]. Ip-administered GEM will have direct contact with the pancreatic tumors and their MDSC but iv-administered GEM will be first metabolized in the liver before it reaches the tumor. This might explain the discrepancies between the human and mouse studies. However, this needs to be further analyzed.

Elderly cancer patients react less efficiently to vaccines than young adults[45,46], which is also true for cancer immunotherapy[47,48], mainly due to lack of naïve T cells later in life[49]. We believe that our approach of reactivating memory T cells generated during childhood overcomes the need for naïve T cells, potentially making this therapeutic

strategy more effective for older patients. This may lead to new treatment modalities against pancreatic cancer where other types of therapies fail.

ACKNOWLEDGEMENTS

This work was supported by the Pancreatic Cancer Action Network (PCAN) 422247, a private donation of Janet and Marty Spatz, NCI Administrative Supplement 3P30CA013330-44S3, and NCI cancer center support P30CA013330 (Flow Cytometry Core, Pathology Core, MicroPET Core, Genetics Core). We greatly thank Ms. Hong Zhang, Department of Pathology, and Dr. Vera DeMarais, Director of Light Microscopy and Image Analysis, Department of Structural and Cell Biology, Einstein for providing outstanding training and support regarding the IHC and image analysis.

AUTHOR CONTRIBUTIONS

Conception, study design, and study supervision; development of methodology; administrative, technical, or material support (i.e., reporting or organizing data, constructing data bases); writing, review, and/or revision of the manuscript: B.C. Selvanesan, D. Chandra, W. Quispe-Tintaya, Z. Yuan, S.K. Libutti, C. Gravekamp

Acquisition of data (provided animals, developed *Listeria*-TT construct, acquired immunological and efficacy data, provided facilities, etc.): B.C. Selvanesan, D. Chandra, W. Quispe-Tintaya, A. Jahangir, A. Patel, K. Meena, R. Alves Da Silva, J. Li, S. Siddiqui, A. Beck, L. Tesfa, W. Koba, Z. Yuan, S.K. Libutti, C. Gravekamp

Analysis and interpretation of data (statistical analysis, biostatistics, computational analysis): B.C. Selvanesan, D. Chandra, W. Quispe-Tintaya, A. Jahangir, A. Patel, K. Meena, R. Alves Da Silva, A. Beck, L. Tesfa, W. Koba, J. Chuy, Z. Yuan, S.K. Libutti, C. Gravekamp

ETHICS APPROVAL AND CONSENT TO PARTICIPATE

All in vivo experiments were approved by the NCI/NIH Animal Care and Use Committee.

DECLARATION OF INTEREST

Dr. Gravekamp has ownership interest in a patent application filed for the *Listeria*-recall antigen concept (96700/2230). No other competing interests were disclosed by the authors.

LEGENDS

Figure 1: (a) Mechanistic view of the *Listeria*-recall antigen concept.

Tetanus vaccine will be used to generate memory T cells to recall antigen TT in mice prior to tumor development. Antigen-presenting cells (DC) take up and present TT protein to naïve T cells. Upon repeated exposures to TT, naïve T cells differentiate into memory T cells, circulating in the blood for life. These memory cells are to be reactivated after appearance of the primary tumor and metastases, as follows. To deliver TT into tumor cells, mice receive a high dose of *Listeria*-TT bacteria, whose replication will lead to more TT protein in the tumor cells. subsequently, frequent low dose immunizations with *Listeria*-TT reactivate specific memory T cells. Finally, TT-specific memory T cells migrate to the tumor and kill tumor cells presenting TT epitopes. Since attenuated *Listeria* bacteria colonize the TME, they will also infect MDSC and macrophages (not depicted).

(b) Protocol for treatment of Panc-02 and KPC mice with *Listeria*-TT+GEM.

In the Panc-02 model, mice were immunized twice with Tetanus vaccine to generate memory T cells. Subsequently, Panc-02 tumor cells were injected and tumors allowed to develop to the early stage of pancreatic cancer (3 mm) or advanced stage (10 mm).

After an initial high ip dose of *Listeria*-TT, it accumulated and multiplied in the TME for 3 days. Periodic doses of GEM were then given for 14 days in order to eliminate MDSC and TAM. At this point, MDSC are no longer required to bring *Listeria*-TT to the TME. Instead, reducing MDSC and TAM populations serves to improve T cell responses. Concomitantly, daily low doses of *Listeria*-TT reactivate TT-specific memory T cells, improved by GEM. Mice were euthanized two days after the last treatment. Panc-02 mice were analyzed for tumor weight and the number of metastases.

In the KPC model, the presence of tumors and/or metastases were first verified by PET scan before mice received the same treatments described above. The metabolic activities (SUVmax) of tumors and metastases in KPC mice were measured by PET scan. Comparisons of SUVmax pre- and post-treatment provide a measure of the growth of tumors and metastases. LM-TT = *Listeria*-TT.

Figure 2: Development and characterization of the *Listeria*-TT vaccine.

(a) *Listeria*-TT construct. $TT_{856\text{-}1313}$, a non-toxic fragment of the C-terminus of TT cDNA (aa position 856-1313, 52 kDa) was cloned as a fusion protein with a truncated non-cytolytic Listeriolysin O (LLO, 48 kDa) into the *Listeria* plasmid pGG34, under the control of the LLO promoter (P). A myc tag was included for detection of the TT protein. **(b)** Western blot detection of TT protein secretion using anti-myc. **Lane 1**: negative control (growth medium); **Lane 2**: supernatant of *Listeria*-TT culture; **Lane 3**: pellet of *Listeria*-TT culture. **(c)** Detection of TT protein in tumor cells. **Lane 1**: Panc-02 tumor cells; **Lane 2**: Panc-02 tumor cells infected with *Listeria* alone; **Lane 3**: Panc-02 tumor cells infected with *Listeria*-TT. **(d)** Panc-02 tumor cells infected with *Listeria*-TT. Average of 2 independent experiments, 3 wells per group. **(e)** Panc-02 tumor cell killing by *Listeria*-TT. Averages of 3 independent experiments; 3 wells per group. **(f)** *Listeria*-TT accumulation in tumors and metastases, but not in normal tissues. A single high dose of *Listeria*-TT,

10^7 CFU/200 μl, was injected ip into Panc-02 mice, and *Listeria*-TT CFU were measured in tumor, metastatic, and normal tissues at different time points. Averages of a single experiment; n=3 mice per timepoint, n=3 tissues per organ/tumor/metastases. In **(d-f)**, error bars represent SEM. **(g)** *Listeria*-TT infecting tumor cells and macrophages (MΦ) in Panc-02-dendra-2 tumors of live mice, by intravital imaging. Tumor cells are green, macrophages blue, and *Listeria*-TT red. **(h)** Immunohistochemical detection of TT protein using polyclonal anti-TT antibody in tumors of KPC mice that received *Listeria*-TT+GEM or *Listeria*-TT treatment. **(i)** Effect of GEM on *Listeria in vitro*. Average of one experiment; n=3 wells per concentration, 3 fields per well. **(j)** Effect of GEM on *Listeria in vivo*. Average of 2 independent experiments; n=3 mice per group. **(k)** ELISPOT analysis of CD45+ IFNγ-producing immune cells isolated from orthotopic Panc-02 tumors in mice treated with *Listeria*-TT+GEM. **(l)** Flow cytometry of IFNγ-producing CD4+ T cells in the CD45+ fraction, isolated from orthotopic Panc-02 tumors. In each group tumors of 5 mice were pooled. Mann-Whitney *p <0.05, **p<0.01, ***p<0.001, ****p<0.0001. LM-TT = *Listeria*-TT.

Figure 3: Generation and recall of memory CD4 and CD8 T cell responses to TT.

(a) Generation of CD4 and CD8 memory T cells to TT by immunization of Panc-02 or KPC mice with Tetanus vaccine, prior to tumor development. **(b)** Reactivation of TT-specific memory CD4 and CD8 T cells in Panc-02 mice post tumor development through the *Listeria*-TT+GEM treatment cycle described in Fig 1b. **(c)** Reactivation of TT-specific memory T cells in KPC mice post tumor development by the *Listeria*-TT+GEM treatment cycle. In **(a-c)**, T cells producing IFNγ were analyzed in a restimulation assay with TT protein by ELISPOT. Representative results of 2 experiments are shown; n=3 mice per group (pooled), 6 wells per group. Statistical significance by Mann-Whitney test: *p<0.05,

***p<0.001 and *****p<0.0001. **(d)** RNAseq analysis of immune responses and tumor cell death pathways in pancreatic tumors of KPC mice in response to *Listeria*-TT+GEM treatment. The heatmap was generated by unbiased hieratical clustering at the following statistical parameters. Statistical parameters for the paired-wise comparison: p<0.05. The signature contains 25 important genes. m1=mouse 1, and m2=mouse 2. **(e)** Flow cytometric analysis of changes in MDSC (CD11b+Gr1+) in blood and tumors, and TAM (CD11b+F4/80+) in tumors of Panc-02 mice in response to the *Listeria*-TT+GEM treatment cycle. Average of a single experiment of MDSC in blood with n=3 mice per group, and the average of 2 independent experiments of MDSC and TAM in tumors with n=3 mice per group. LM-TT = *Listeria*-TT.

Figure 4: Tetanus protein attracts CD4 memory T cells to the TME.

KPC mice were treated with saline, GEM, *Listeria*-TT, or *Listeria*-TT+GEM as outlined in Fig 1b. Three days after the last treatment, the pancreas with tumors including lymph node like structures (LNS) were excised and processed for CD4 and CD8 staining by IHC. **(a)** CD4 T cells in the KPC tumors and the presence of LNS were analyzed in all treatment groups. **(b)** Isolation and flow cytometry analysis of CD4 and CD8 T cells in a LNS of a mouse that received *Listeria*-TT. The CD45+ cells were gated, followed by CD3CD4 or CD3CD8 gating, followed by gating of CD3CD4 and CD3CD8 T cells producing intracellular IFNγ, followed by staining to identify T cells with memory phenotype (CD44+CD62L-). **(c)** Production of Perforin and Granzyme B in KPC tumors, by IHC. (d) **(d)** Production of Perforin and Granzyme B in KPC LNS, by IHC. **(e)** Quantification of CD4 T cells in KPC tumors and the production of perforin and Granzyme B in the KPC tumors and LNS. CD4 T cell numbers were counted in the tumor areas of all treatment groups. Also, the number of perforin and granzyme B-producing cells were counted in the tumor areas and LNS of all treatment groups. In

each group, four-ten fields were measured, and the number of cells per 1000 μm^2 was calculated. Results of three mice per group were averaged. Mann-Whitney *p<0.05, ** p<0.01, ***p<0.001. LM-TT = *Listeria*-TT. Scale bars=100μm.

Figure 5: *Listeria*-TT+GEM robustly reduces advanced pancreatic cancer in Panc-02 and KPC mice.

Panc-02 and KPC mice received the combined treatment as outlined in Fig 1b. **(a)** Effect of treatment on advanced pancreatic cancer in the peritoneal cavity Panc-02 mouse model. Averages of two experiments, with 4-5 mice per group, are shown. **(b)** Effect of treatment on advanced pancreatic cancer in the orthotopic Panc-02 mouse model. Averages are shown for a single experiment with 5 mice in each group. **(c)** Effect of treatment on advanced pancreatic cancer in KPC mice. Averages are shown for a single experiment with 5 mice in the *Listeria*-TT+GEM group, and 2 mice in each other treatment group. *Listeria*-TT+GEM was started at age 3–5.5 months, after tumors and metastases were verified through PET scan. SUVmax of tumors and metastases were measured prior to and post-treatment. (a-c) were analyzed by the Mann-Whitney test. *p <0.05, **p<0.01, ***p<0.001, ****p<0.0001. **(d-f)** Examples for each treatment group of pancreatic tumors in Panc-02 mice (orthotopic model) and for KPC mice. LM-TT = *Listeria*-TT.

REFERENCES

1 Kulke, M. H. *et al.* Capecitabine plus erlotinib in gemcitabine-refractory advanced pancreatic cancer. *J Clin Oncol* **25**, 4787-4792, doi:10.1200/JCO.2007.11.8521 (2007).

2 Maitra, A. & Hruban, R. H. Pancreatic cancer. *Annual review of pathology* **3**, 157-188, doi:10.1146/annurev.pathmechdis.3.121806.154305 (2008).

3 Moore, M. J. *et al.* Erlotinib plus gemcitabine compared with gemcitabine alone in patients with advanced pancreatic cancer: a phase III trial of the National Cancer Institute of Canada Clinical Trials Group. *J Clin Oncol* **25**, 1960-1966, doi:10.1200/JCO.2006.07.9525 (2007).

4 Abbruzzese, J. L. *et al.* A phase I clinical, plasma, and cellular pharmacology study of gemcitabine. *J Clin Oncol* **9**, 491-498 (1991).

5 Von Hoff, D. D. *et al.* Gemcitabine plus nab-paclitaxel is an active regimen in patients with advanced pancreatic cancer: a phase I/II trial. *J Clin Oncol* **29**, 4548-4554, doi:10.1200/JCO.2011.36.5742 (2011).

6 Valsecchi, M. E., Diaz-Canton, E., de la Vega, M. & Littman, S. J. Recent treatment advances and novel therapies in pancreas cancer: a review. *J Gastrointest Cancer* **45**, 190-201, doi:10.1007/s12029-013-9561-z (2014).

7 Thind, K., Padrnos, L. J., Ramanathan, R. K. & Borad, M. J. Immunotherapy in pancreatic cancer treatment: a new frontier. *Therap Adv Gastroenterol* **10**, 168-194, doi:10.1177/1756283X16667909 (2017).

8 Schumacher, T. N. & Schreiber, R. D. Neoantigens in cancer immunotherapy. *Science* **348**, 69-74, doi:10.1126/science.aaa4971 (2015).

9 Balachandran, V. P. *et al.* Identification of unique neoantigen qualities in long-term survivors of pancreatic cancer. *Nature* **551**, 512-516, doi:10.1038/nature24462 (2017).

10 Chandra, D., Jahangir, A., Quispe-Tintaya, W., Einstein, M. H. & Gravekamp, C. Myeloid-derived suppressor cells have a central role in attenuated Listeria monocytogenes-based immunotherapy against metastatic breast cancer in young and old mice. *British Journal of Cancer* **108**, 2281-2290, doi:10.1038/bjc.2013.206 (2013).

11 Ostrand-Rosenberg, S. & Sinha, P. Myeloid-derived suppressor cells: linking inflammation and cancer. *Journal of immunology* **182**, 4499-4506, doi:10.4049/jimmunol.0802740 (2009).

12 Gabrilovich, D. I. & Nagaraj, S. Myeloid-derived suppressor cells as regulators of the immune system. *Nature reviews. Immunology* **9**, 162-174, doi:10.1038/nri2506 (2009).

13 Xia, H. *et al.* Suppression of FIP200 and autophagy by tumor-derived lactate promotes naive T cell apoptosis and affects tumor immunity. *Sci Immunol* **2**, doi:10.1126/sciimmunol.aan4631 (2017).

14 Jahangir, A. *et al.* Immunotherapy with Listeria reduces metastatic breast cancer in young and old mice through different mechanisms. *Oncoimmunology* **6**, e1342025, doi:10.1080/2162402X.2017.1342025 (2017).

15 Kim, S. H. *et al.* Mage-b vaccine delivered by recombinant Listeria monocytogenes is highly effective against breast cancer metastases. *British journal of cancer* **99**, 741-749, doi:10.1038/sj.bjc.6604526 (2008).

16 Alvarez-Dominguez, C., Carrasco-Marin, E. & Leyva-Cobian, F. Role of complement component C1q in phagocytosis of Listeria monocytogenes by murine macrophage-like cell lines. *Infect Immun* **61**, 3664-3672 (1993).

17 Croize, J., Arvieux, J., Berche, P. & Colomb, M. G. Activation of the human complement alternative pathway by Listeria monocytogenes: evidence for direct

binding and proteolysis of the C3 component on bacteria. *Infect Immun* **61**, 5134-5139 (1993).

18 Drevets, D. A., Sawyer, R. T., Potter, T. A. & Campbell, P. A. Listeria monocytogenes infects human endothelial cells by two distinct mechanisms. *Infect Immun* **63**, 4268-4276 (1995).

19 Quispe-Tintaya, W. *et al.* Nontoxic radioactive Listeria(at) is a highly effective therapy against metastatic pancreatic cancer. *Proc Natl Acad Sci U S A* **110**, 8668-8673, doi:10.1073/pnas.1211287110 (2013).

20 Bayne, L. J. *et al.* Tumor-derived granulocyte-macrophage colony-stimulating factor regulates myeloid inflammation and T cell immunity in pancreatic cancer. *Cancer cell* **21**, 822-835, doi:10.1016/j.ccr.2012.04.025 (2012).

21 Portnoy, D. A., Auerbuch, V. & Glomski, I. J. The cell biology of Listeria monocytogenes infection: the intersection of bacterial pathogenesis and cell-mediated immunity. *The Journal of cell biology* **158**, 409-414, doi:10.1083/jcb.200205009 (2002).

22 Kim, S. H., Castro, F., Paterson, Y. & Gravekamp, C. High efficacy of a Listeria-based vaccine against metastatic breast cancer reveals a dual mode of action. *Cancer Research* **69**, 5860-5866, doi:10.1158/0008-5472.CAN-08-4855 (2009).

23 Chandra, D. *et al.* 32-Phosphorus selectively delivered by listeria to pancreatic cancer demonstrates a strong therapeutic effect. *Oncotarget* **8**, 20729-20740, doi:10.18632/oncotarget.15117 (2017).

24 Zhou, S., Gravekamp, C., Bermudes, D. & Liu, K. Tumour-targeting bacteria engineered to fight cancer. *Nat Rev Cancer*, doi:10.1038/s41568-018-0070-z (2018).

25 Singh, M. *et al.* Direct incorporation of the NKT-cell activator alpha-galactosylceramide into a recombinant Listeria monocytogenes improves breast

cancer vaccine efficacy. *Br J Cancer* **111**, 1945-1954, doi:10.1038/bjc.2014.486 (2014).

26 Zorde Khvalevsky, E. *et al.* Mutant KRAS is a druggable target for pancreatic cancer. *Proc Natl Acad Sci U S A* **110**, 20723-20728, doi:10.1073/pnas.1314307110 (2013).

27 Hingorani, S. R. *et al.* Trp53R172H and KrasG12D cooperate to promote chromosomal instability and widely metastatic pancreatic ductal adenocarcinoma in mice. *Cancer cell* **7**, 469-483, doi:10.1016/j.ccr.2005.04.023 (2005).

28 Qiu, W. *et al.* Disruption of p16 and activation of Kras in pancreas increase ductal adenocarcinoma formation and metastasis in vivo. *Oncotarget* **2**, 862-873, doi:10.18632/oncotarget.357 (2011).

29 Gunn, G. R. *et al.* Two Listeria monocytogenes vaccine vectors that express different molecular forms of human papilloma virus-16 (HPV-16) E7 induce qualitatively different T cell immunity that correlates with their ability to induce regression of established tumors immortalized by HPV-16. *Journal of immunology* **167**, 6471-6479 (2001).

30 Pamer, E. G. Immune responses to Listeria monocytogenes. *Nat Rev Immunol* **4**, 812-823, doi:10.1038/nri1461 (2004).

31 Ovchinnikov, D. A. *et al.* Expression of Gal4-dependent transgenes in cells of the mononuclear phagocyte system labeled with enhanced cyan fluorescent protein using Csf1r-Gal4VP16/UAS-ECFP double-transgenic mice. *J Leukoc Biol* **83**, 430-433, doi:10.1189/jlb.0807585 (2008).

32 Groom, J. R. & Luster, A. D. CXCR3 in T cell function. *Experimental cell research* **317**, 620-631, doi:10.1016/j.yexcr.2010.12.017 (2011).

33 Slaney, C. Y., Kershaw, M. H. & Darcy, P. K. Trafficking of T cells into tumors. *Cancer Res* **74**, 7168-7174, doi:10.1158/0008-5472.CAN-14-2458 (2014).

34 Elgueta, R. *et al.* Molecular mechanism and function of CD40/CD40L engagement in the immune system. *Immunol Rev* **229**, 152-172, doi:10.1111/j.1600-065X.2009.00782.x (2009).

35 Anagnostou, V. *et al.* Evolution of Neoantigen Landscape during Immune Checkpoint Blockade in Non-Small Cell Lung Cancer. *Cancer Discov* **7**, 264-276, doi:10.1158/2159-8290.CD-16-0828 (2017).

36 Efremova, M., Finotello, F., Rieder, D. & Trajanoski, Z. Neoantigens Generated by Individual Mutations and Their Role in Cancer Immunity and Immunotherapy. *Front Immunol* **8**, 1679, doi:10.3389/fimmu.2017.01679 (2017).

37 Stromnes, I. M., Hulbert, A., Pierce, R. H., Greenberg, P. D. & Hingorani, S. R. T-cell Localization, Activation, and Clonal Expansion in Human Pancreatic Ductal Adenocarcinoma. *Cancer Immunol Res* **5**, 978-991, doi:10.1158/2326-6066.CIR-16-0322 (2017).

38 Fink, D. M., Steele, M. M. & Hollingsworth, M. A. The lymphatic system and pancreatic cancer. *Cancer letters* **381**, 217-236, doi:10.1016/j.canlet.2015.11.048 (2016).

39 Keenan, B. P. *et al.* A Listeria vaccine and depletion of T-regulatory cells activate immunity against early stage pancreatic intraepithelial neoplasms and prolong survival of mice. *Gastroenterology* **146**, 1784-1794 e1786, doi:10.1053/j.gastro.2014.02.055 (2014).

40 Deng, W. *et al.* Recombinant Listeria promotes tumor rejection by CD8(+) T cell-dependent remodeling of the tumor microenvironment. *Proc Natl Acad Sci U S A* **115**, 8179-8184, doi:10.1073/pnas.1801910115 (2018).

41 Toussaint, B., Chauchet, X., Wang, Y., Polack, B. & Le Gouellec, A. Live-attenuated bacteria as a cancer vaccine vector. *Expert Rev Vaccines* **12**, 1139-1154, doi:10.1586/14760584.2013.836914 (2013).

42 Forbes, N. S. *et al.* White paper on microbial anti-cancer therapy and prevention. *J Immunother Cancer* **6**, 78, doi:10.1186/s40425-018-0381-3 (2018).

43 Ullenhag, G. J., Mozaffari, F., Broberg, M., Mellstedt, H. & Liljefors, M. Clinical and Immune Effects of Lenalidomide in Combination with Gemcitabine in Patients with Advanced Pancreatic Cancer. *PLoS One* **12**, e0169736, doi:10.1371/journal.pone.0169736 (2017).

44 Takeuchi, S. *et al.* Chemotherapy-Derived Inflammatory Responses Accelerate the Formation of Immunosuppressive Myeloid Cells in the Tissue Microenvironment of Human Pancreatic Cancer. *Cancer Res* **75**, 2629-2640, doi:10.1158/0008-5472.CAN-14-2921 (2015).

45 McElhaney, J. E., Meneilly, G. S., Lechelt, K. E. & Bleackley, R. C. Split-virus influenza vaccines: do they provide adequate immunity in the elderly? *J Gerontol* **49**, M37-43 (1994).

46 Effros, R. B. Role of T lymphocyte replicative senescence in vaccine efficacy. *Vaccine* **25**, 599-604, doi:10.1016/j.vaccine.2006.08.032 (2007).

47 Gravekamp, C. The impact of aging on cancer vaccination. *Curr Opin Immunol* **23**, 555-560, doi:10.1016/j.coi.2011.05.003 (2011).

48 Castro, F. *et al.* Vaccination with Mage-b DNA induces CD8 T-cell responses at young but not old age in mice with metastatic breast cancer. *British journal of cancer* **101**, 1329-1337, doi:10.1038/sj.bjc.6605329 (2009).

49 Utsuyama, M. *et al.* Differential age-change in the numbers of CD4+CD45RA+ and CD4+CD29+ T cell subsets in human peripheral blood. *Mech Ageing Dev* **63**, 57-68 (1992).

50 Corbett, T. H. *et al.* Induction and chemotherapeutic response of two transplantable ductal adenocarcinomas of the pancreas in C57BL/6 mice. *Cancer Res* **44**, 717-726 (1984).

51 Aslakson, C. J. & Miller, F. R. Selective events in the metastatic process defined by analysis of the sequential dissemination of subpopulations of a mouse mammary tumor. *Cancer Research* **52**, 1399-1405 (1992).

52 Lelekakis, M. *et al.* A novel orthotopic model of breast cancer metastasis to bone. *Clin Exp Metastasis* **17**, 163-170, doi:10.1023/a:1006689719505 (1999).

53 Medaglini, D. *et al.* Immunization with recombinant Streptococcus gordonii expressing tetanus toxin fragment C confers protection from lethal challenge in mice. *Vaccine* **19**, 1931-1939, doi:10.1016/s0264-410x(00)00434-5 (2001).

54 Reece, J. C., Geysen, H. M. & Rodda, S. J. Mapping the major human T helper epitopes of tetanus toxin. The emerging picture. *Journal of immunology* **151**, 6175-6184 (1993).

55 Rice, J., Buchan, S. & Stevenson, F. K. Critical components of a DNA fusion vaccine able to induce protective cytotoxic T cells against a single epitope of a tumor antigen. *Journal of immunology* **169**, 3908-3913 (2002).

56 Partecke, L. I. *et al.* A syngeneic orthotopic murine model of pancreatic adenocarcinoma in the C57/BL6 mouse using the Panc02 and 6606PDA cell lines. *Eur Surg Res* **47**, 98-107, doi:10.1159/000329413 (2011).

57 Qiu, W. & Su, G. H. Development of orthotopic pancreatic tumor mouse models. *Methods in molecular biology* **980**, 215-223, doi:10.1007/978-1-62703-287-2_11 (2013).

58 Entenberg, D. *et al.* Time-lapsed, large-volume, high-resolution intravital imaging for tissue-wide analysis of single cell dynamics. *Methods* **128**, 65-77, doi:10.1016/j.ymeth.2017.07.019 (2017).

59 Entenberg, D. *et al.* Setup and use of a two-laser multiphoton microscope for multichannel intravital fluorescence imaging. *Nat Protoc* **6**, 1500-1520, doi:10.1038/nprot.2011.376 (2011).

60 Yamamoto, T. *et al.* Over-expression of facilitative glucose transporter genes in human cancer. *Biochem Biophys Res Commun* **170**, 223-230 (1990).

61 Kim, S. H. *et al.* Mage-b vaccine delivered by recombinant Listeria monocytogenes is highly effective against breast cancer metastases. *Br J Cancer* **99**, 741-749, doi:10.1038/sj.bjc.6604526 (2008).

62 Chandra, D. *et al.* STING ligand c-di-GMP improves cancer vaccination against metastatic breast cancer. *Cancer Immunol Res* **2**, 901-910, doi:10.1158/2326-6066.CIR-13-0123 (2014).

63 Smallwood, S. A. *et al.* Single-cell genome-wide bisulfite sequencing for assessing epigenetic heterogeneity. *Nat Methods* **11**, 817-820, doi:10.1038/nmeth.3035 (2014).

64 Wang, L., Wang, S. & Li, W. RSeQC: quality control of RNA-seq experiments. *Bioinformatics* **28**, 2184-2185, doi:10.1093/bioinformatics/bts356 (2012).

65 Trapnell, C. *et al.* Transcript assembly and quantification by RNA-Seq reveals unannotated transcripts and isoform switching during cell differentiation. *Nature biotechnology* **28**, 511-515, doi:10.1038/nbt.1621 (2010).

66 Lien, W. H. *et al.* Genome-wide maps of histone modifications unwind in vivo chromatin states of the hair follicle lineage. *Cell stem cell* **9**, 219-232, doi:10.1016/j.stem.2011.07.015 (2011).

67 Trapnell, C. *et al.* Differential gene and transcript expression analysis of RNA-seq experiments with TopHat and Cufflinks. *Nat Protoc* **7**, 562-578, doi:10.1038/nprot.2012.016 (2012).

Methods

Animal care

C57BL/6 male and female mice aged 3 months were obtained from Charles River. KPC mice (*LSL-p53*$^{R172/+}$*; LSL*^{KrasG12D}*; Pdx1-Cre*)[27] were generated in the laboratories of Drs. Gravekamp and Libutti, as described previously[23]. C57Bl/6N-Tg(Cfms-gal4-vp16)-(UAS-eCFP)[31] were maintained in the laboratory of Dr. Condeelis. All mice were housed in the animal husbandry facility at Albert Einstein College of Medicine according to the Association and Accreditation of Laboratory Animal Care guidelines, and kept under BSL-2 conditions as required for *Listeria* treatments. All KPC mice were genotyped by Transnetyx (Cordova, TN).

Cell lines

The Panc-02 cell line with the Kras-G12D mutant allele was derived from a methylcholanthrene-induced ductal adenocarcinoma growing in a C57BL/6 female mouse[50]. Panc-02 cells were cultured in McCoy's5A medium supplemented with 10% fetal bovine serum, 2 mM glutamine, non-essential amino acids, 1 mM sodium pyruvate, and 100 U/ml Pen/Strep. The Panc-02 cell line expressing Dendra-2 was developed in the laboratory of Dr. Gravekamp. Briefly, Panc-02 cells were transfected with pDendra2C (ClonTech), and positive cells were selected using neomycin and FACS sorting. The 4T1 cell line was derived from a spontaneous mammary carcinoma in a BALB/c mouse[51]. Various 4T1 sub lines have been generated with different patterns of metastases[52], which is kindly provided to our lab by Dr. Fred Miller, Karmanos Institute, Wayne State University, Michigan, MI). The 4T1 cell line used in this study is highly aggressive, metastasizing predominantly to the mesenteric lymph nodes (MLN), and less frequently to the diaphragm, portal liver, spleen and kidneys (Gravekamp *et al*, 2008).

Listeria and *Listeria*-TT

In this study, an attenuated *Listeria monocytogenes* (*Listeria*) was used as the vehicle for delivery of $TT_{856-1313}$[53] to the TME and inside tumor cells. The *Listeria* plasmid pGG-34, expressing the non-cytolytic truncated form of Listeriolysin O (LLO) under control of the hemolysin promoter *(Phly)* and the positive regulatory factor A (prfA), with mutations to further reduce pathogenicity, have been described elsewhere[29]. *Listeria*-$TT_{856-1313}$ was developed in our laboratory **(Fig 2a)**. Briefly, $TT_{856-1313}$[53] was cloned by PCR into pCR2.1 using primers containing XHoI and XMaI restriction sites and a myc Tag for detection of TT. (**PrF5':** CTC GAG TCA ACA CCA ATT CCA TTT; **PrR5':** CCC GGG TTA TAG ATC TTC TTC TGA AAT TAG TTT TTG TTC TGT CCA TCC TTC ATC TGT) Subsequently the pCR2.1-XHoI-$TT_{856-1313}$-Myc-XmaI and pGG34 plasmids were digested with XHoI and XMaI, and the XHoI-$TT_{856-1313}$-myc-XMaI DNA fragment was cloned into the pGG34 vector, and then electroporated into the *Listeria* background strain XFL7[29]. The *Listeria*-$TT_{856-1313}$ was characterized by DNA sequencing and by evaluating the secretion of $TT_{856-1313}$ into the culture medium **(Fig 2a).** The $TT_{856-1313}$ fragment contains both mouse and human immunodominant T cell epitopes[54,55].

Infection of tumor cells *in vitro*

The *in vitro* infectivity of Panc-02 tumor cells was assessed as described previously[22]. Briefly, 10^6 cells/ml were infected with 10^7 CFU of *Listeria* or *Listeria* -TT for 1 hr at 37°C in culture medium, then incubated with gentamicin (50 μg/ml) for 1 hr to kill extracellular *Listeria*. Finally, cells were washed with phosphate-buffered saline (PBS), lysed in water, and serial dilutions were plated onto LB agar to quantify the infection rate the next day.

Evaluation of cell death

As described previously[22], tumor cell killing by *Listeria* or *Listeria*-TT was determined *in vitro* as follows. Panc-02 cells ($3x10^3$) plated in 96 well plates were infected with 10^7 CFU/well of *Listeria* or *Listeria*-TT for 3 hrs at 37°C, then gentamicin (50 μg/ml) was added. Live and dead cells were counted the next day using Trypan blue staining.

Biodistribution of *Listeria*-TT

C57Bl/6 mice were injected with $2x10^6$ tumor cells as described above, and 14 days later injected with a single large dose 10^7 CFU of *Listeria*-TT. Mice were euthanized at various time points after the injection, and metastases, tumors and normal tissues were dissected, weighed, and analyzed for CFU of *Listeria*-TT, as described previously[23].

Dose-limiting toxicity

C57Bl6 mice were injected ip with various doses of *Listeria*-TT, and survival was monitored over the next 20 days, as described previously[23].

Tumor development

Panc-02 tumor cells were injected into the mammary fat pad (peritoneal cavity model) (10^5) or orthotopically into the pancreas (10^6) of C57Bl/6 mice. When injected into the mammary fad pat, a primary tumor develops at the place of injection and tumor cells metastasize via the peritoneal cavity to other organs, predominantly to the pancreas and liver, and less abundantly to mesenchymal lymph nodes along the gastrointestinal tract and the diaphragm[19], but when injected into the pancreas tumor cells a primary tumor develops in the pancreas and tumor cells metastasize to the liver only[56]. In KPC mice, multiple primary tumors develop spontaneously in the pancreas, metastasizing to the liver and lungs[23,27].

Orthotopic Panc-02 model

Orthotopic Panc-02 tumors were generated in C57Bl/6 mice as described previously[57]. Briefly, mice were anesthetized with Ketamine/Xylazine (respectively 100 mg and 10 mg/Kg, ip), the hair was removed at the location of the spleen, and the skin was sterilized with betadine followed by 70% alcohol. The animal was covered with gauze sponge surrounding the incision site. A 1 cm incision was made in the abdominal skin and muscle just lateral to the midline and directly above the spleen/pancreas to allow visualization. The spleen/pancreas was gently retracted and positioned to allow injection of 1×10^6 KPC tumor cells directly into the pancreas, from the tail all the way to the head of the pancreas. To prevent leakage of injected cell suspension, the injection site was tied off after tumor cell injections with dissolvable suture. The spleen/pancreas were then replaced within the abdominal cavity, and both muscle and skin layers closed with sutures. Following recovery from surgery, mice were monitored and weighed daily. A palpable tumor appeared within 2 weeks in the pancreas, and metastases in the liver began to develop within 2-4 weeks.

Protocol for treatment of Panc-02 and KPC mice with *Listeria*-TT+GEM.

A detailed rationale for this treatment protocol and schematic view of all treatments are shown in **Fig 1b.** Panc-02 mice. To generate memory T cells to TT, C57Bl/6 mice were immunized twice intramuscularly with the Tetanus vaccine (the same used for childhood vaccinations, 0.3 µg/50 µL) 1 week apart. Subsequently, Panc-02 tumor cells (10^5/100 µL) were injected into mammary fat pad. A single high dose of *Listeria*-TT (10^7 CFU) was injected ip, either 3-5 days after tumor cell injection when tumors were 3 mm (early pancreatic cancer) or 10-14 days after tumor cell injection when tumors were 10 mm (advanced pancreatic cancer). Three days later, GEM (Gemizan: Zuventus, Mombay, India) treatment was started (1.2 mg/mouse, every 3 days) and continued for 14 days

(six doses in total). Concomitantly, low doses of *Listeria*-TT were administered daily for 2 weeks (14 doses in total). All mice were euthanized 2 days after the last treatment, and visually analyzed for tumor weight and the number of metastases, as described previously[19]. KPC mice. KPC mice, age 3.5-5 months, received the same treatment described above, after verification of the presence of tumors and metastases by PET scan.

Intravital multiphoton imaging (IVMI)

Panc-02 tumor cells (10^6) expressing Dendra-2 were injected into the pancreas of transgenic mice [C57Bl/6N-Tg(Cfms-gal4-vp16)-(UAS-eCFP)][31] in which the macrophages were labeled with cyan fluorescent protein (CFP). Three weeks later, when a pancreatic tumor developed and on the same day as imaging, *Listeria*-TT was labeled *ex vivo* with Alexa-680 by incubation with rabbit anti-*Listeria* polyclonal antiserum (dilution 1:200) and anti-rabbit IgG-Alexa-680 (dilution 1:250). *Listeria*-TT-Alexa-680 was injected ip, and four hours later, when *Listeria*-TT had accumulated in the TME and infected tumor cells, mice were anesthetized using isoflurane. Pancreatic tumors were externalized through a small incision (~0.7 cm) through the skin and peritoneal wall, and stabilized for imaging using previously published protocols[58]. Multiphoton intravital microscopy was performed using a custom-built two-laser multiphoton microscope[59]. Tumors were imaged with a femtosecond laser set to 880 nm for excitation of CFP or the green form of Dendra-2, and an optical parametric oscillator set to 1240 nm for excitation of Alexa 680. Z-stacks to a depth of 45 μm were acquired with a 1 μm slice interval. During the course of imaging, the animal was placed in a heated chamber maintained at physiological temperature. Mice were monitored for heart rate, breathing rate, pulse distension, breath distension and oxygen saturation using a pulse oximeter (MouseSTAT, Kent Scientific).

PET scan

Positron emission tomography (PET) was performed as described previously[60]. Briefly, the effect of the *Listeria*-TT+GEM treatment on the tumor and metastases was monitored by microPET (Siemens Imaging System) prior to and post-treatment. For this purpose, mice were injected with the positron emitter [^{18}F]-labeled deoxyglucose. The uptake of ^{18}F-FDG by tumors and metastases was quantified by microPET as described previously[19]. Increased FDG uptake reflects increased metabolic activity of cancer cells, expressed as SUVmax.

Flow cytometry

Immune cells from spleens, blood, or metastases of mice were isolated as described previously[48]. Anti-CD3 and anti-CD8 antibodies were used to identify CD8 T cells, anti-CD3 and anti-CD4 to identify CD4 T cells, anti-CD11b and anti-Gr1 to identify MDSC, and anti-CD11b and anti-F4/80 to identify TAM. To detect intracellular cytokine production, the cells were incubated with GolgiPlug (1 µg/ml) for 6 hrs, then treated with Cytofix/Cytoperm according to the manufacturer's instructions, before staining with antibodies to intracellular cytokines, IFNγ, Granzyme B, Perforin, IL-6, IL-10, TNFα, and other markers such as the T cell response inhibitor MARCO, the T cell activation marker CD69, or the costimulator CD80. Appropriate isotype controls were included for each sample. 50,000-100,000 cells were acquired by scanning using a special order LSR-II Fluorescence Activated Cell Sorter system (Beckton and Dickinson), and analyzed using FlowJo 7.6 software. Cell debris and dead cells were excluded from the analysis based on scatter signals and use of Fixable Blue or Green Live/Dead Cell Stain Kit.

ELISPOT

Spleen cells were isolated from treated and control Panc-02 and KPC mice for ELISPOT (BD Biosciences, cat# 551083) analysis, as described previously[61]. To detect T cell responses to TT, 10^5 spleen cells were incubated with purified TT protein (5 μg/ml). The frequency of IFNγ-producing spleen cells was measured 72 hrs later using an ELISPOT reader (CTL Immunospot S4 analyzer). To determine the frequency of IFNγ-producing CD4 and CD8 T cells, spleen cells were depleted for CD4 and CD8 T cells using magnetic bead depletion techniques according to the manufacturer's instructions.

Western blotting

Expression of TT protein in tumor cells was analyzed by western blotting as described previously[62]. Briefly, cells were lysed in RIPA buffer containing protease inhibitors, and proteins were separated on 4-12% gradient SDS-polyacrylamide gels, then electro-transferred to PVDF membrane. Membranes were incubated with rabbit anti-myc IgG, followed by horseradish peroxidase-conjugated goat anti-rabbit IgG. Detection was with a chemiluminescence detection kit. Antibody to β-actin was used to ensure equal loading.

Immunohistochemistry (IHC)

Tumors were dissected from pancreas and immediately fixed with buffered formalin, and the tissue was embedded in paraffin. Sections (5 μm) were sliced and placed on slides, then deparaffinized at 60ºC for 1 hr, followed by xylene, an ethanol gradient (100-70%), water, and PBS. Slides were then incubated for 30 min in 3% hydrogen peroxide followed by boiling in citrate buffer for 20 min. Once the slides were cooled, washed, and blocked with 5% goat serum, the sections were incubated with primary antibodies such as anti-CD4 (1:100 dilution), anti-CD8α (1:400 dilution), anti-Perforin (1:300 dilution),

anti-Granzyme (1:200 dilution), anti-CD31 (1:100 dilution) or anti-TT (1:50 dilution), followed by incubation with secondary antibody (mouse anti-goat IgG-HRP), and SignalStain® Boost IHC Detection Reagent (Cell Signaling Technology, cat# 8114S). Subsequently, the slides were incubated with 3,3'-diaminobenzidine (DAB)(Vector Laboratories, cat# SK-4100), counterstained with hematoxylin, dehydrated through an ethanol gradient (70-100%) and xylene, and mounted with Permount. The slides were scanned with a 3D Histech P250 High Capacity Slide Scanner to acquire images and quantification data.

RNAseq

Sample preparation for RNA seq. Total RNA was isolated from the metastasis and tumor tissues, treated with DNase, and evaluated using the Agilent Bioanalyzer. The purified high quality total RNA was submitted to the Epigenetics Shared Facility (ESF) for assay and analysis. An RNAseq assay using 25 ng of RNA was performed and validated by the ESF.

Whole-transcriptome library preparation and high-throughput RNA sequencing. ESF personnel performed rRNA-depletion using a Ribo-Zero rRNA Removal Kit, and reverse transcription using random hexamers and oligo(dT) to synthesize ds-cDNA. Libraries were prepared with adapters and barcodes for multiplex sequencing, and sequenced using the Illumina HiSeq 2500. Raw FASTQ files were trimmed for adapter sequences using quart. FASTQ file sequence quality was evaluated using FastQC[63], and read coverage determined using the RSeQC package[64].

RNAseq data analysis. We generated a total of 150 RNAseq runs. For each run we obtained at least 20 million reads, with >70% of them aligned to the mouse genome. We used the Bowtie/Tophat/Cufflinks/Cuffdiff software suite[65-67], applying the Tuxedo protocol.

Statistics

To statistically compare the effects of *Listeria*-TT+GEM on the growth of metastases and tumors or on immune responses in the mouse models, the Mann-Whitney was applied using Prism. *$p<0.05$, **<0.01, ***<0.001, ****<0.0001. Values of $p<0.05$ were considered statistically significant.

Further information on research design is available as a Supplemental file linked to this article.

Figure 1

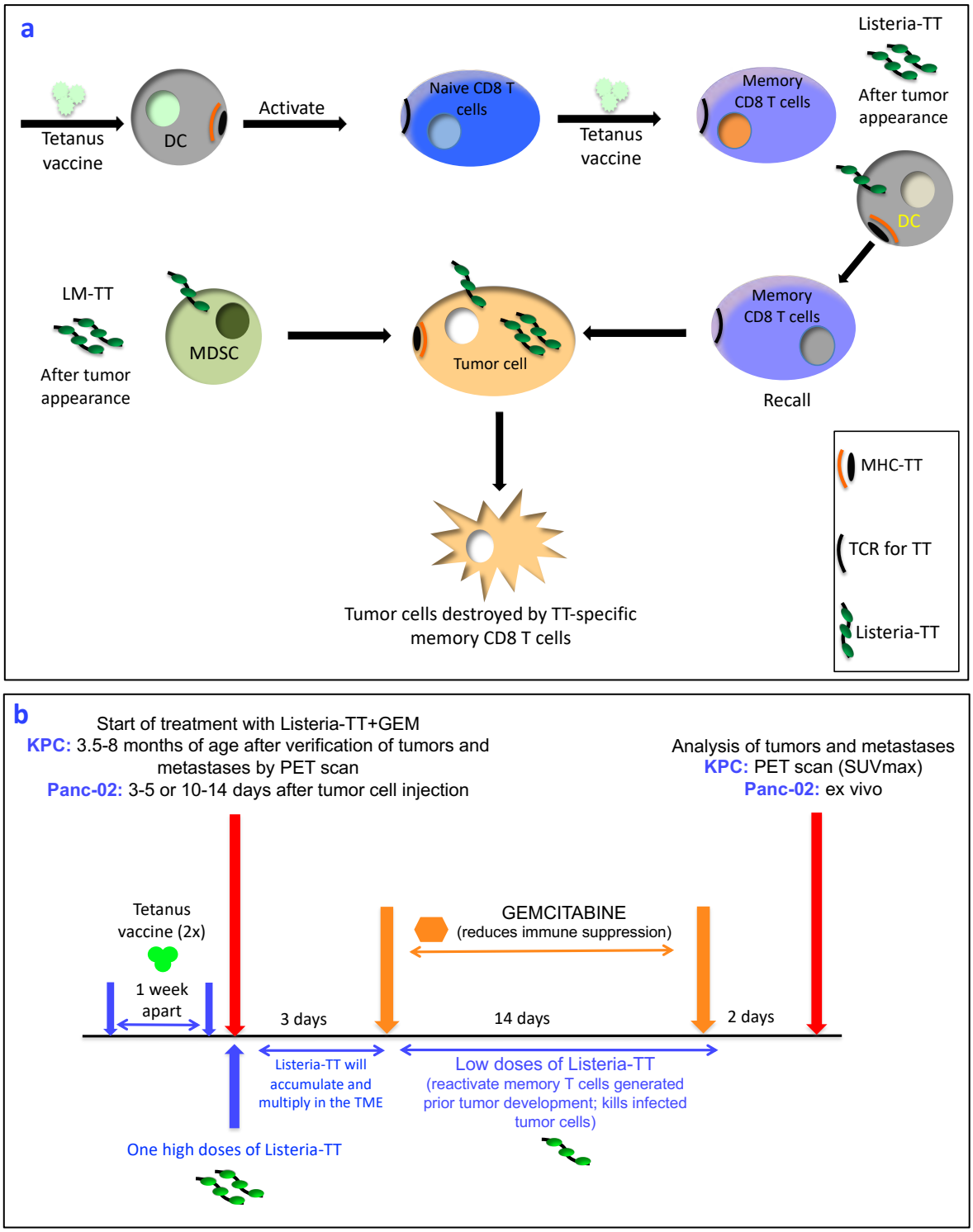
a
Tetanus vaccine
DC
Activate
Naive CD8 T cells
Tetanus vaccine
Memory CD8 T cells
Listeria-TT
After tumor appearance
DC
Memory CD8 T cells
Recall
Tumor cell
MDSC
LM-TT
After tumor appearance
Tumor cells destroyed by TT-specific memory CD8 T cells
MHC-TT
TCR for TT
Listeria-TT
b
Start of treatment with Listeria-TT+GEM
KPC: 3.5-8 months of age after verification of tumors and metastases by PET scan
Panc-02: 3-5 or 10-14 days after tumor cell injection
Analysis of tumors and metastases
KPC: PET scan (SUVmax)
Panc-02: ex vivo
Tetanus vaccine (2x)
1 week apart
GEMCITABINE
(reduces immune suppression)
3 days
14 days
2 days
Listeria-TT will accumulate and multiply in the TME
Low doses of Listeria-TT
(reactivate memory T cells generated prior tumor development; kills infected tumor cells)
One high doses of Listeria-TT

Figure 2

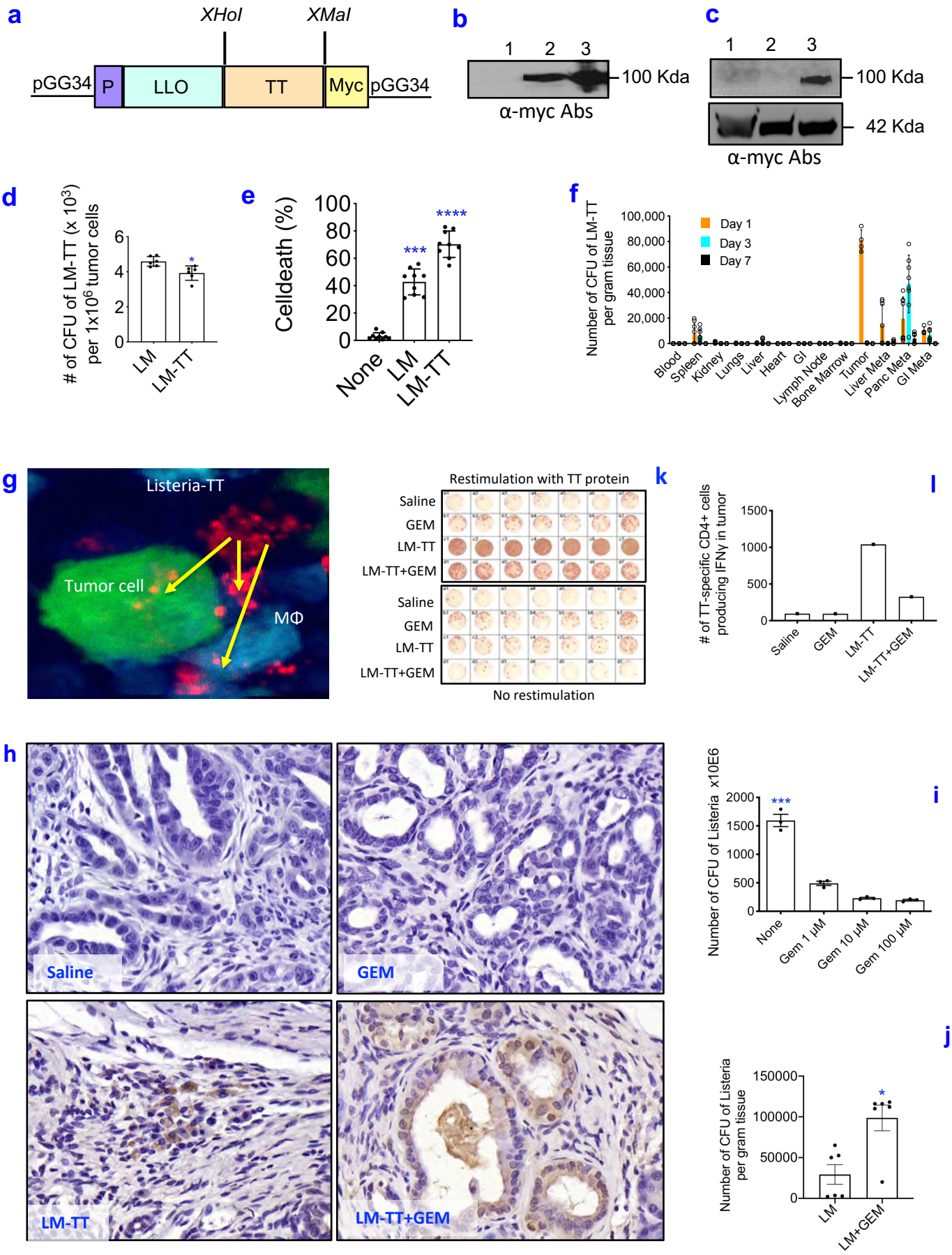
a
XHoI
XMaI
pGG34
P
LLO
TT
Myc
pGG34
b
1 2 3
100 Kda
α-myc Abs
c
1 2 3
100 Kda
42 Kda
α-myc Abs
d
# of CFU of LM-TT (x 10^3) per 1x10^6 tumor cells
LM
LM-TT
e
Celldeath (%)
None
LM
LM-TT
f
Number of CFU of LM-TT per gram tissue
Day 1
Day 3
Day 7
Blood
Spleen
Kidney
Lungs
Liver
Heart
GI
Lymph Node
Bone Marrow
Tumor
Liver Meta
Panc Meta
GI Meta
g
Listeria-TT
Tumor cell
MΦ
Restimulation with TT protein
Saline
GEM
LM-TT
LM-TT+GEM
No restimulation
k
l
# of TT-specific CD4+ cells producing IFNγ in tumor
Saline
GEM
LM-TT
LM-TT+GEM
h
Saline
GEM
LM-TT
LM-TT+GEM
i
Number of CFU of Listeria x10E6
None
Gem 1 μM
Gem 10 μM
Gem 100 μM
j
Number of CFU of Listeria per gram tissue
LM
LM+GEM

Figure 3

Prior tumor development **a**

Panc-02 mice

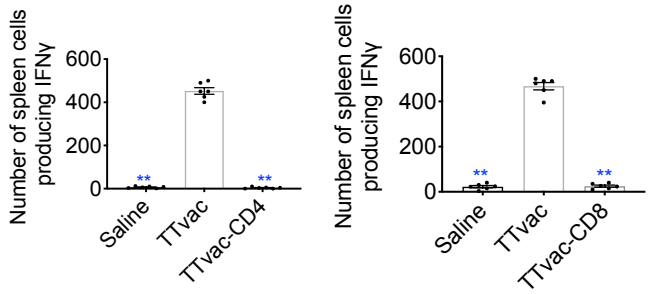

Post tumor development **b**

Panc-02 mice

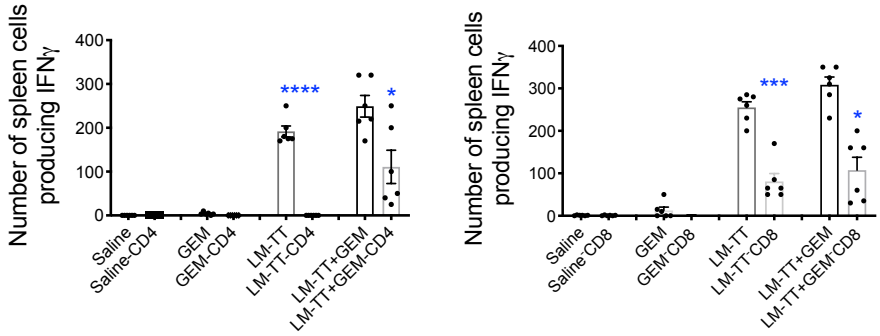

Post tumor development **c**

KPC mice

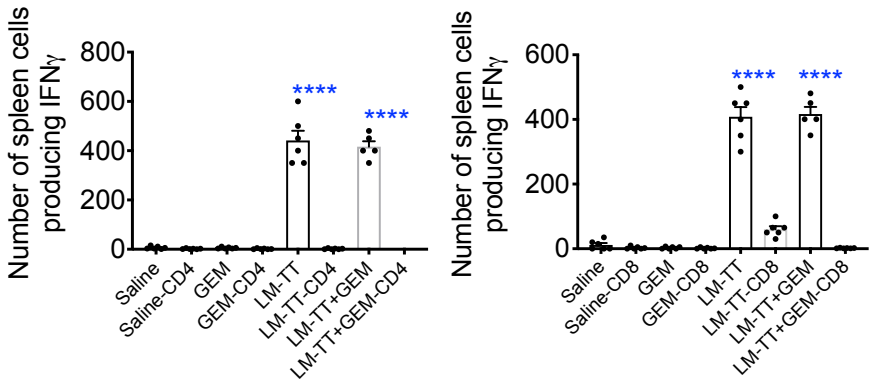

d

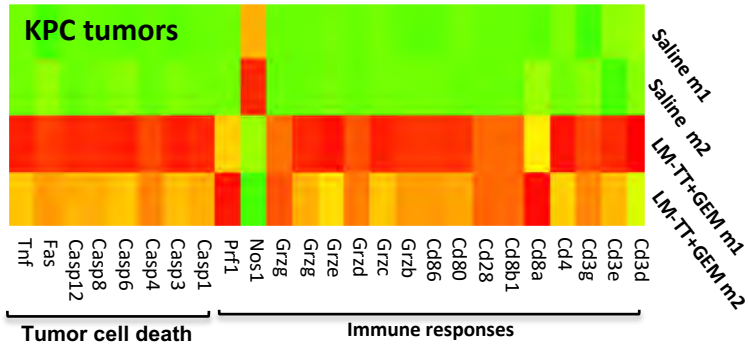

e

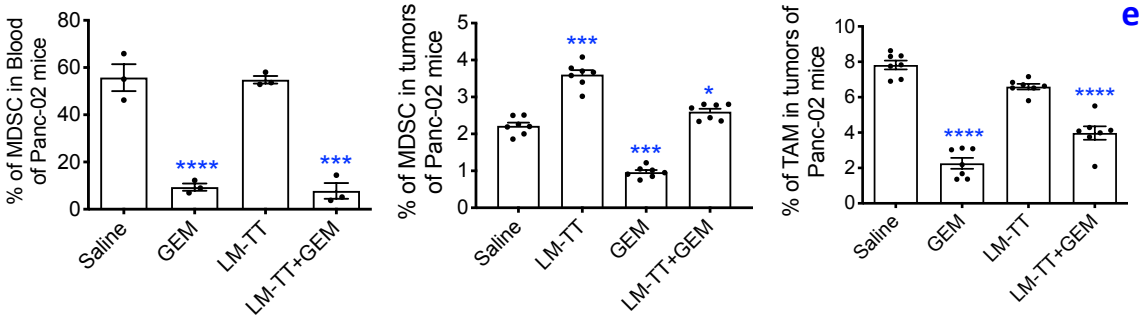

Figure 4

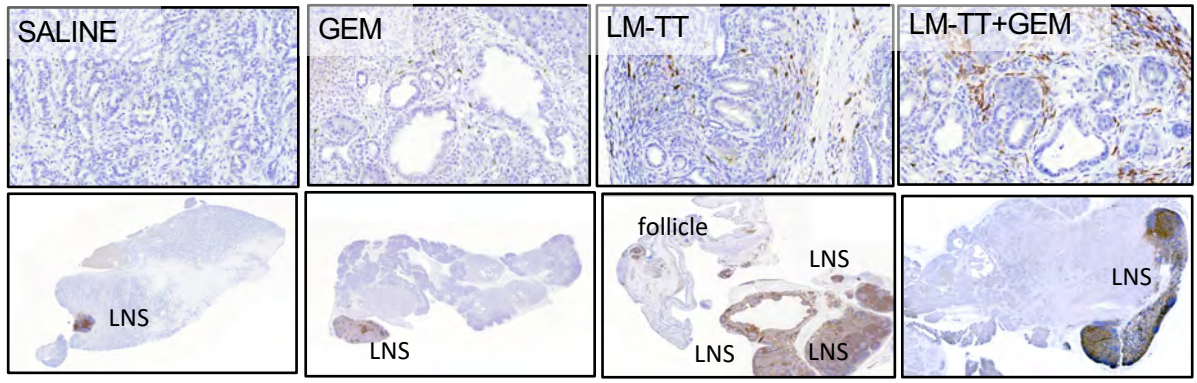
SALINE
GEM
LM-TT
LM-TT+GEM
Tumor
CD4 T cells
a
LNS
LNS
follicle
LNS
LNS
LNS
LNS

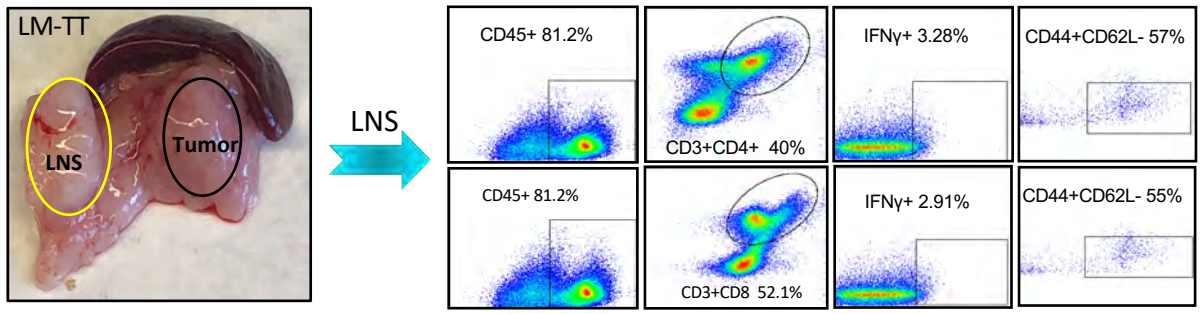
LM-TT
LNS
Tumor
LNS
CD45+ 81.2%
CD3+CD4+ 40%
IFNγ+ 3.28%
CD44+CD62L- 57%
CD4/LNS
b
CD45+ 81.2%
CD3+CD8 52.1%
IFNγ+ 2.91%
CD44+CD62L- 55%
CD8/LNS

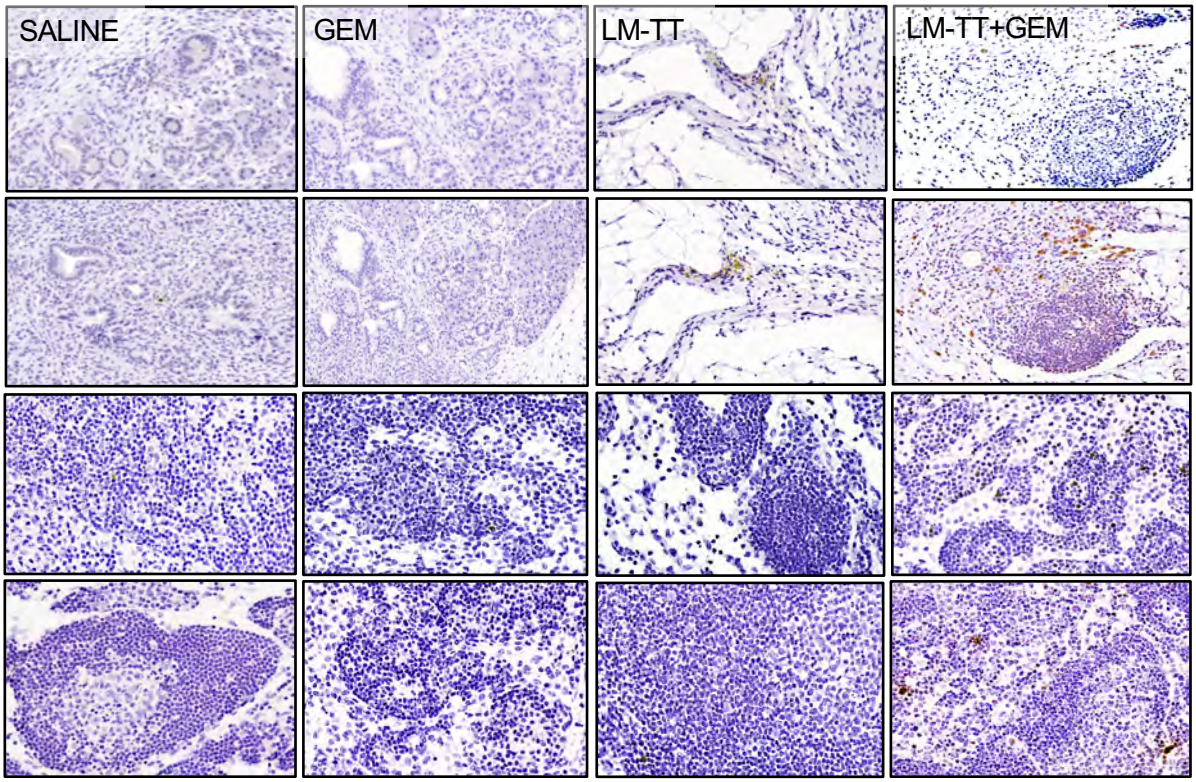
SALINE
GEM
LM-TT
LM-TT+GEM
Perforin
Tumor
c
GranzB
Perforin
LNS
d
GranzB

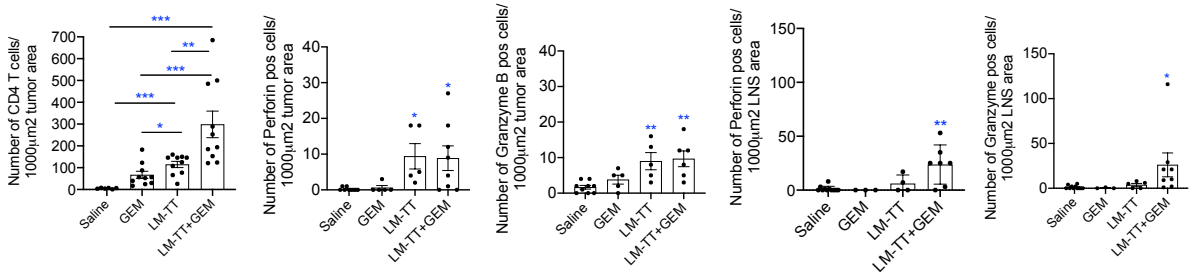
e
Number of CD4 T cells/ 1000μm2 tumor area
Number of Perforin pos cells/ 1000μm2 tumor area
Number of Granzyme B pos cells/ 1000μm2 tumor area
Number of Perforin pos cells/ 1000μm2 LNS area
Number of Granzyme pos cells/ 1000μm2 LNS area
Saline
GEM
LM-TT
LM-TT+GEM

Figure 5

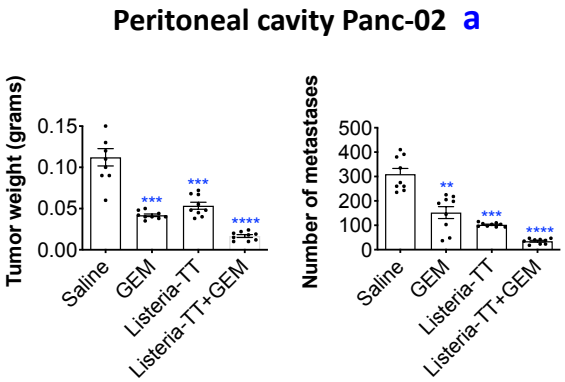
Peritoneal cavity Panc-02 a
Tumor weight (grams)
0.15
0.10
0.05
0.00
***
***
****
Saline
GEM
Listeria-TT
Listeria-TT+GEM
Number of metastases
500
400
300
200
100
0
**
***
****
Saline
GEM
Listeria-TT
Listeria-TT+GEM

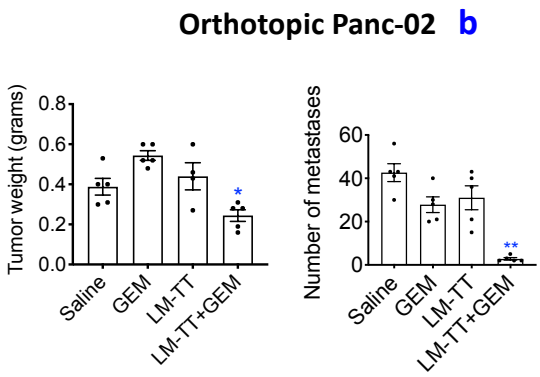
Orthotopic Panc-02 b
Tumor weight (grams)
0.8
0.6
0.4
0.2
0.0
*
Saline
GEM
LM-TT
LM-TT+GEM
Number of metastases
60
40
20
0
**
Saline
GEM
LM-TT
LM-TT+GEM

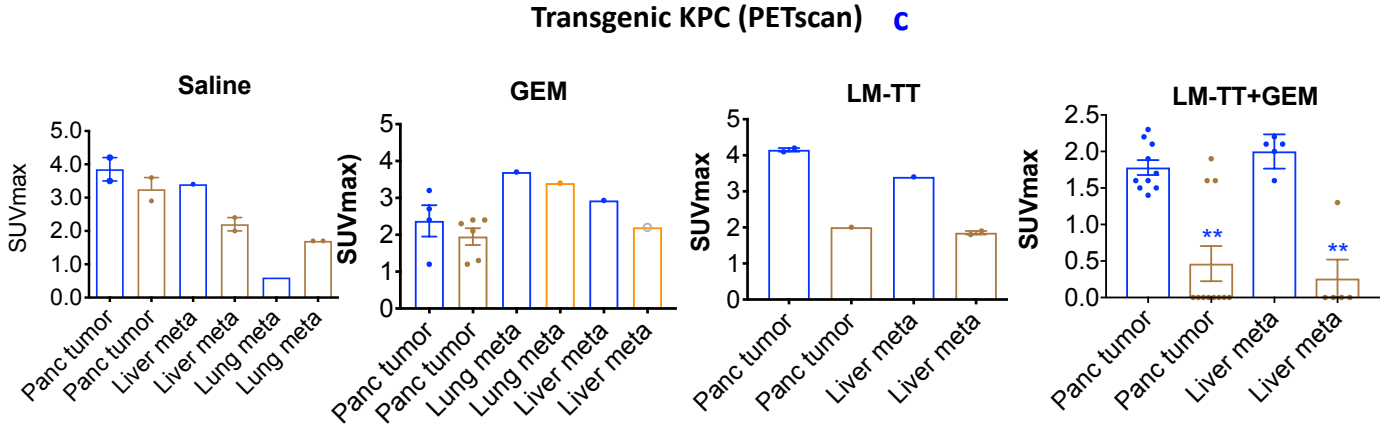
Transgenic KPC (PETscan) c
Saline
SUVmax
5.0
4.0
3.0
2.0
1.0
0.0
Panc tumor
Panc tumor
Liver meta
Liver meta
Lung meta
Lung meta
GEM
SUVmax)
5
4
3
2
1
0
Panc tumor
Panc tumor
Lung meta
Lung meta
Liver meta
Liver meta
LM-TT
SUVmax
5
4
3
2
1
0
Panc tumor
Panc tumor
Liver meta
Liver meta
LM-TT+GEM
SUVmax
2.5
2.0
1.5
1.0
0.5
0.0
**
**
Panc tumor
Panc tumor
Liver meta
Liver meta

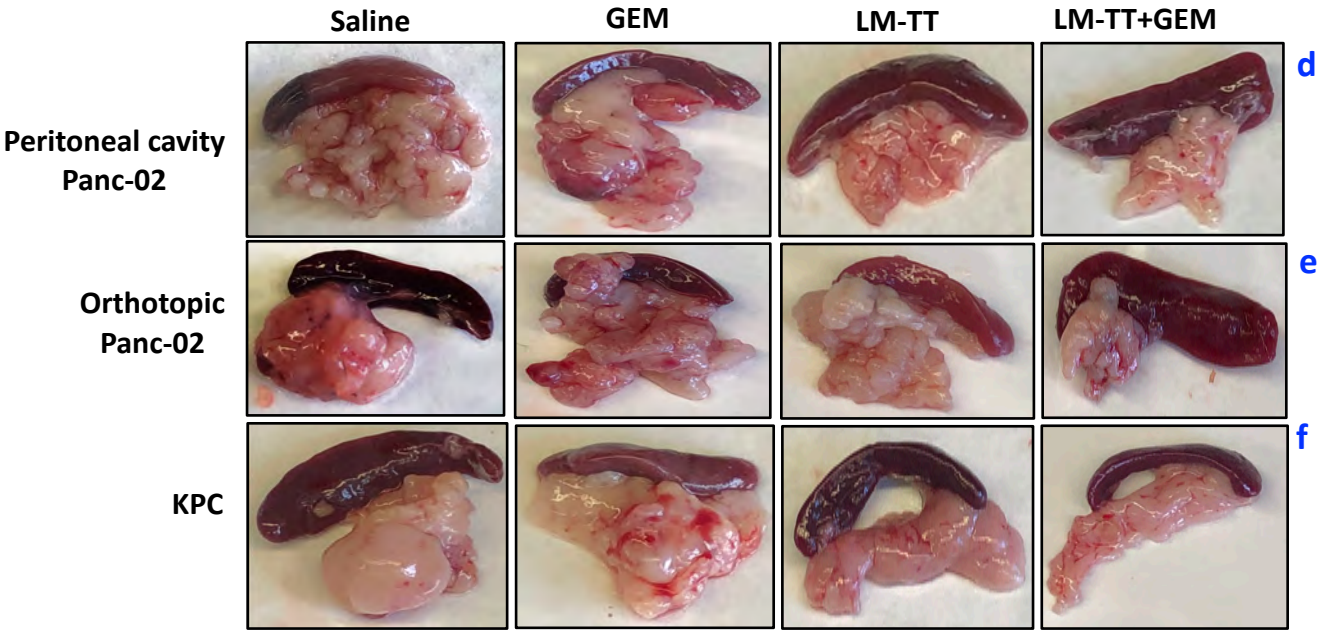
Saline
GEM
LM-TT
LM-TT+GEM
d
Peritoneal cavity Panc-02
e
Orthotopic Panc-02
f
KPC

Table 1a: Listeria-TT and GEM increases CD4 and CD8 T cell responses *in vivo* in Panc-02 mice

T cell responses*	Saline	GEM	LM-TT	LM-TT+GEM
CD3CD4CD69	15.5	14.2	14.2	28.5
CD3CD8CD69	16.7	15.5	15.5	33.2
CD3CD4Perforin	7.9	14.9	14.9	22.7
CD3CD8Perforin	2.1	4.8	4.9	6.2
CD3CD4Granzyme B	4.9	4.8	5.9	9.9
CD3CD8Granzyme B	1.2	1.1	1.2	2.4
CD3CD4IFNγ	2.6	2.7	3.0	5.0
CD3CD8IFNγ	0.5	0.4	0.4	0.9

* T cell responses are provided in percentages (Flow cytometry).
An example of gating T cells is shown in **SI Fig 2ab**
All mice were treated as outlined in **Fig 1b.** LM-TT = Listeria-TT
n=3 mice per group (spleen cells were pooled). Representative of 2 experiments

Table 1b: Listeria-TT and GEM increases CD4 and CD8 T cell responses *in vivo* in KPC mice

T cell responses	Saline	GEM	LM-TT	LM-TT+GEM
CD3CD4CD69	13.5	10.01	6.59	17.34
CD3CD8CD69	12.3	17.5	18.8	23.92
CD3CD4Perforin	0.26	7.90	8.22	14.27
CD3CD8Perforin	0.25	15.60	14.73	16.70
CD3CD4Granzyme B	3.1	3.5	4.82	12.17
CD3CD8Granzyme B	1.6	9.71	9.82	12.60
CD3CD4IFNγ	0.3	0.0	0.41	0.16
CD3CD8IFNγ	0.0	1.7	1.85	3.33

*T cell responses are provided in percentages (Flow cytometry).
All mice were treated as outlined in **Fig 1b.** LM-TT = Listeria-TT
n=3 mice per group (spleen cells were pooled). Representative of 2 experiments.

Table 1c: Listeria-TT and GEM reduce immune suppressive function of MDSC (CD11b+Gr1+) in metastases of Panc-02 mice

MDSC responses*	Saline	LM-TT	GEM	LM-TT+GEM
IL-10	3.46	2.44	2.76	1.45
IL-6	4.25	4.05	3.59	1.97
TNFα	3.64	8.42	8.49	11.6
MARCO	3.38	3.70	3.84	1.79
CD80	1.28	1.08	1.78	1.17

*MDSC responses are provided in percentages (Flow cytometry).
An example of gating the MDSC is shown in **SI Fig 5a.**
All mice were treated as outlined in **Fig 1b.** LM-TT = Listeria-TT
n=3 mice per group (CD45+ cells were pooled). This experiment was performed once.

Table 1d: Listeria-TT and GEM reduce immune suppressive function of TAM (CD11b+F4/80+) in metastases of Panc-02 mice

TAM responses*	Saline	LM-TT	GEM	LM-TT+GEM
IL-10	1.45	0.65	1.47	0.72
IL-6	1.09	0.76	1.25	0.42
TNFα	4.78	8.73	8.85	8.04
MARCO	1.96	2.16	1.94	1.33
CD80	1.93	3.07	4.28	5.26

*TAM responses are provided in percentages (Flow cytometry).
An example of gating TAM is shown in **SI Fig 5b.**
All mice were treated as outlined in **Fig 1b.** LM-TT = Listeria-TT
n=3 mice per group (CD45+ cells were pooled). This experiment was performed once.

SUPPLEMENTARY INFORMATION

Tumor-targeted delivery of childhood vaccine recall antigens by attenuated *Listeria* reduces pancreatic cancer

Benson Chellakkan Selvanesan[1$], Dinesh Chandra[1$], Wilber Quispe-Tintaya[1$], Arthee Jahangir[1], Ankur Patel[1], Kiran Meena[1], Rodrigo Alves Da Silva[1], Steven K Libutti[2], Ziqiang Yuan[2], Jenny Li[1], Sarah Siddiqui1, Amanda Beck[3], Lydia Tesfa[4], Wade Koba[5], Jennifer Chuy[6], John C. McAuliffe[7], Rojin Jafari[8], David Entenberg[8,9,10], Yarong Wang[8,9,10], John Condeelis[8,9,10,11], and Claudia Gravekamp[1*].

SI Figure S1: Intraperitoneally but not intravenously injected *Listeria* colonizes tumors and metastases.

Experiments conducted in three different mouse models showed that *Listeria* colonized the TME efficiently if injected intraperitoneally (ip), but very poorly or not at all when injected intravenously (iv). **(a)** Balb/C mice were injected into the mammary fat pad with 4T1 tumor cells, resulting in primary tumors in the peritoneal membrane and multiple metastases in the liver, pancreas and along the GI, as described previously[1]. After tumors and metastases had developed, *Listeria* (10^7 CFU) was injected ip or iv, and the number of *Listeria* bacteria was determined 1, 3, or 4 days later in blood and all organs, including tumors and metastases, as done previously[2]. **(b)** A similar experiment in the Panc-02 mouse peritoneal cavity model. Panc-02 tumor cells were injected into the mammary fat pad of Panc-02 mice, resulting in a primary tumor in the peritoneal membrane and multiple metastases in the pancreas, liver and gastrointestinal tract, as described previously[3]. Ten days later, when primary tumor was palpable at the place of injection and metastases had developed, *Listeria*-TT was administered as above. CFU in the blood, tumors, metastases and normal tissue (spleen) were determined 3 days later as described previously[3]. **(c)** A similar experiment in the 4T1 model. Injection of 4T1 tumor cells into the mammary fat pad resulted in a primary mammary tumor and metastases in the lungs within 4 weeks, *Listeria*-TT was administered, and CFU measured 3 days later, as described previously[4]. In **a-c,** n=3 mice per timepoint and multiple tissues per organ/tumor/metastases have been analyzed.

SI Figure 2: Gating of CD4 and CD8 T cells in spleens of tumor-bearing Panc-02 mice treated with *Listeria*-TT and GEM, in combination or separately.

Examples of gating **(a)** the CD4 T cells and **(b)** CD8 T cells isolated from spleens of treated and control mice. CD3CD4-pos cells and CD3CD8-pos cells were gated, followed by

gating of CD4 or CD8 T cells producing IFNγ, Perforin, Granzyme B, or expressing CD69. A similar gating protocol was used to analyze CD4 and CD8 T cells in spleens of KPC mice.

LM-TT = *Listeria*-TT.

SI Figure 3: Detail of CD4 and CD8 T cells in tumors of *Listeria*-TT+GEM-treated and control mice.

KPC mice received treatment with *Listeria*-TT+GEM, or control treatments, as outlined in **Fig 1b.** Two days after the last treatment, tumor tissues were analyzed by IHC for the presence of CD4 **(a-d)** and CD8 **(e-h)** T cells. CD8, and particularly CD4 T cells, were predominantly observed in the tumor areas of KPC mice that received *Listeria*-TT or *Listeria*-TT+GEM.

LM-TT = *Listeria*-TT.

SI Figure 4: Detail of lymph node-like structures associated with pancreatic tumors in mice.

CD4 T cells **(a)** in tumor areas with TT **(b)** and CD31 **(c)** expression by IHC of KPC mice treated with *Listeria*-TT+GEM. Circles mark tumor areas. **(d)** Example of LNS in close proximity to a pancreatic tumor of a KPC mouse. In the overview of the lymphoid structure, there were well-developed follicular structures, many of which contained a pale germinal area at the center. CD4+ T cells were concentrated in the cortex and in the deep cortical zone/paracortex, where they were arranged in sheets rather than follicles. CD8+ T cells were concentrated within the deep cortical zone/paracortex. Below are views of the lymphoid structure at higher magnification, to visualize the density of CD4+ and CD8+ T cells. CD4+ cells were located mostly within the cortex, surrounding and within the follicles, and in the paracortex. CD8+ cells were primarily within the paracortex. **(e)** Production of

Granzyme B and Perforin in LNS of KPC mice treated with saline, GEM, *Listeria*-TT, or *Listeria*-TT+GEM, detected by IHC.

LM-TT = *Listeria*-TT.

SI Figure 5: Effect of LM-TT+GEM treatment on expression of genes involved in T cell migration, efficacy and safety

(a) Detection of chemokines and their receptors in pancreatic tumors of *Listeria* TT+GEM-treated or untreated KPC mice by RNAseq. Results of 2 mice are shown in each group. Log2-fold increase in the group of *Listeria*-TT+GEM compared to the untreated mice. The heatmap was generated by unbiased hieratical clustering at the following statistical parameters. Statistical parameters for the paired-wise comparison: $p<0.05$. **(b)** LM-TT+GEM testing in the Panc-02 mouse peritoneal cavity model of early pancreatic cancer. C57Bl6 mice were immunized twice with Tetanus vaccine, and challenged one week later with Panc-02 tumor cells in the mammary fat pad as described previously[3]. Treatments began three days after tumor cell injection. Mice were euthanized after treatment, and analyzed for tumor weight and the number of metastases. Two independent experiments with 5 mice per group were averaged. Error bars represent standard error of the mean. Mann-Whitney *$p<0.05$, *** $p<0.01$. **(c)** Dose-limiting toxicity study of *Listeria*-TT in tumor-naive C57Bl6 mice (n=5 mice per group).

SI Figure 6: Flow cytometry demonstration of MDSC and TAM in metastases of tumor-bearing Panc-02 mice.

(a) Example of gating of MDSC cells present in metastases of treated and control mice. First, live cells were gated. Subsequently, CD11bGr1-pos cells (MDSC) were gated in the live cell population, followed by the gating of Gr1-pos cells producing IL-10, IL-6, TNFα,

or expressing MARCO or CD80 as indicated in the figure. **(b)** Example of gating TAMs present in metastases of treated and control mice. First, CD45+ leukocytes were gated to exclude tumor cells, followed by gating of CD11bF4/80-pos cells, followed by F4/80-pos cells producing IL-10, IL-6, TNFα, or expressing MARCO or CD80.

REFERENCES

1. Kim, S.H.*, et al.* Mage-b vaccine delivered by recombinant Listeria monocytogenes is highly effective against breast cancer metastases. *British journal of cancer* **99**, 741-749 (2008).
2. Chandra, D.*, et al.* 32-Phosphorus selectively delivered by listeria to pancreatic cancer demonstrates a strong therapeutic effect. *Oncotarget* **8**, 20729-20740 (2017).
3. Quispe-Tintaya, W.*, et al.* Nontoxic radioactive Listeria(at) is a highly effective therapy against metastatic pancreatic cancer. *Proc Natl Acad Sci U S A* **110**, 8668-8673 (2013).
4. Chandra, D.*, et al.* Cryoablation and Meriva have strong therapeutic effect on triple-negative breast cancer. *Oncoimmunology* **5**, e1049802 (2016).

SI Figure 1

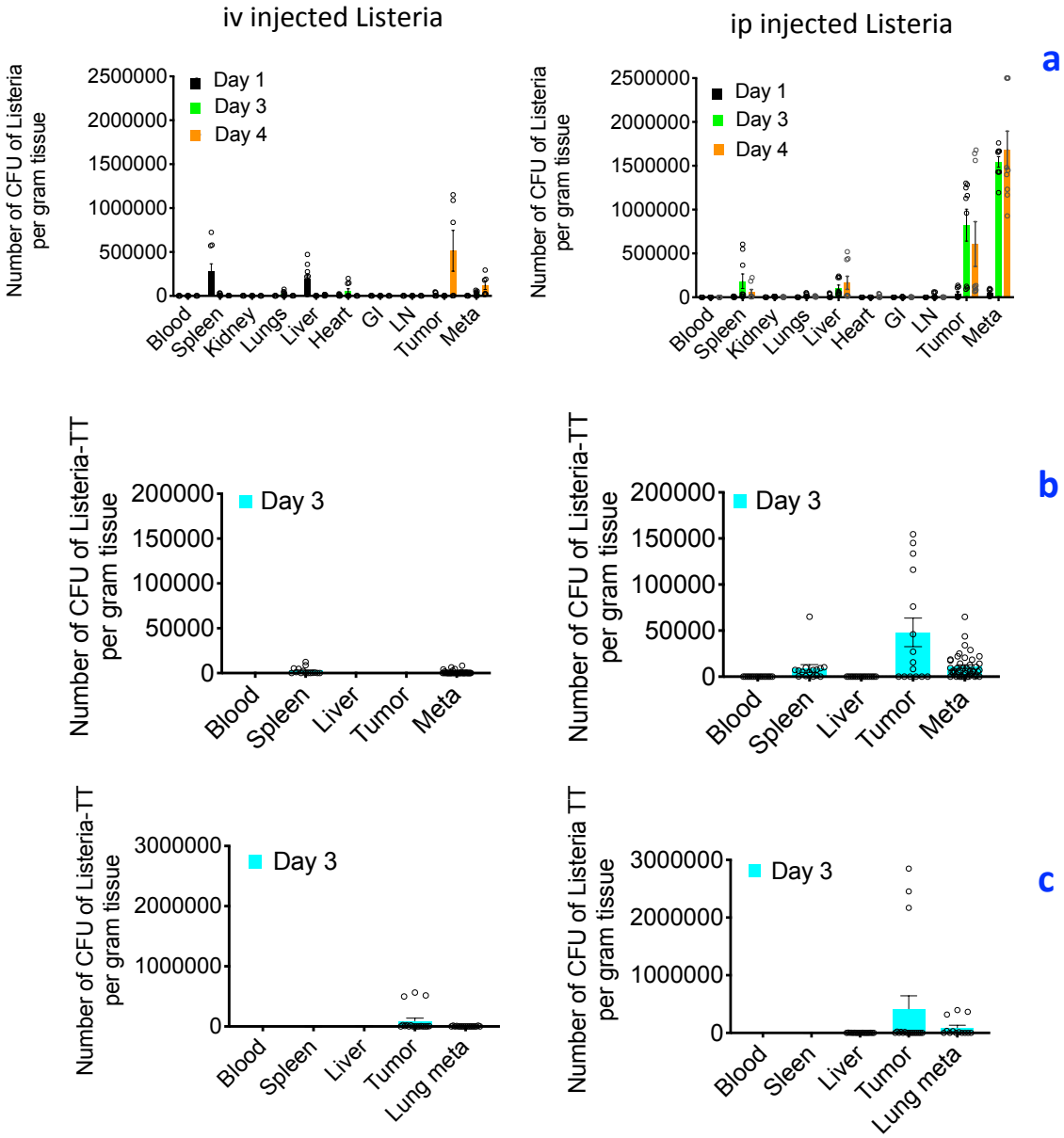
iv injected Listeria
ip injected Listeria
a
Number of CFU of Listeria per gram tissue
Day 1
Day 3
Day 4
2500000
2000000
1500000
1000000
500000
0
Blood
Spleen
Kidney
Lungs
Liver
Heart
GI
LN
Tumor
Meta
b
Number of CFU of Listeria-TT per gram tissue
Day 3
200000
150000
100000
50000
0
Blood
Spleen
Liver
Tumor
Meta
c
Number of CFU of Listeria-TT per gram tissue
Number of CFU of Listeria TT per gram tissue
Day 3
3000000
2000000
1000000
0
Blood
Spleen
Sleen
Liver
Tumor
Lung meta

SI Figure 2a

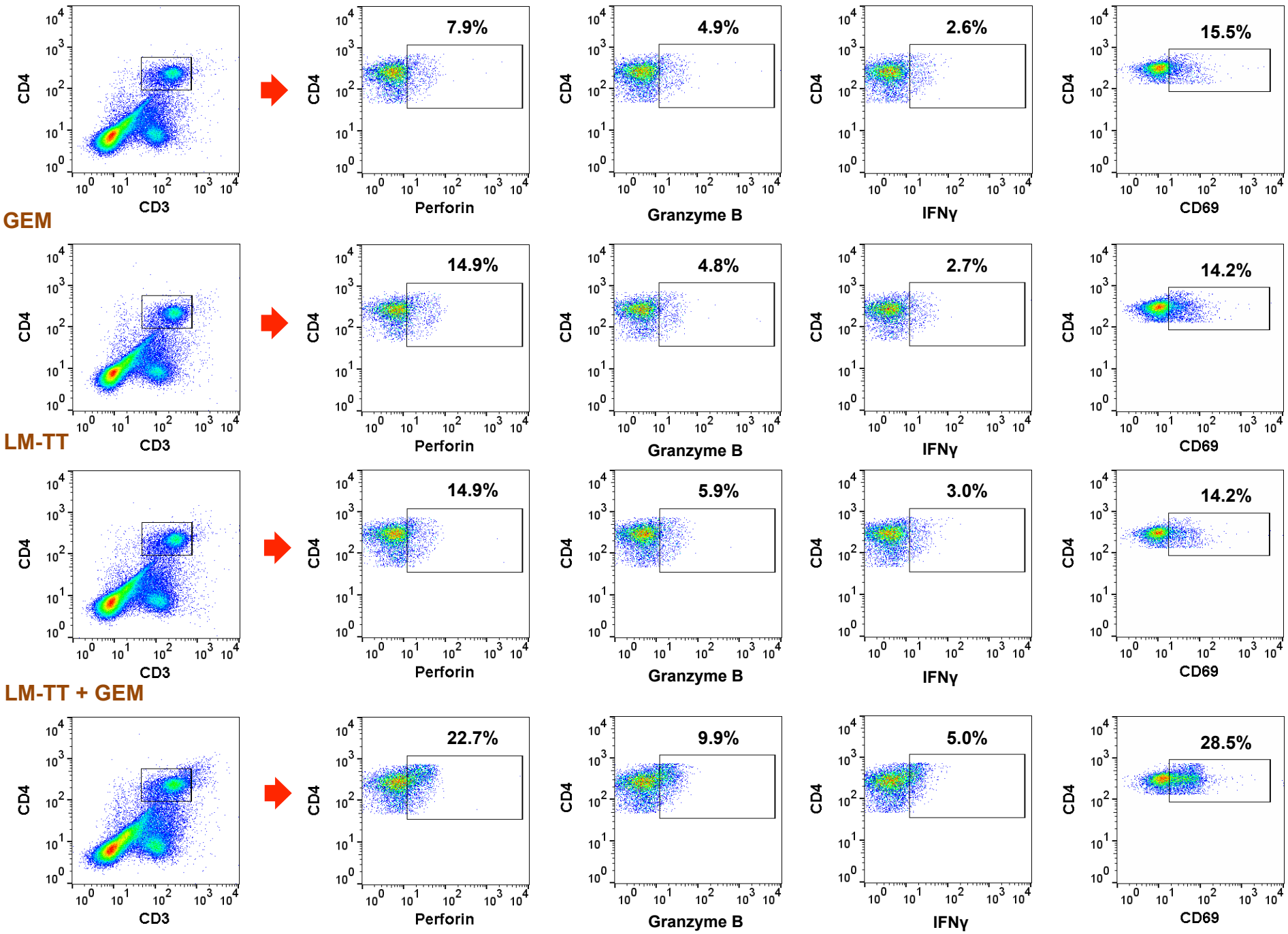
Saline
GEM
LM-TT
LM-TT + GEM
CD4
CD3
Perforin
Granzyme B
IFNγ
CD69
7.9%
4.9%
2.6%
15.5%
14.9%
4.8%
2.7%
14.2%
14.9%
5.9%
3.0%
14.2%
22.7%
9.9%
5.0%
28.5%

SI Figure 2b

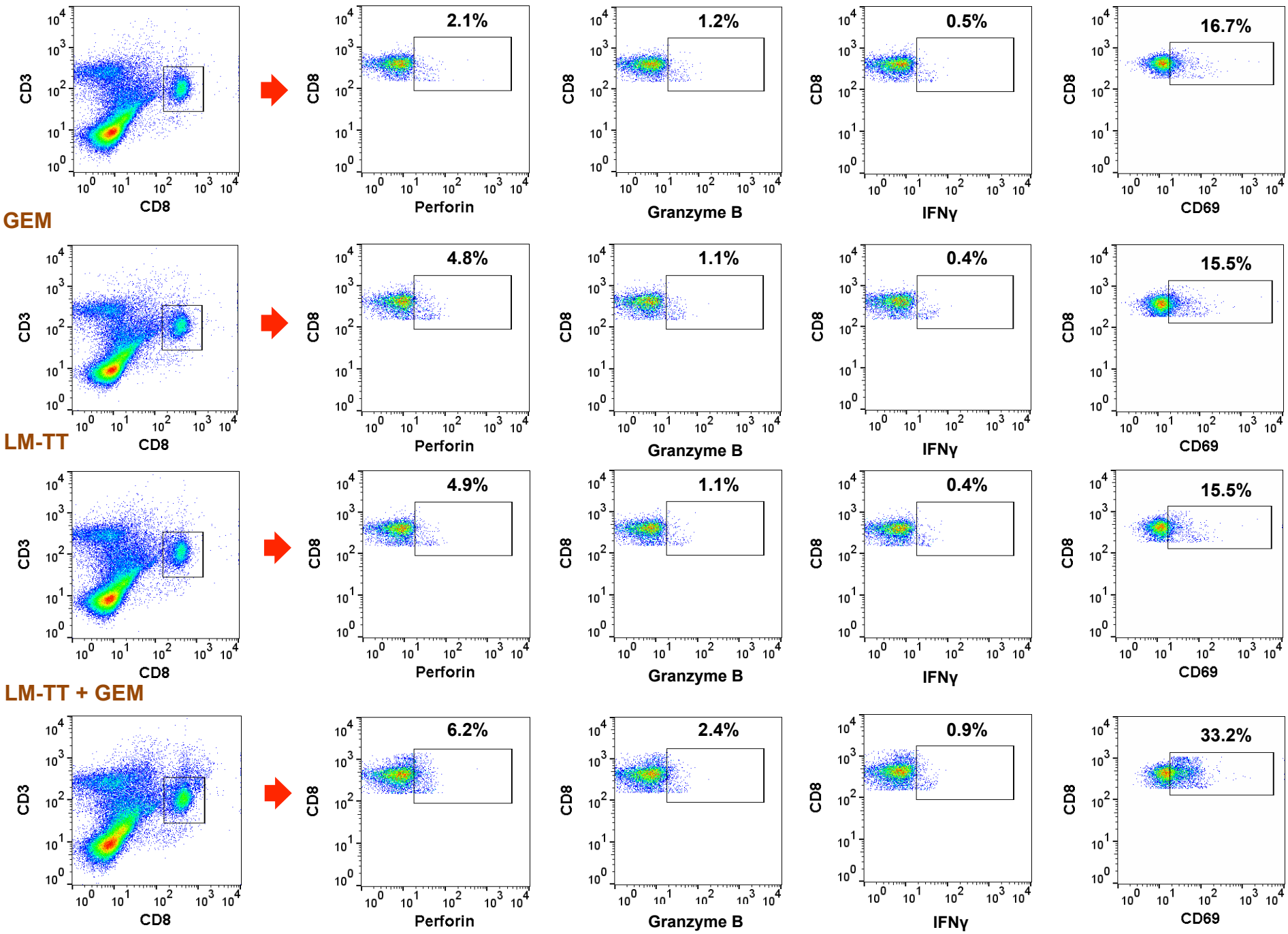
Saline
GEM
LM-TT
LM-TT + GEM
CD3
CD8
Perforin
Granzyme B
IFNγ
CD69
2.1%
1.2%
0.5%
16.7%
4.8%
1.1%
0.4%
15.5%
4.9%
1.1%
0.4%
15.5%
6.2%
2.4%
0.9%
33.2%

Saline
CD4

SI Figure 3a

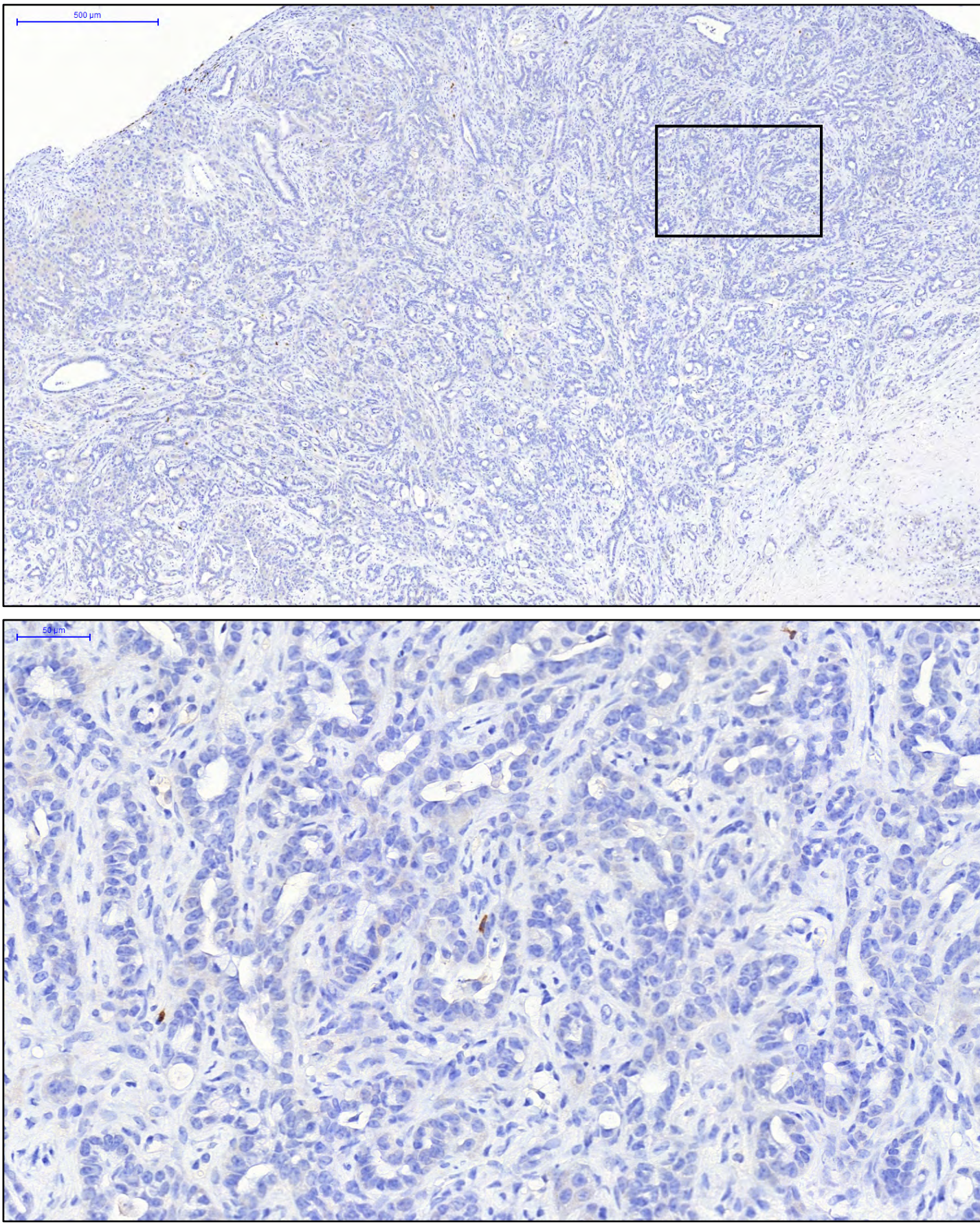

SI Figure 3b

GEM
CD4

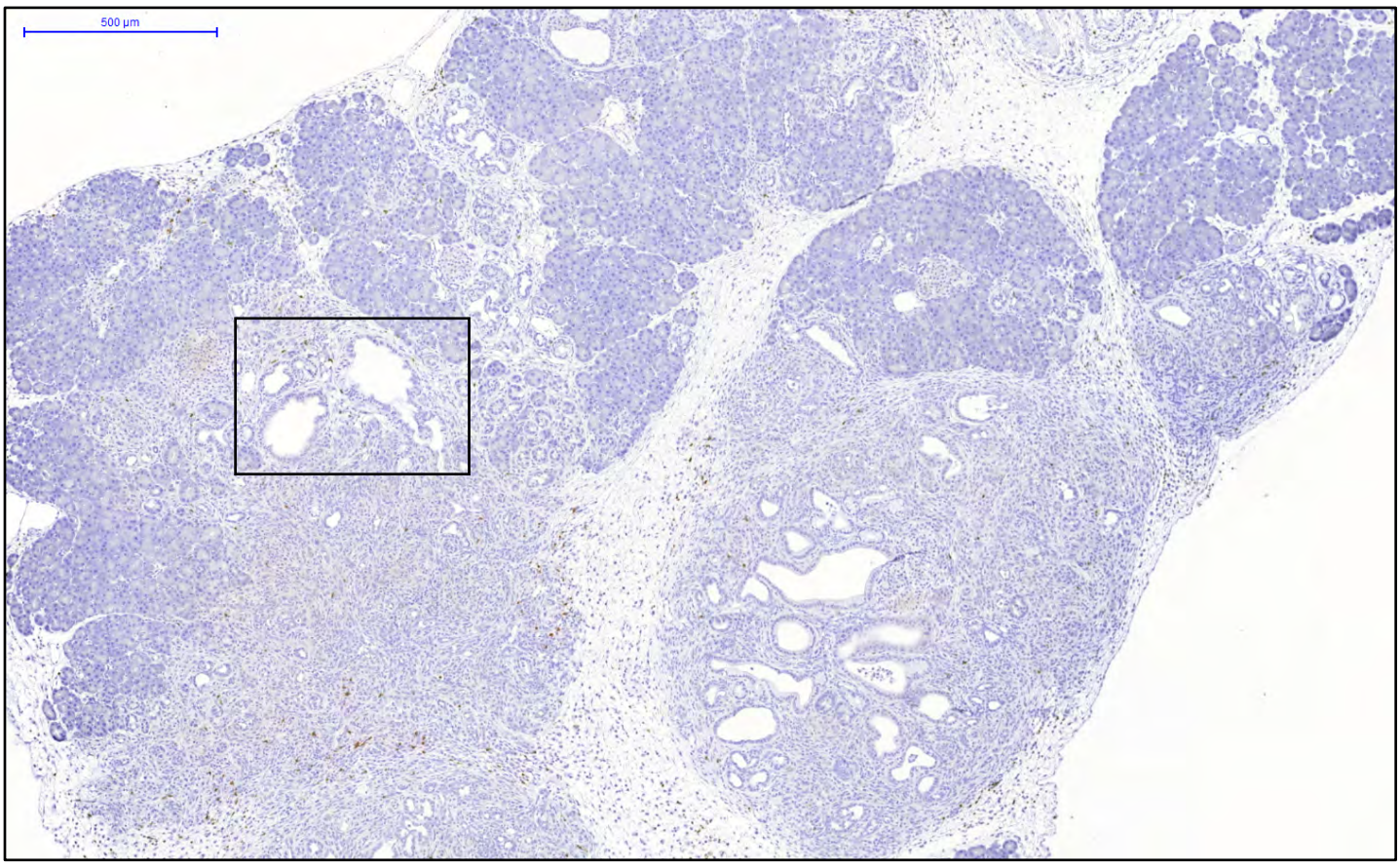

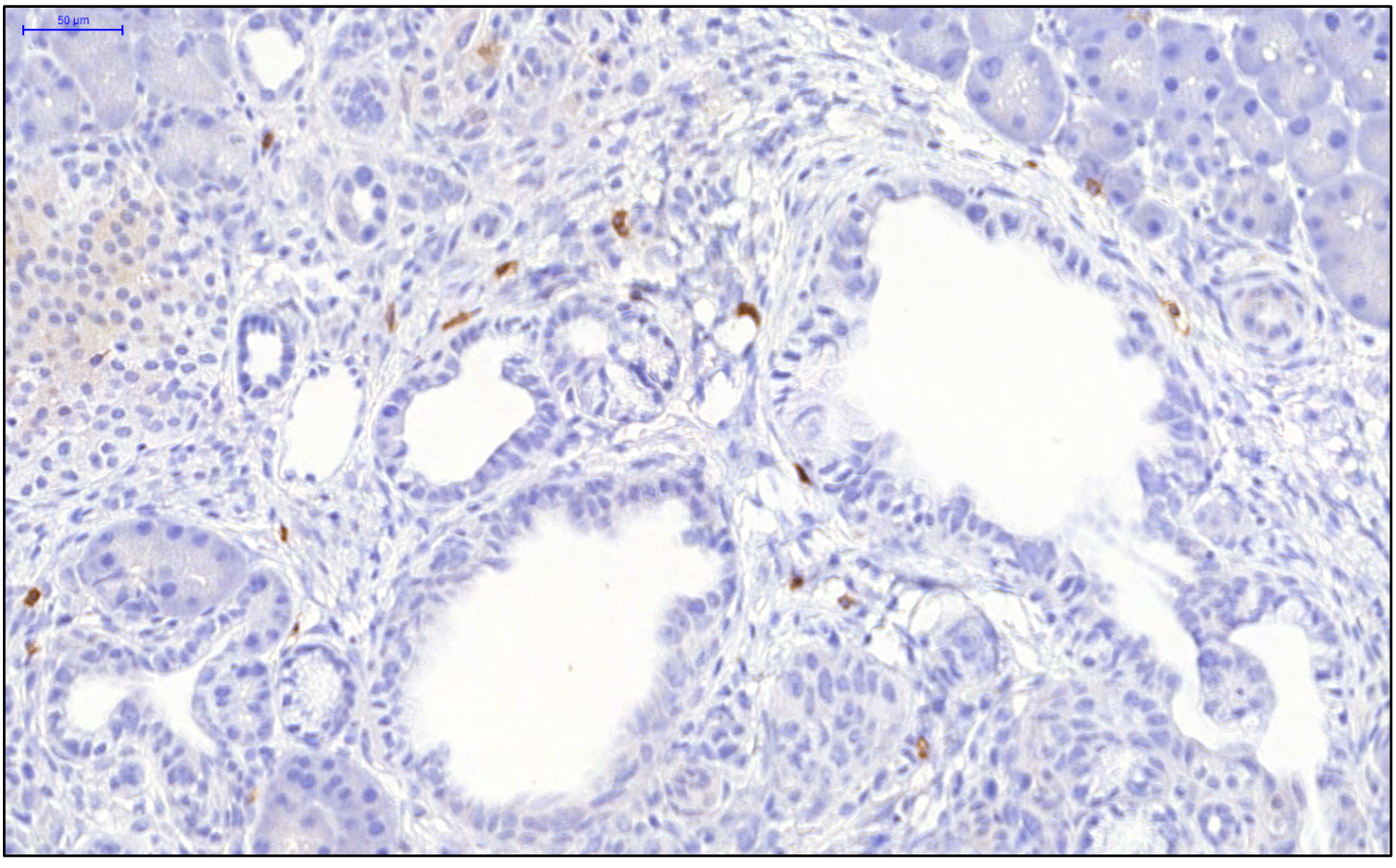

LM-TT
CD4

SI Figure 3c

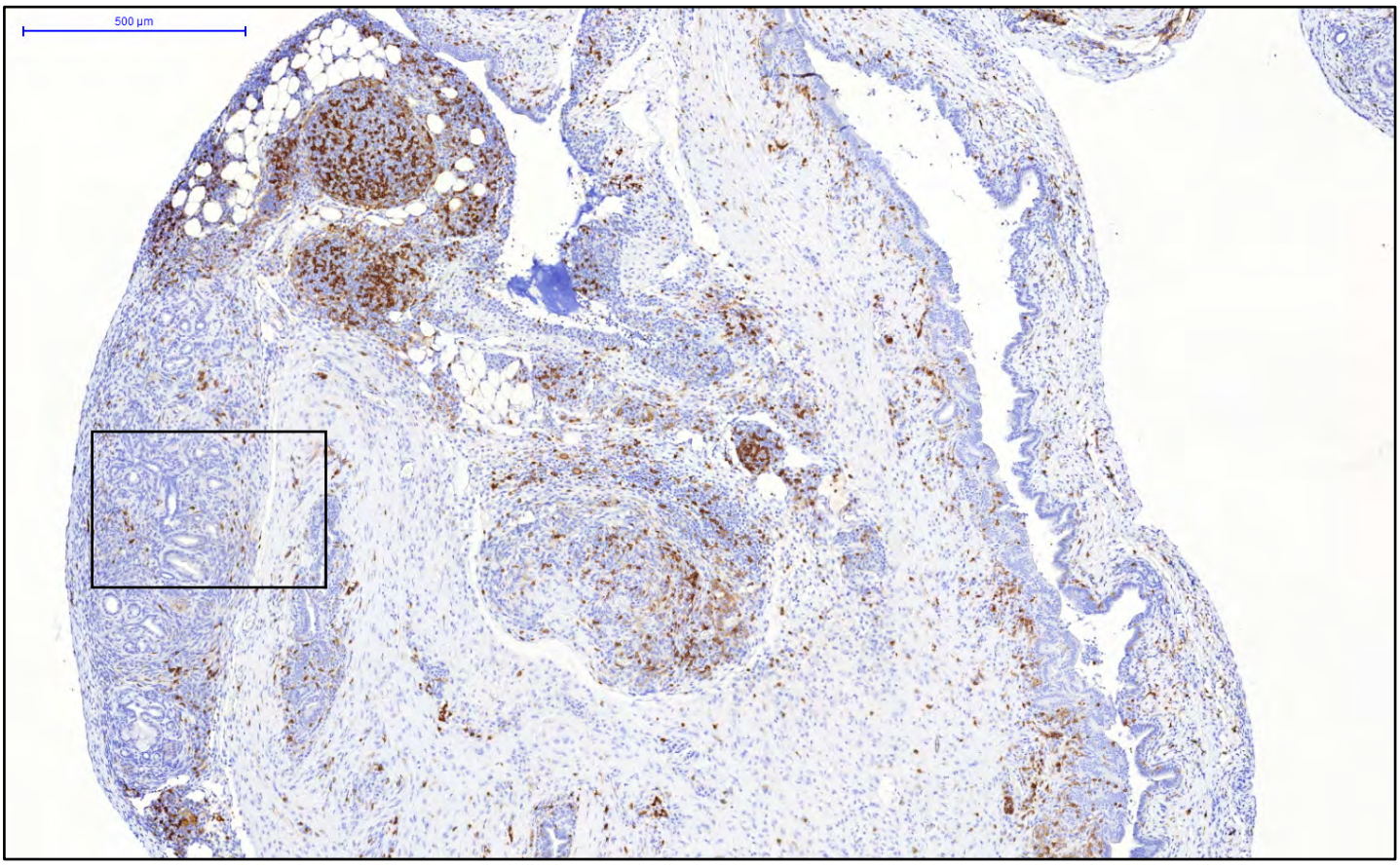

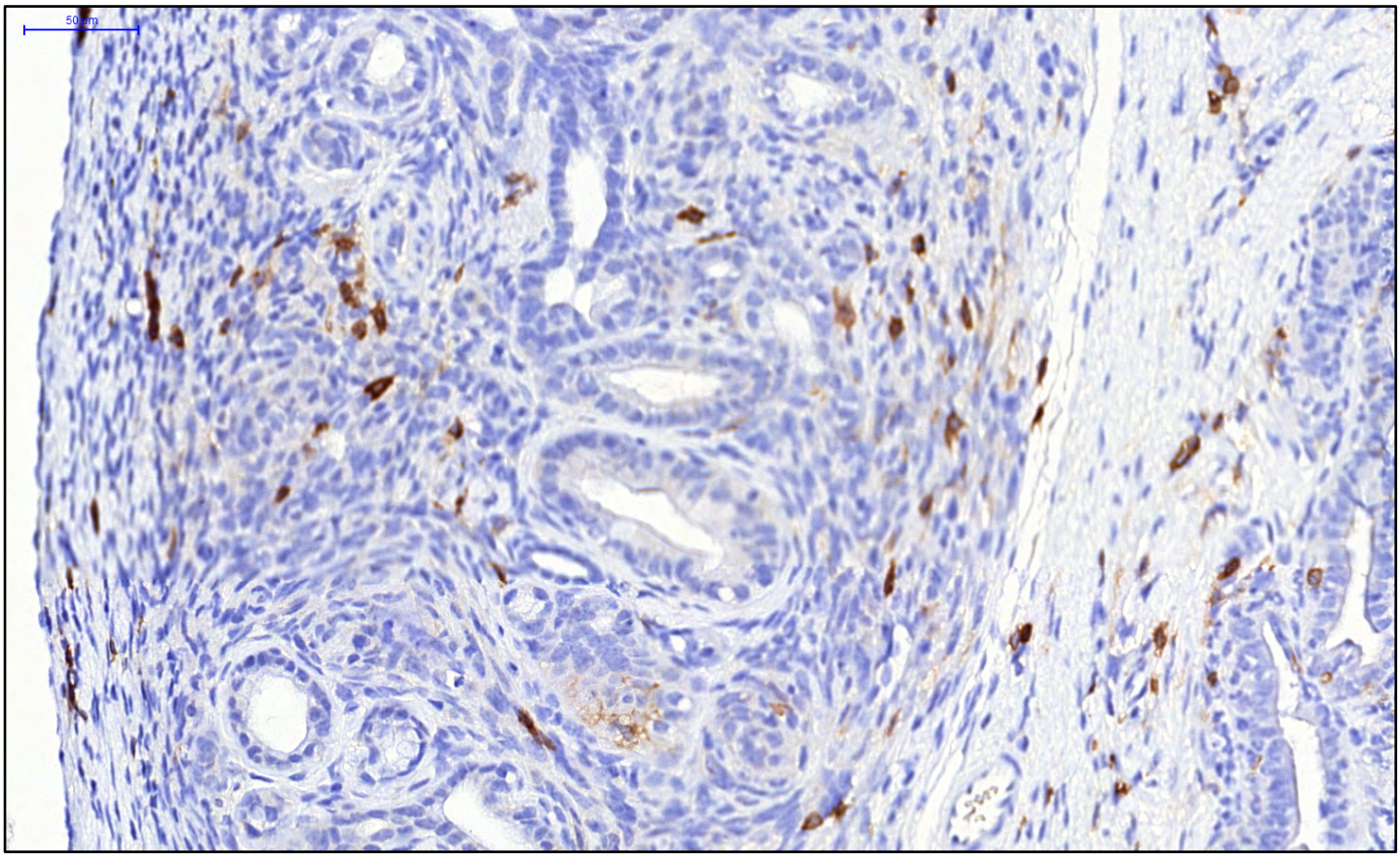

LM-TT+GEM
CD4

SI Figure 3d

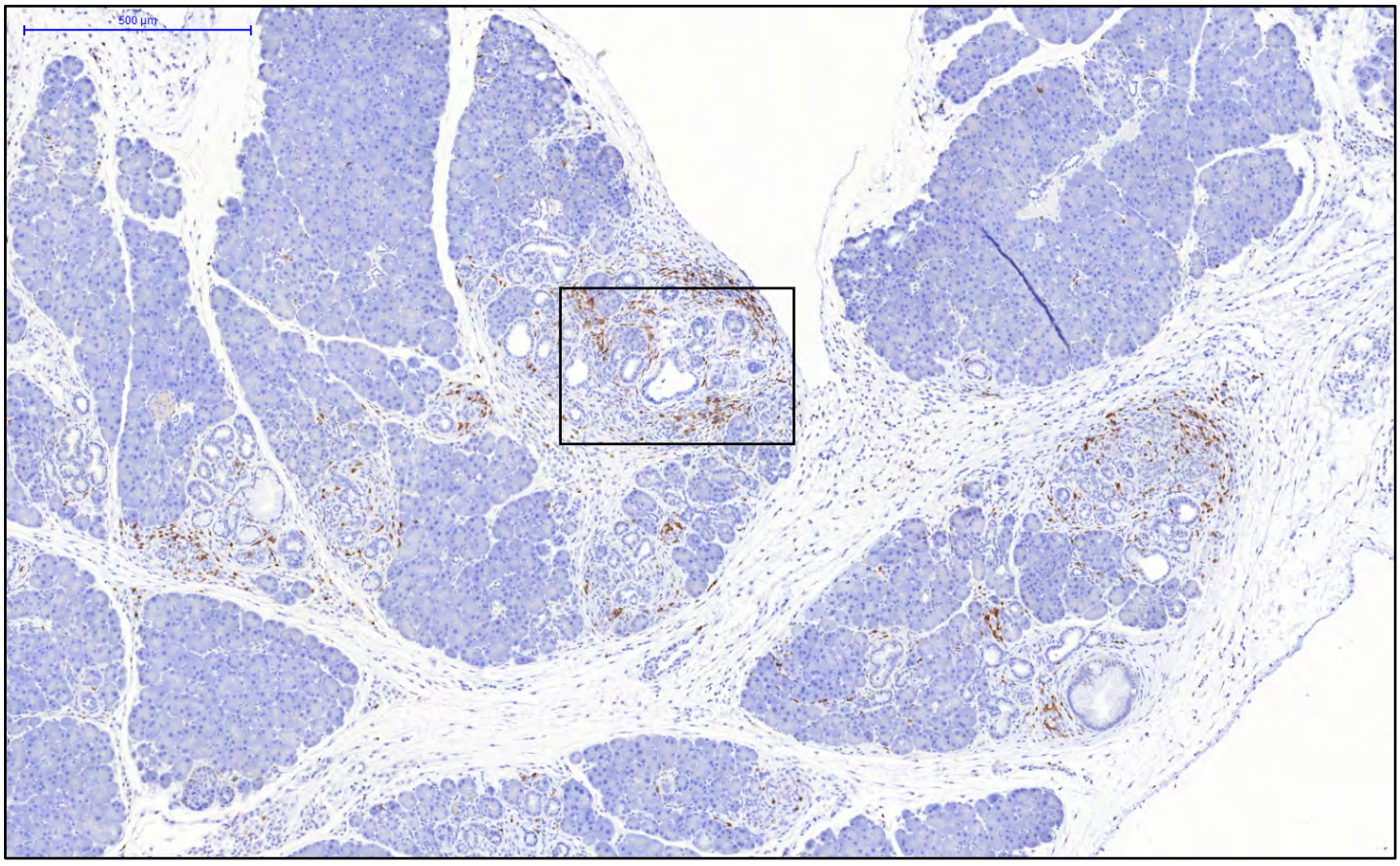

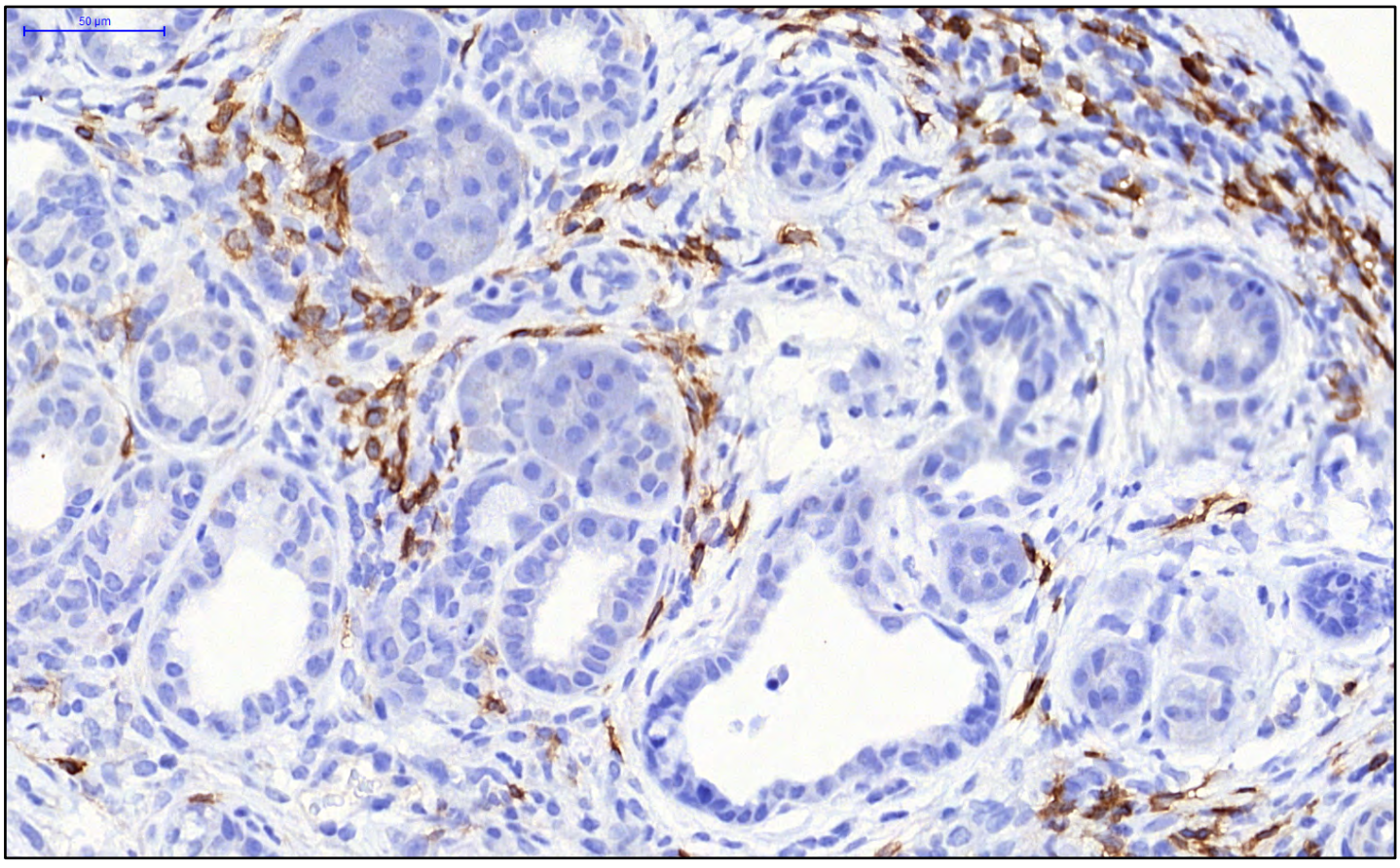

Saline
CD8

SI Figure 3e

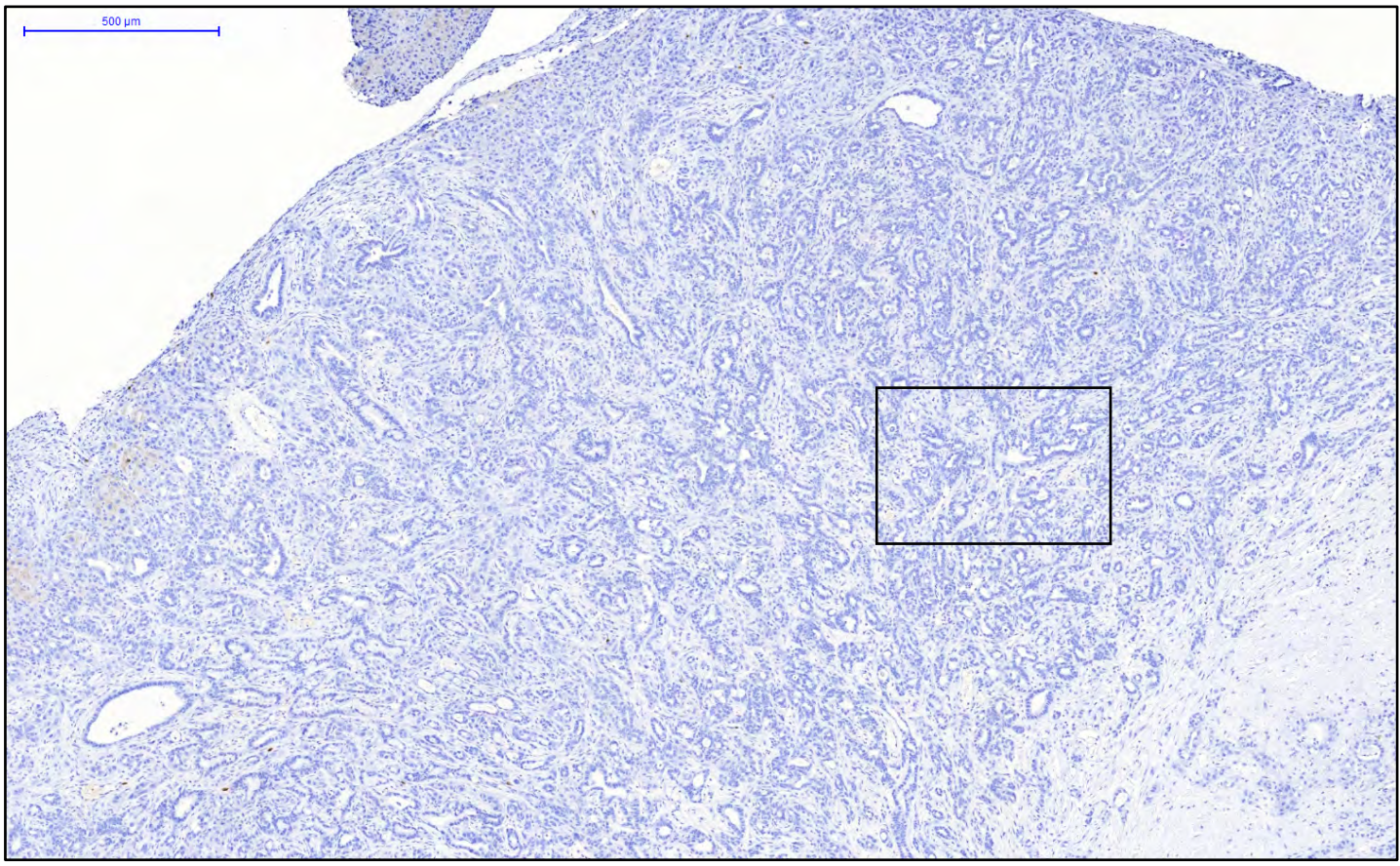

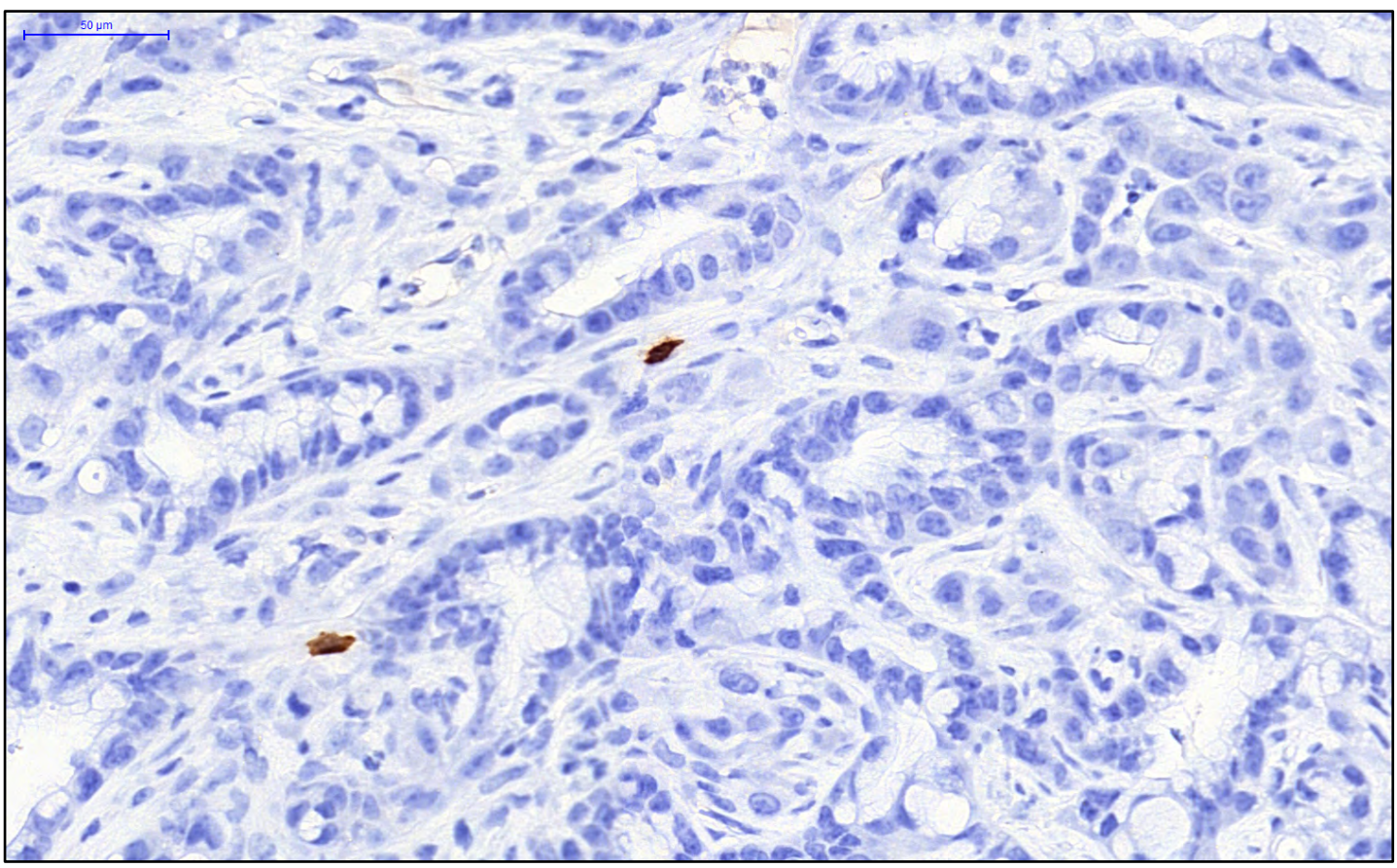

SI Figure 3f

GEM
CD8

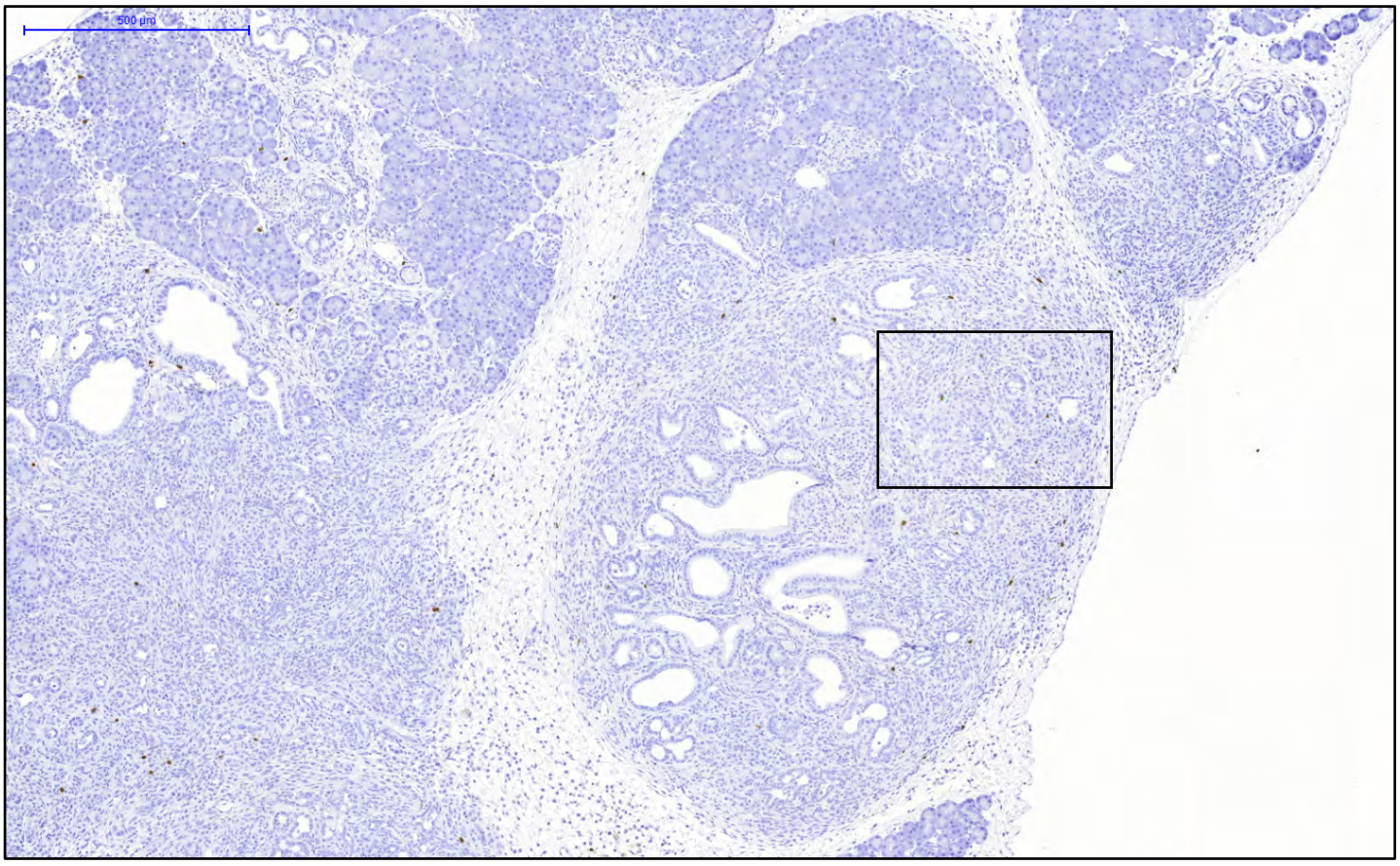

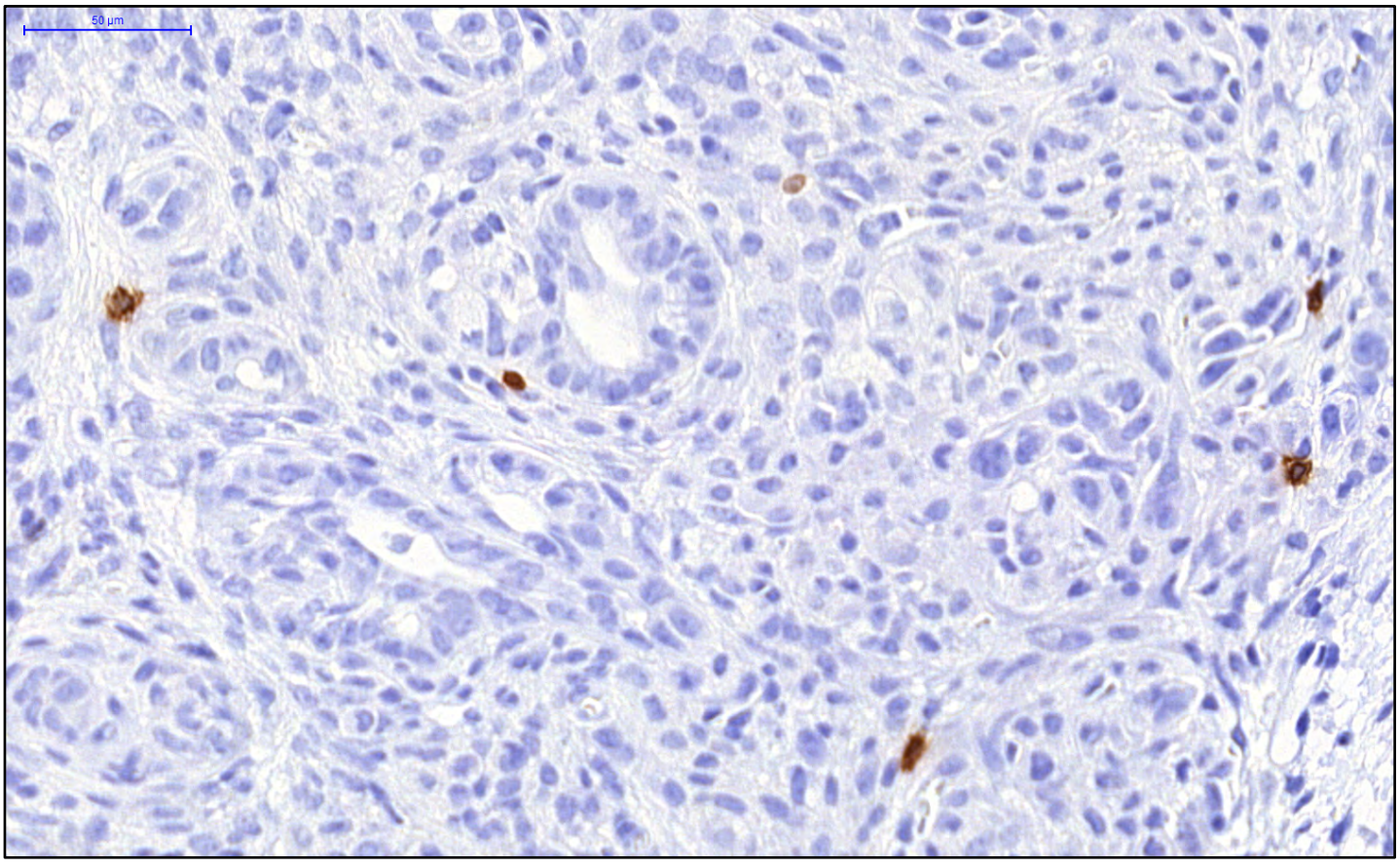

SI Figure 3g

LM-TT
CD8

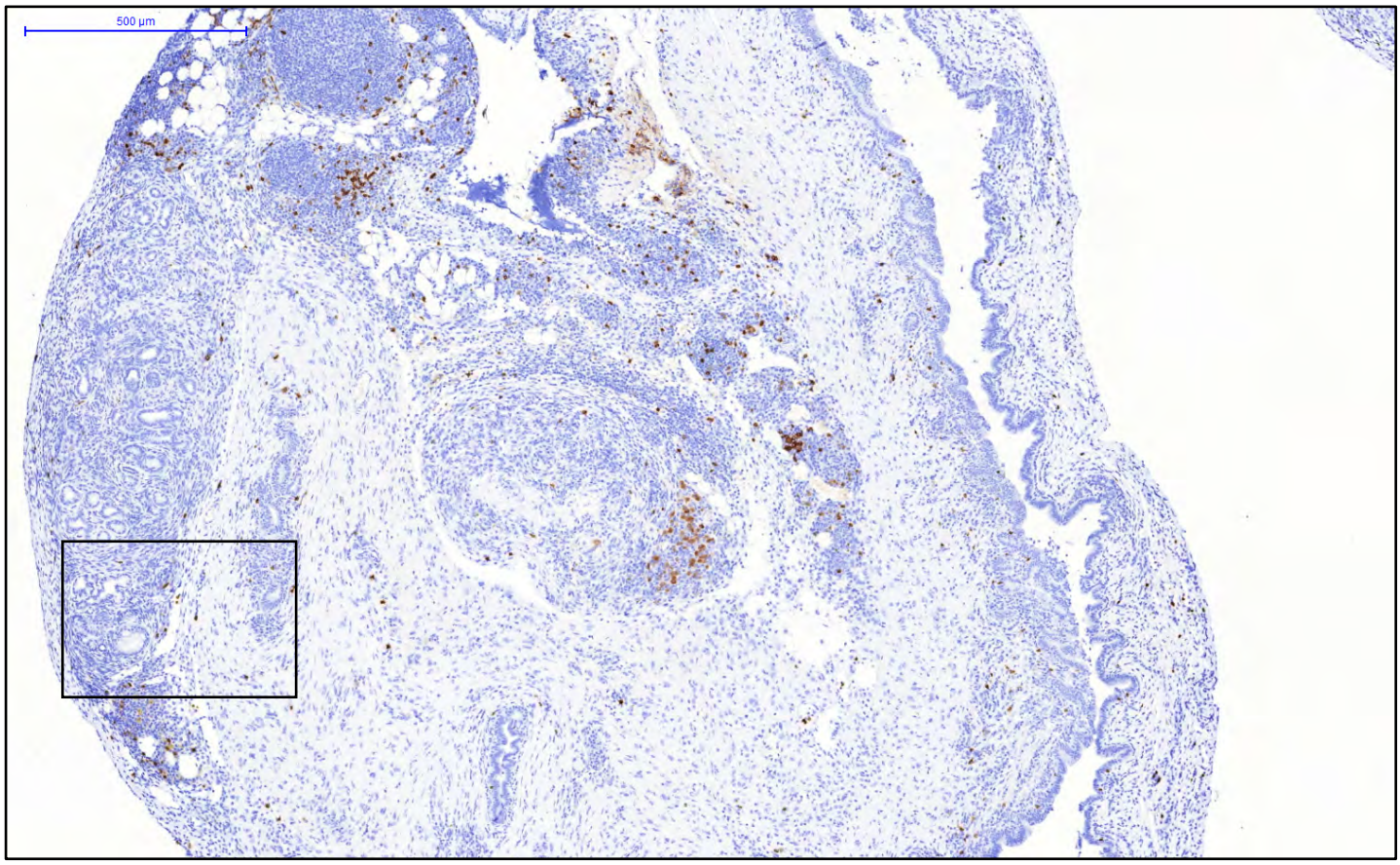

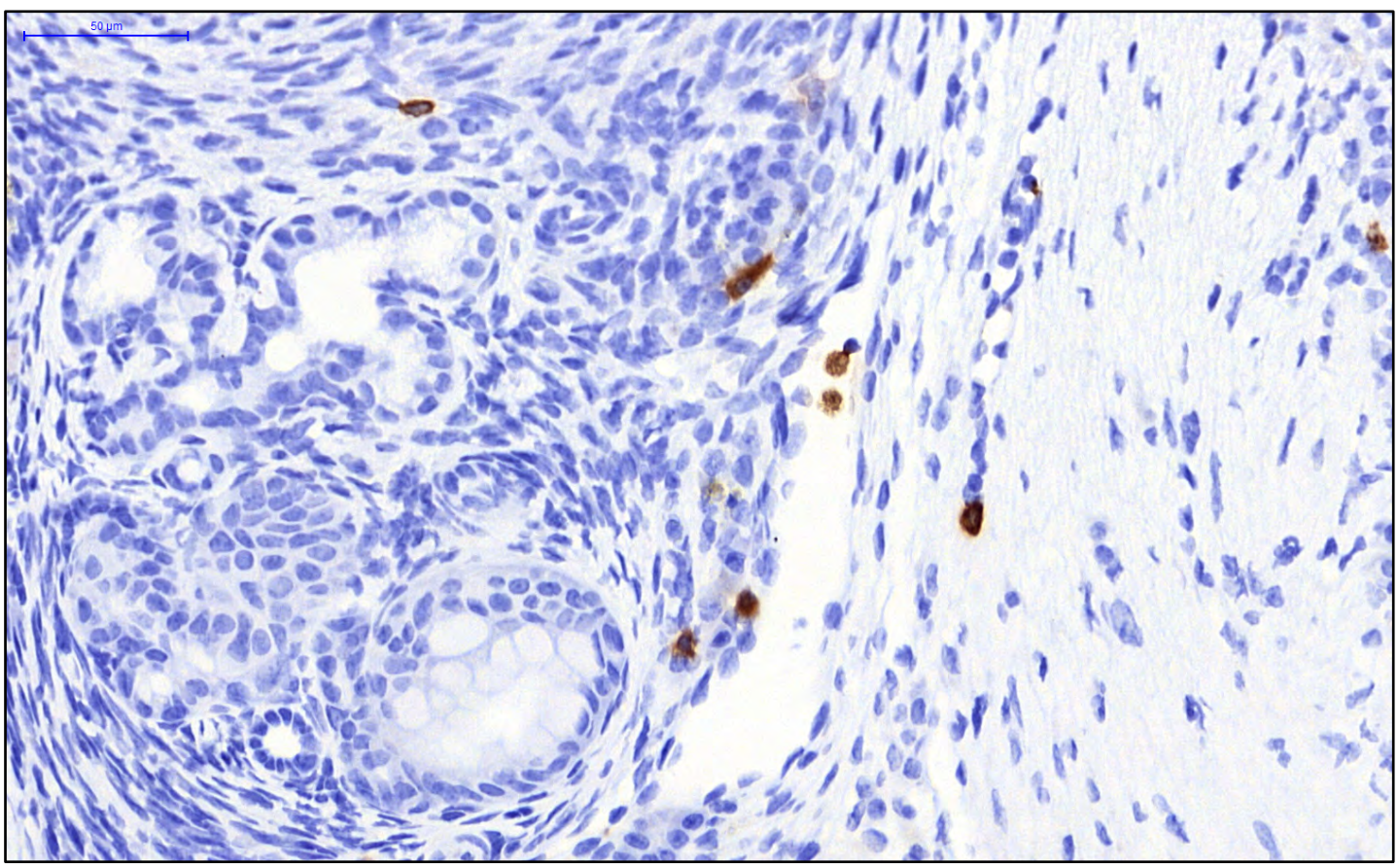

LM-TT+GEM
CD8

SI Figure 3h

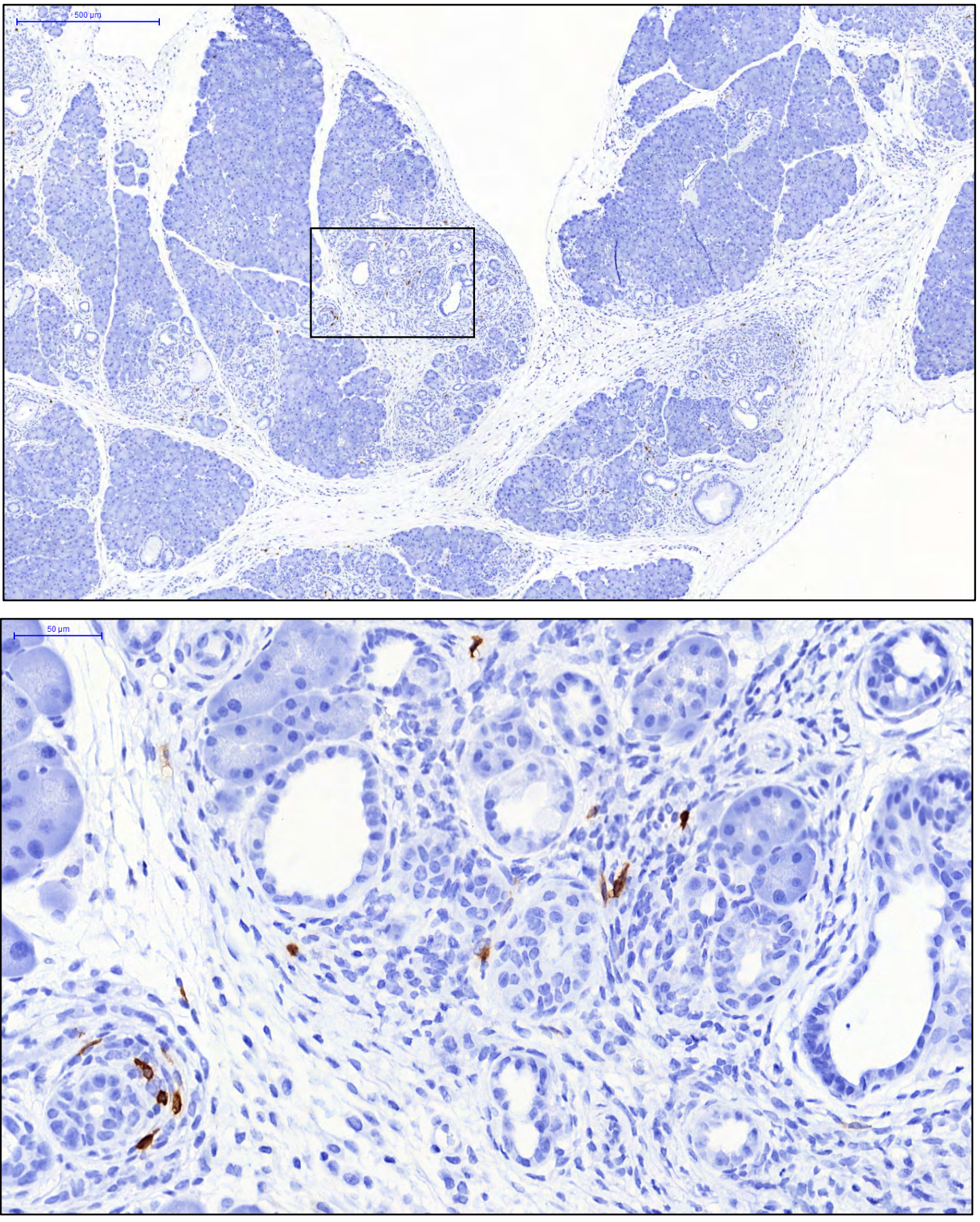

SI Figure 4abc

a

CD4-staining

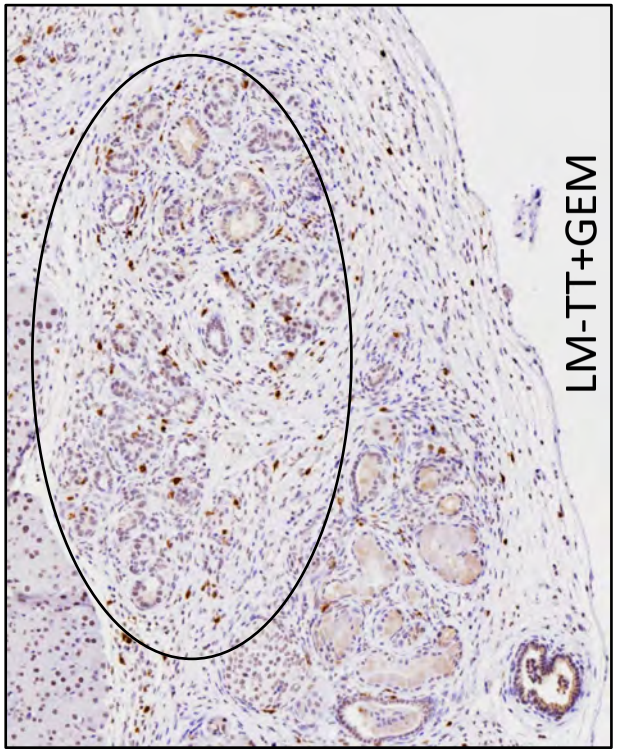

b

TT-staining

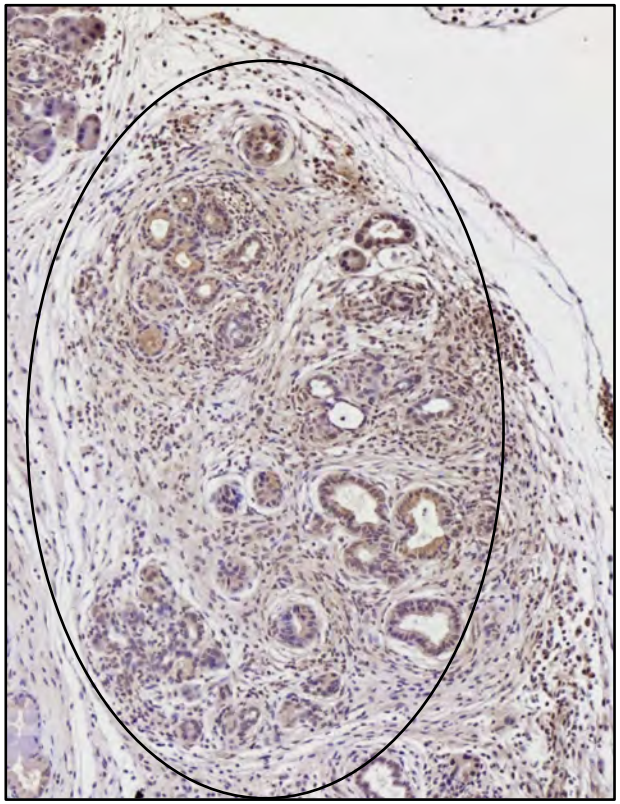

c

CD31 staining

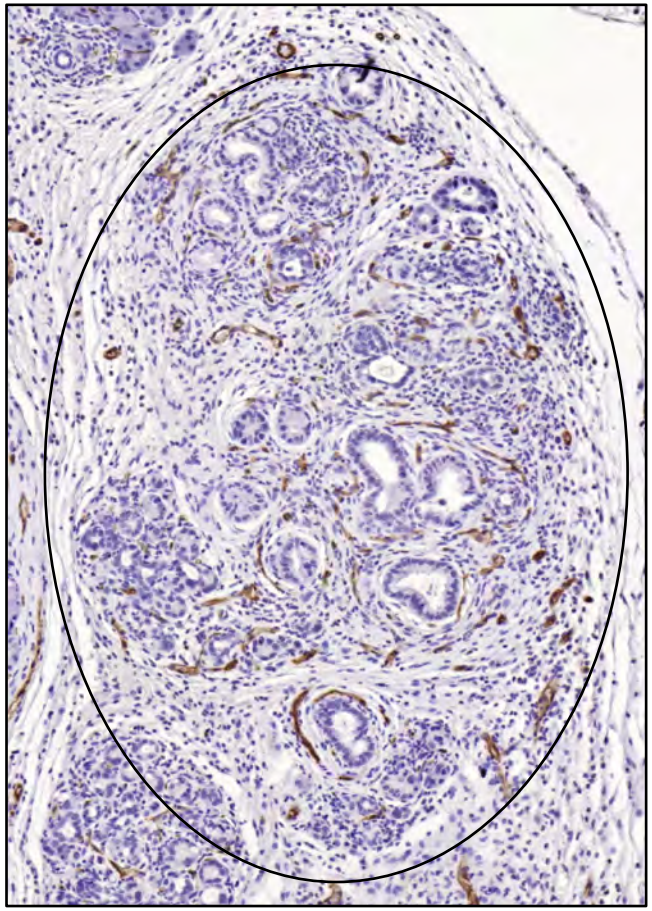

SI Figure 4d

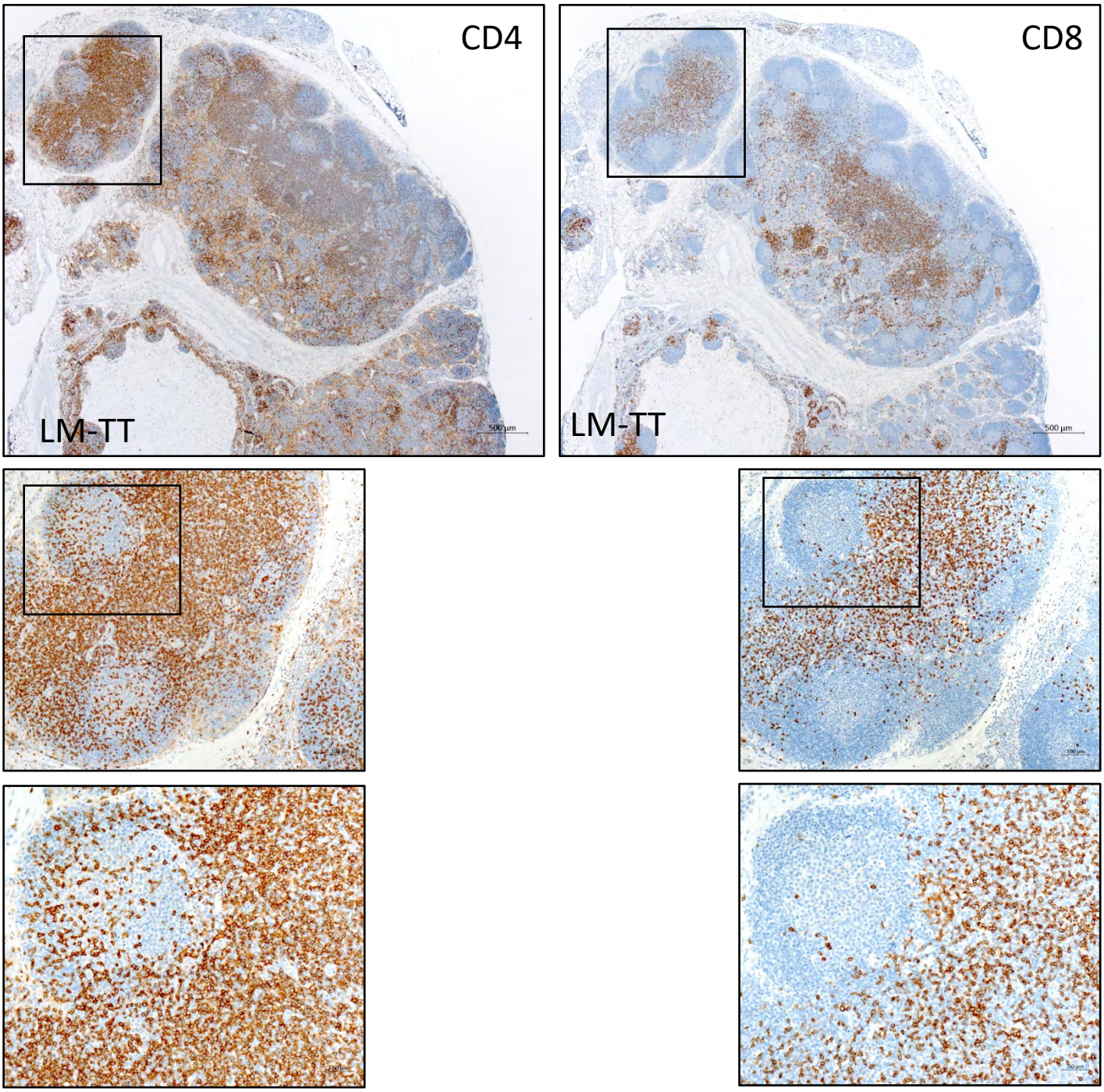

SI Figure 4e

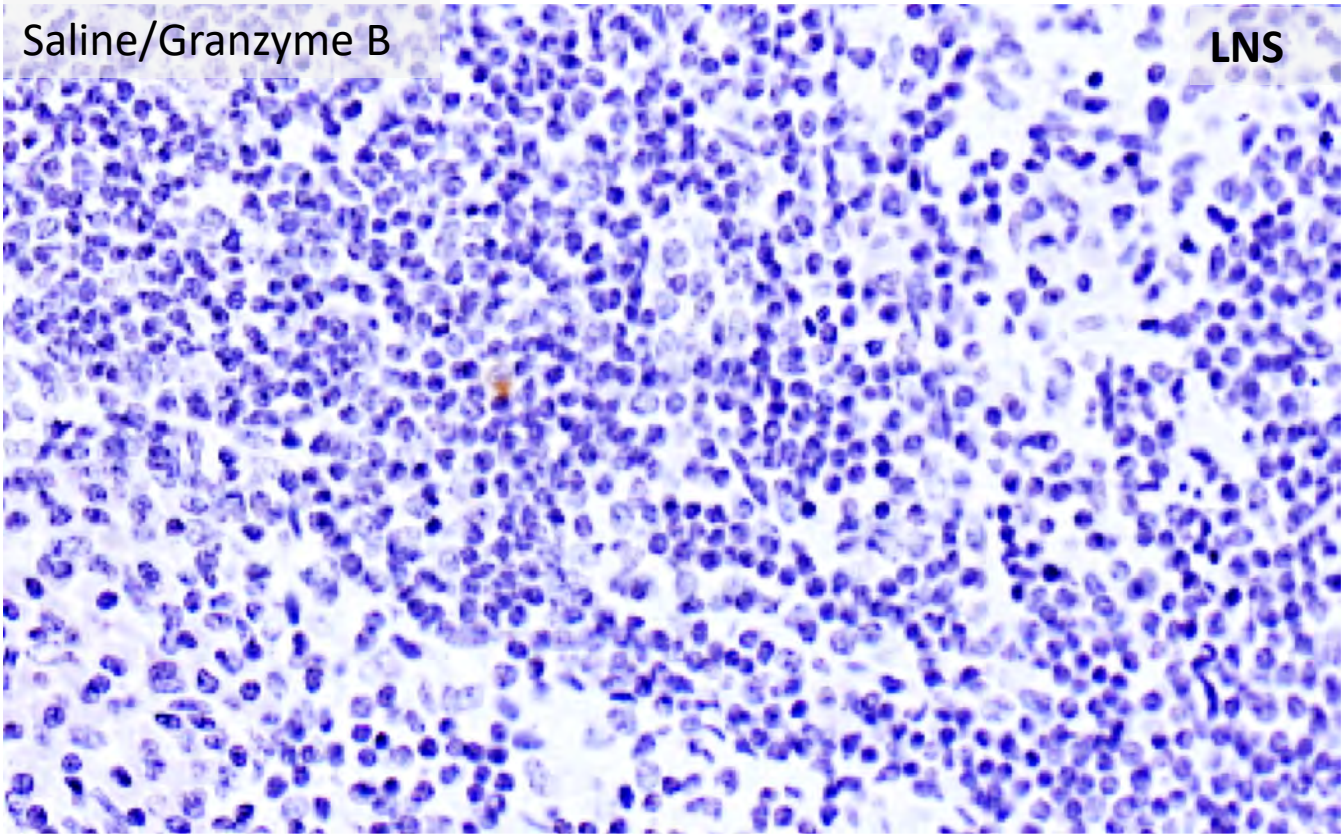

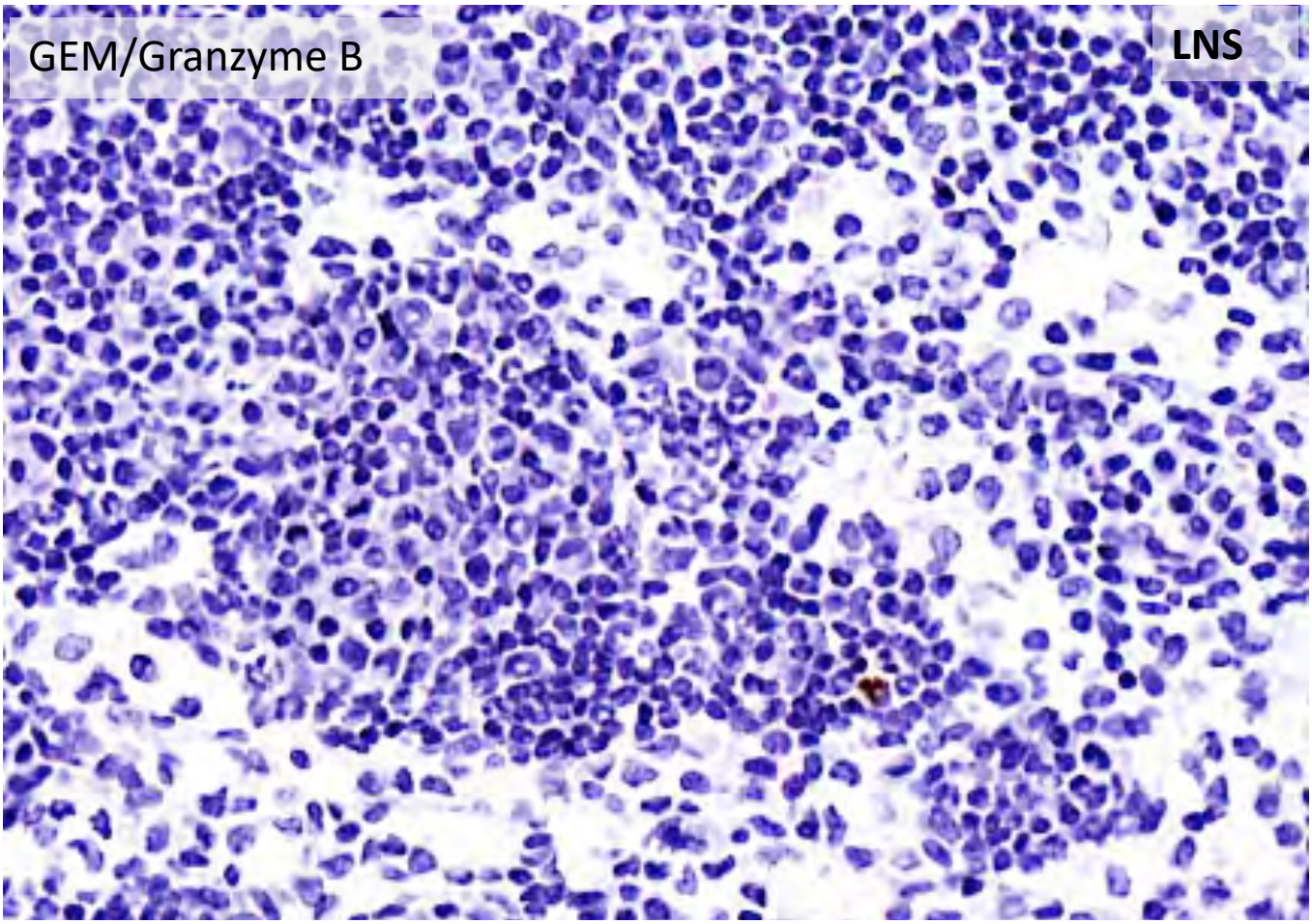

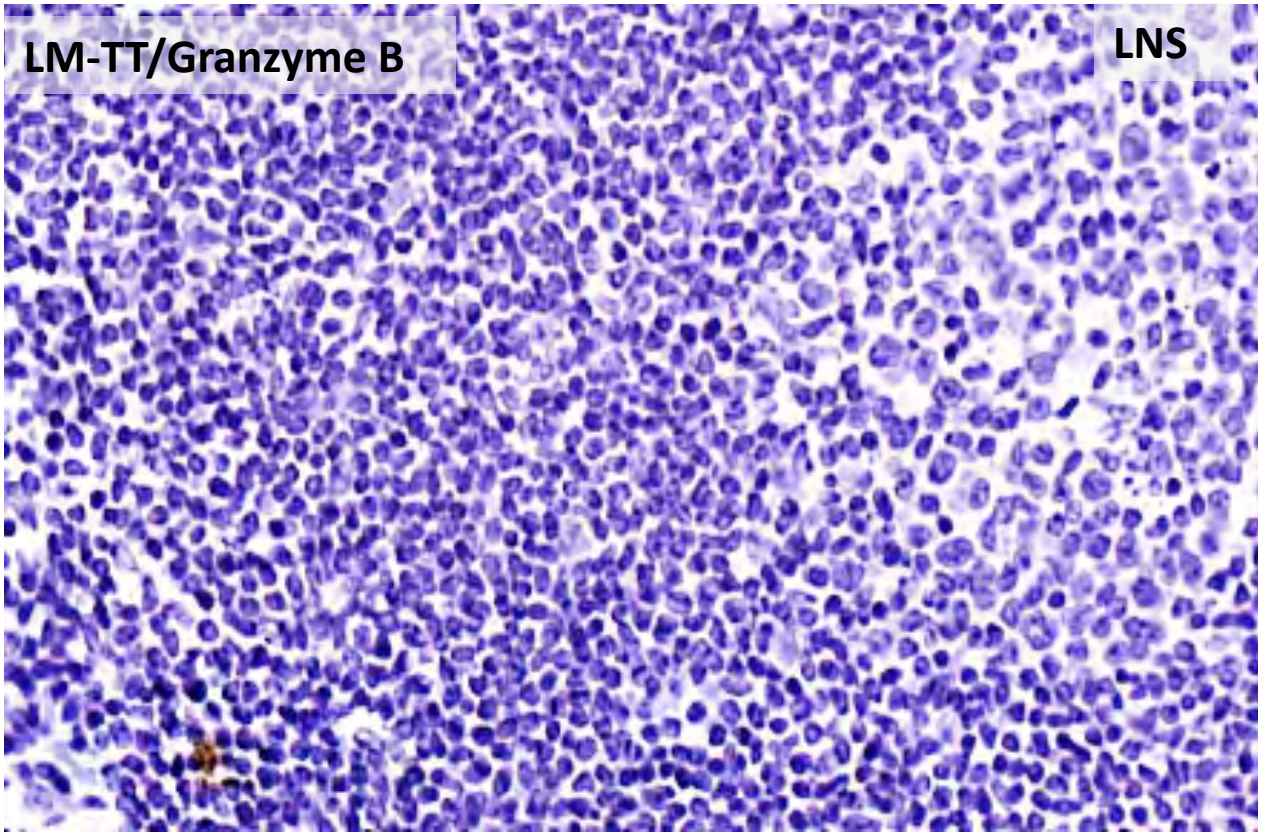
LM-TT/Granzyme B
LNS

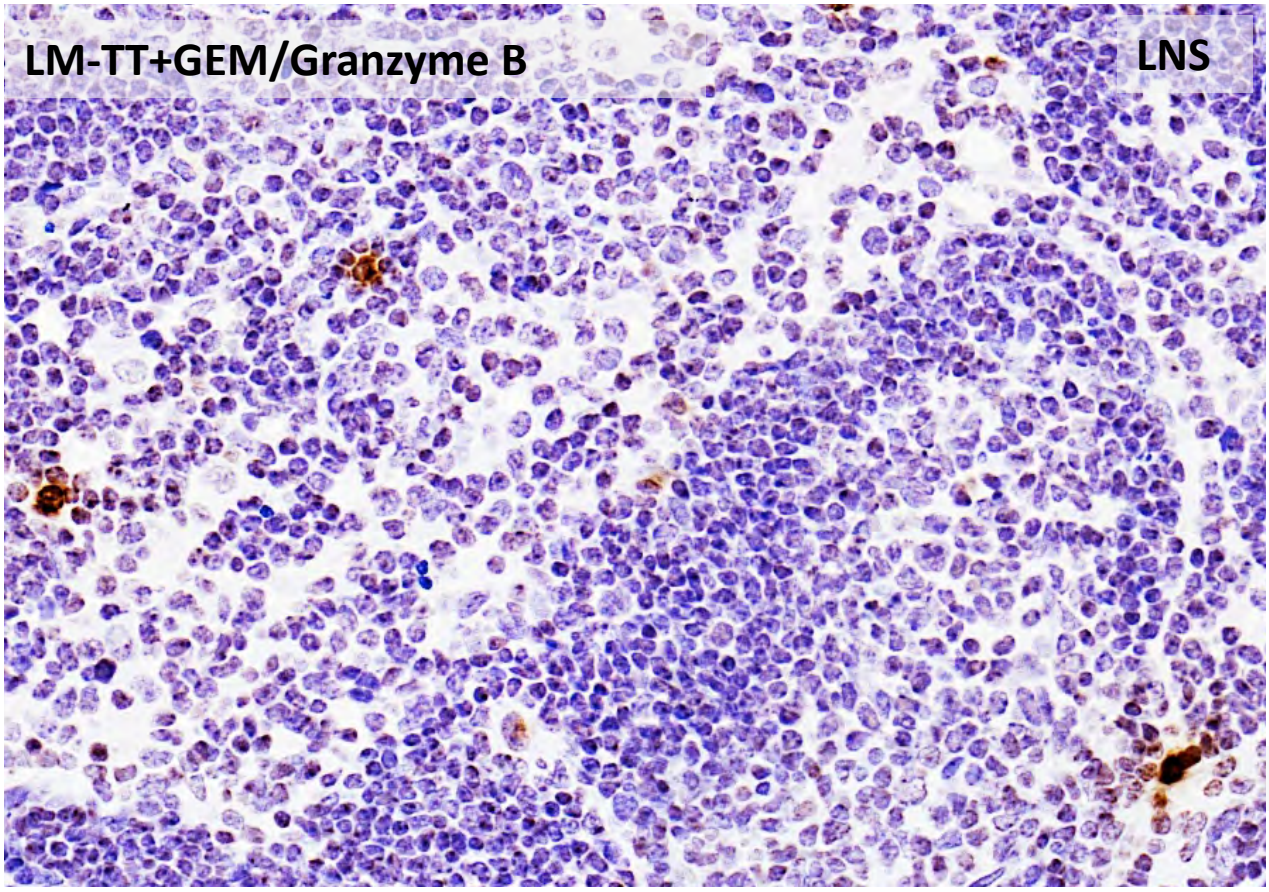
LM-TT+GEM/Granzyme B
LNS

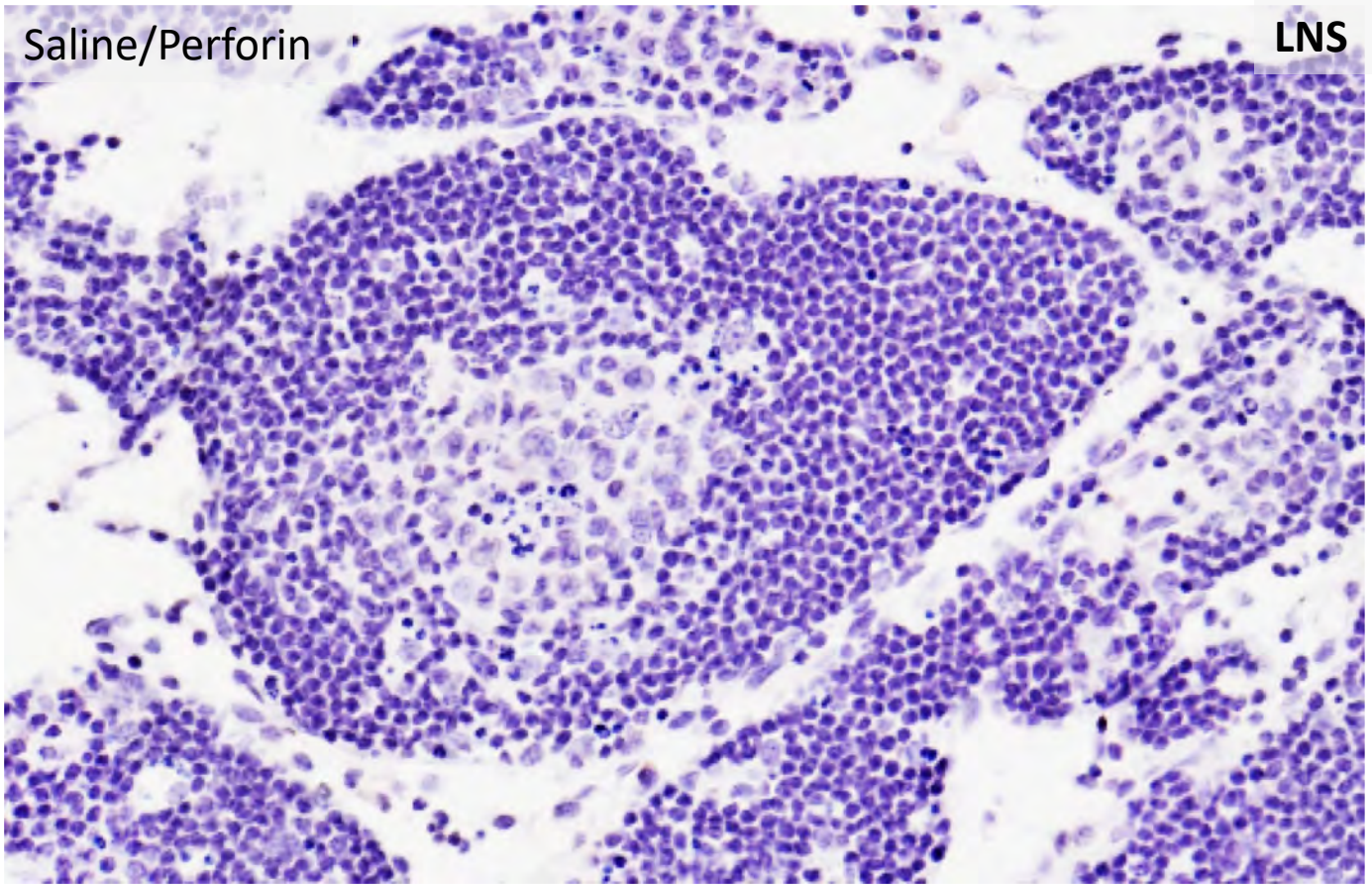
Saline/Perforin
LNS

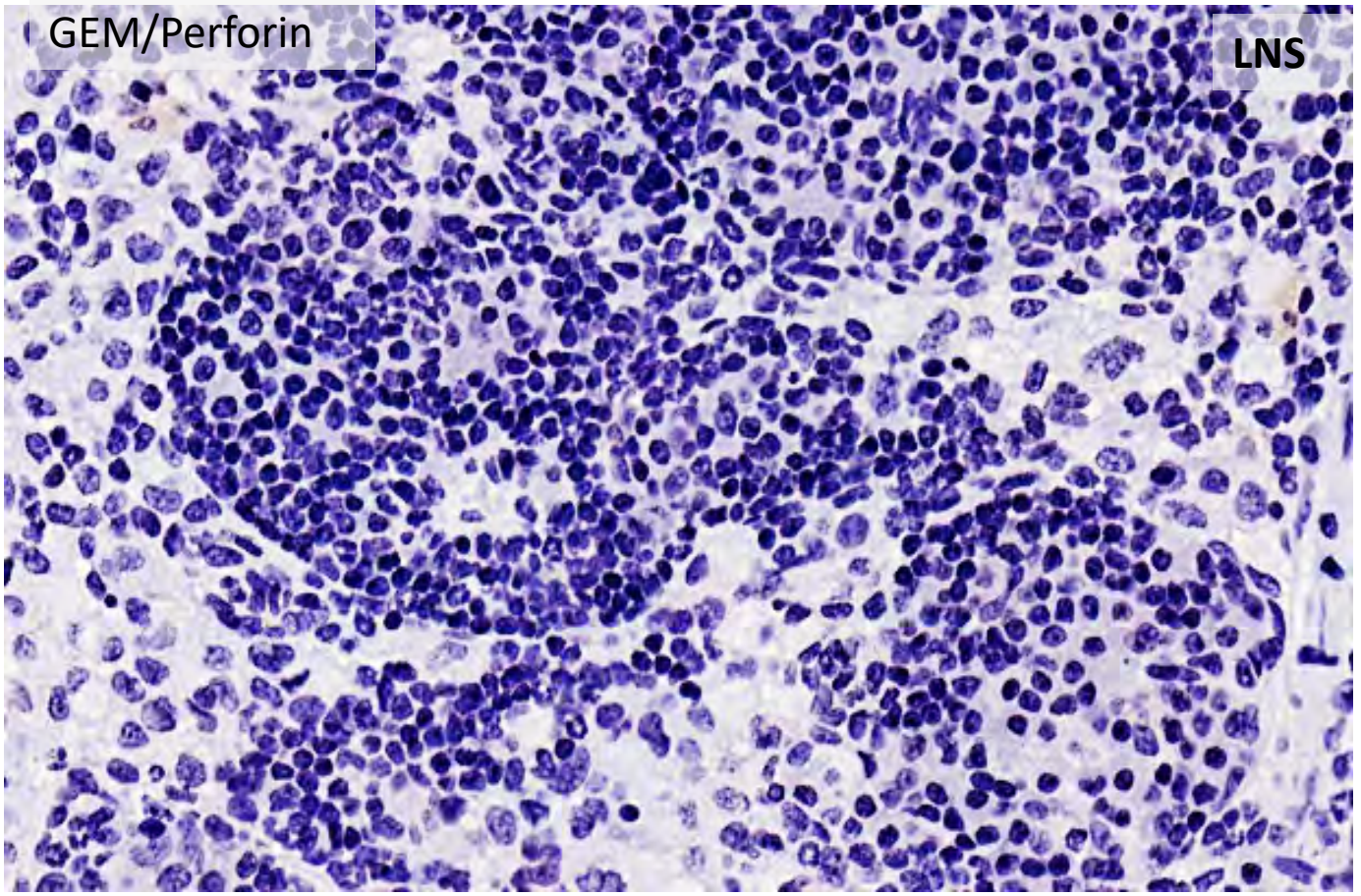
GEM/Perforin
LNS

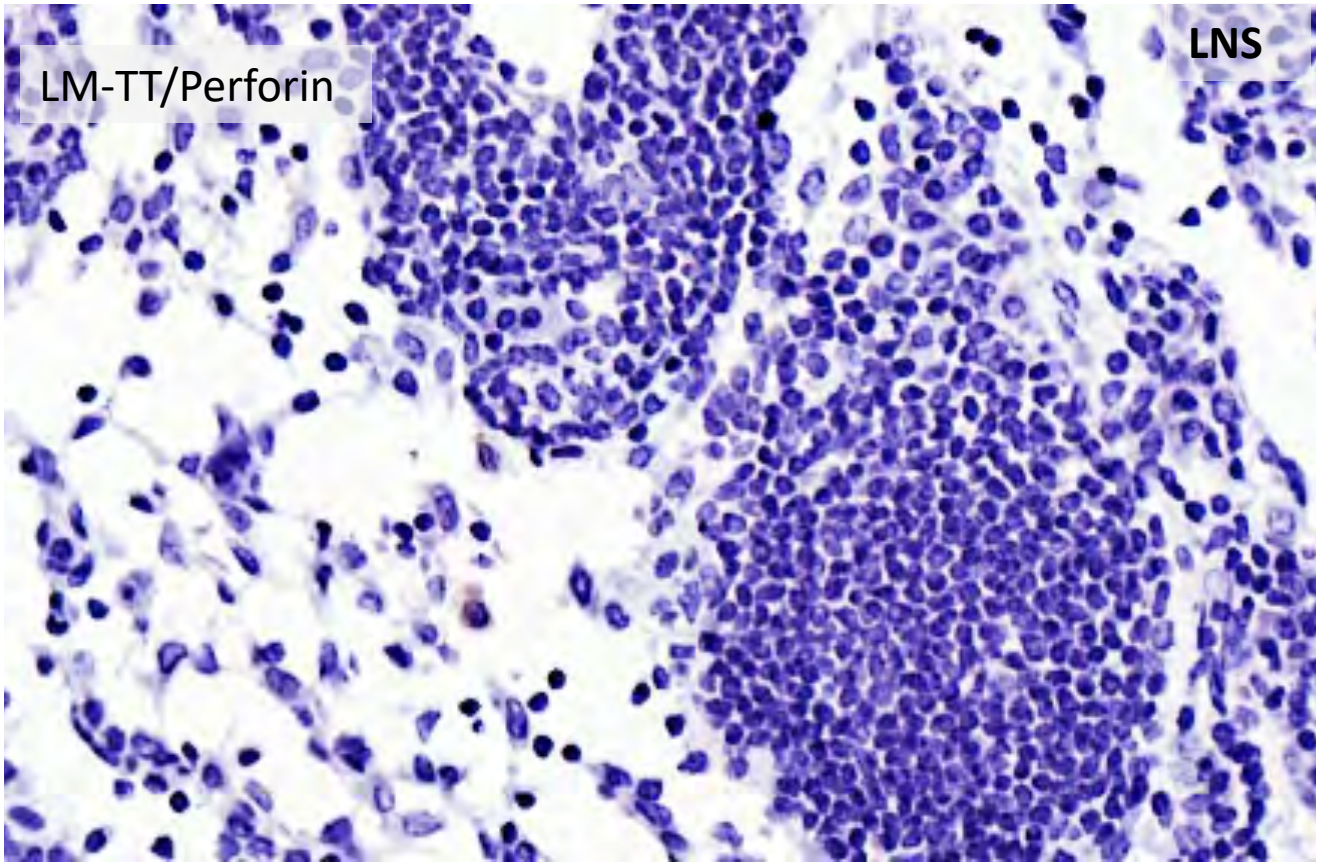
LM-TT/Perforin
LNS

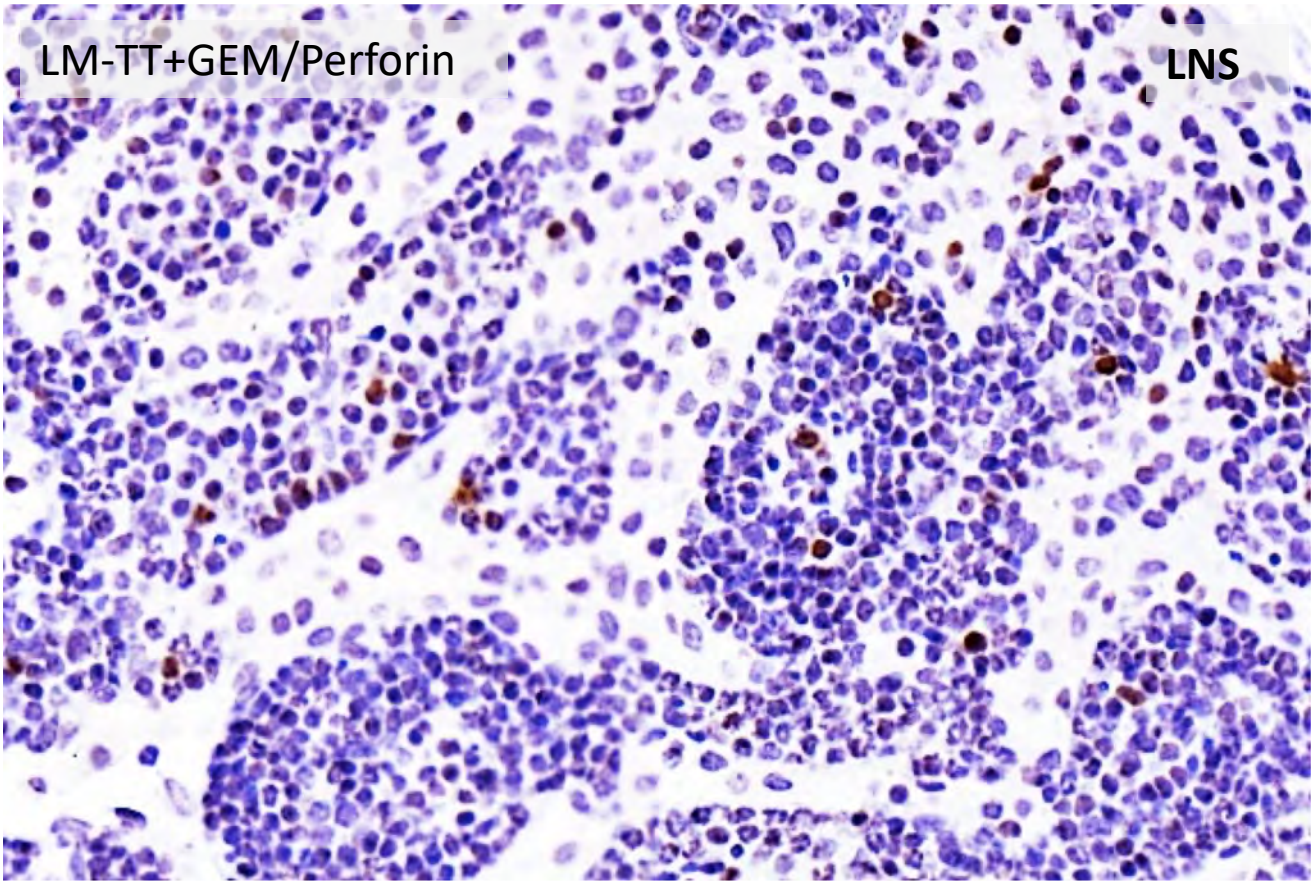
LM-TT+GEM/Perforin
LNS

SI Figure 5

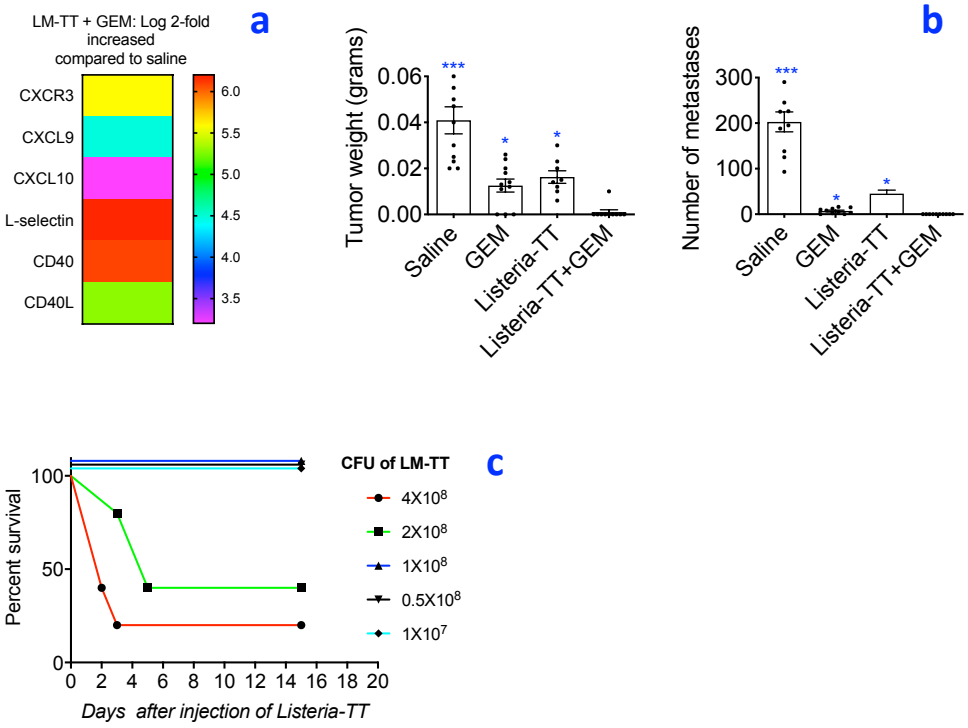
a
LM-TT + GEM: Log 2-fold increased compared to saline
CXCR3
CXCL9
CXCL10
L-selectin
CD40
CD40L
6.0
5.5
5.0
4.5
4.0
3.5
b
Tumor weight (grams)
0.06
0.04
0.02
0.00
***
*
*
Saline
GEM
Listeria-TT
Listeria-TT+GEM
Number of metastases
300
200
100
0
***
*
*
Saline
GEM
Listeria-TT
Listeria-TT+GEM
c
Percent survival
100
50
0
0 2 4 6 8 10 12 14 16 18 20
Days after injection of Listeria-TT
CFU of LM-TT
4X10^8
2X10^8
1X10^8
0.5X10^8
1X10^7

SI Figure 6a

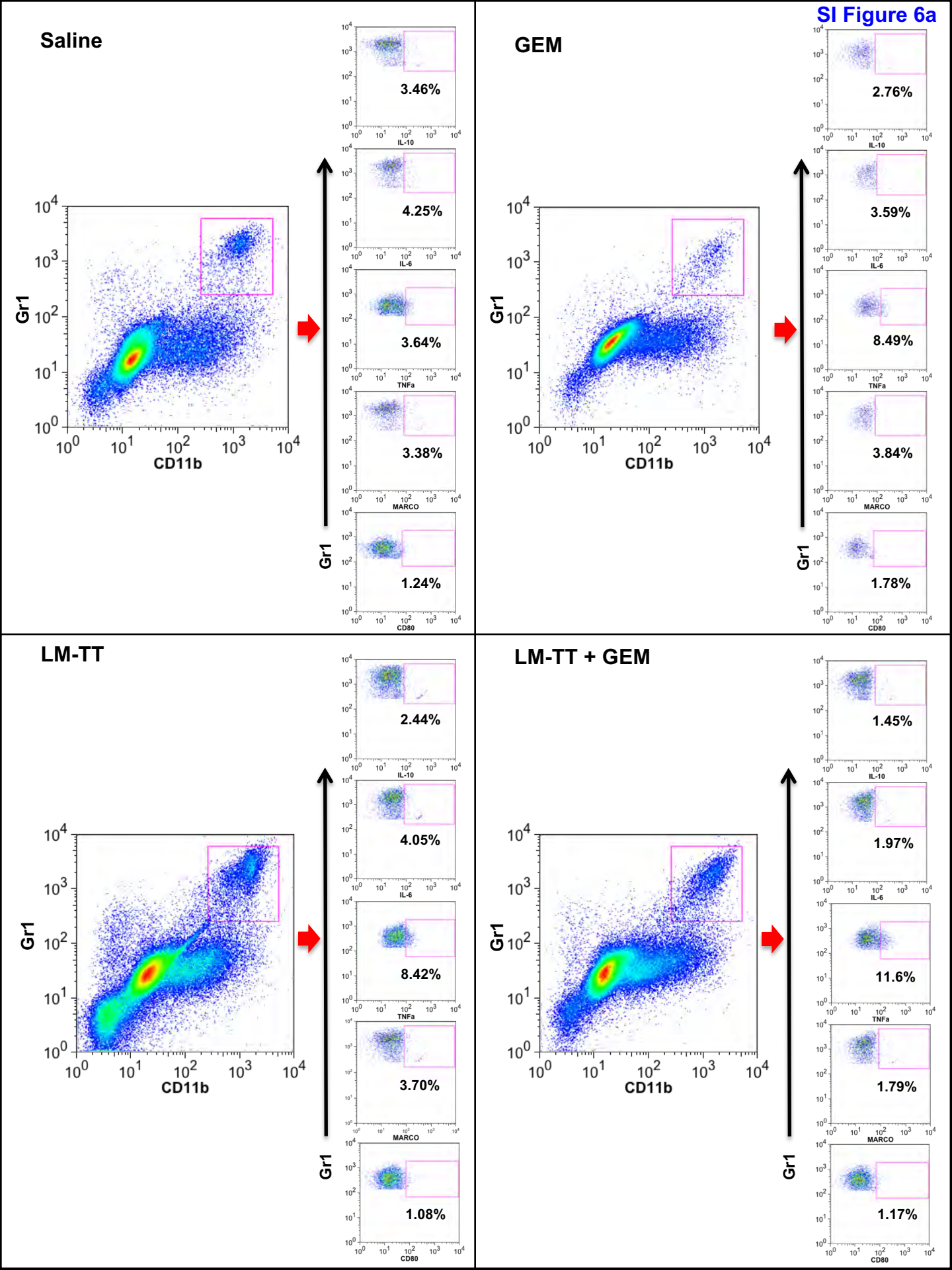
Saline
GEM
LM-TT
LM-TT + GEM
Gr1
CD11b
IL-10
IL-6
TNFa
MARCO
CD80
3.46%
4.25%
3.64%
3.38%
1.24%
2.76%
3.59%
8.49%
3.84%
1.78%
2.44%
4.05%
8.42%
3.70%
1.08%
1.45%
1.97%
11.6%
1.79%
1.17%

SI Figure 6b

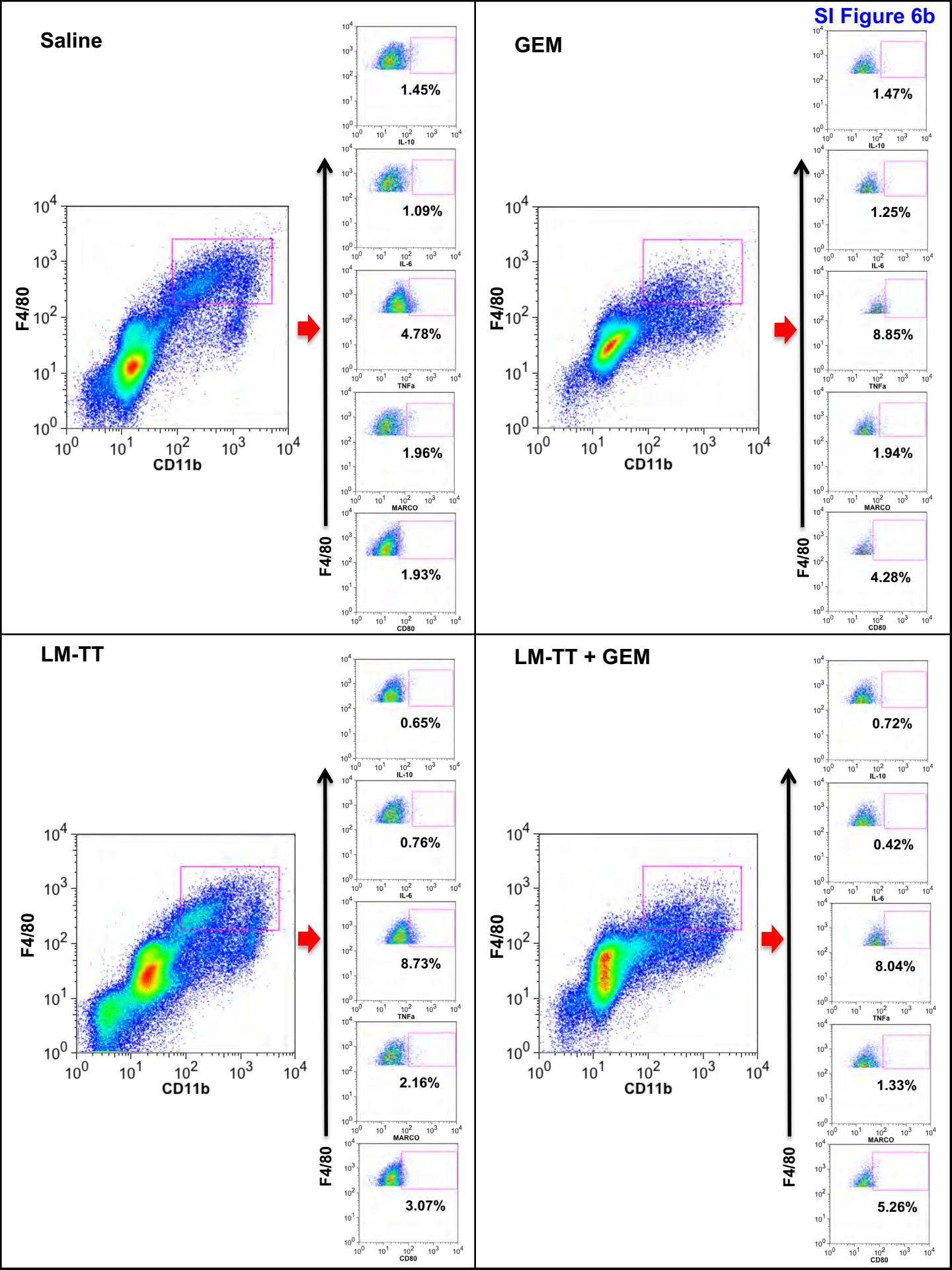
Saline
GEM
LM-TT
LM-TT + GEM
F4/80
CD11b
IL-10
IL-6
TNFa
MARCO
CD80
1.45%
1.09%
4.78%
1.96%
1.93%
1.47%
1.25%
8.85%
1.94%
4.28%
0.65%
0.76%
8.73%
2.16%
3.07%
0.72%
0.42%
8.04%
1.33%
5.26%

SI Table 1a: Pathological examination of tissues in C57Bl/6 mice 2 days after the last treatment with Listeria-TT and Gemcitabine

Treatment	**Saline**			**Listeria-TT+Gem**		
Mouse	**1**	**2**	**3**	**1**	**2**	**3**
Liver						
Random foci of mixed leukocytes	1	1	1	0	1	1
Individual hepatocyte cell death	1	0	0	0	1	1
Extramedullary hematopoiesis	0	0	0	0	0	1
Hepatocellular cytoplasmic vacuolation	0	0	0	0	0	0
Foci of necrosis	0	0	0	0	0	0
Kidney						
Tubular ectasia, cortex	0	0	0	0	0	0
Tubular ectasia, medulla	0	0	0	0	0	1
Tubular epithelial cell cytoplasmic vacuolation, cortex	0	0	0	0	1	0
Tubular epithelial cell cytoplasmic vacuolation, medulla	0	0	0	0	0	0
Regenerative tubules, cortex	0	0	0	1-2	1-2	0
Regenerative tubules, medulla	0	0	0	0	0	0
Tubular proteinosis, cortex	0	0	0	0	0	0
Tubular proteinosis, medulla	0	0	0	0	0	1
Spleen						
Lymphoid hyperplasia, white pulp	2	2	2	0	0	0
Extramedullary hematopoiesis, red pulp	0	2	2	3	3	3
Lung						
Increased mixed leukocytes, alveolar septae	2-3	2-3	2-3	2-3	2-3	2-3
Perivascular/peribronchiolar lymphocytic to lymphohistiocytic infiltrates	1	0	0	1-2	0	0

The samples were graded on a scale of 0-5; 0=no significant findings, 1=minimal finding, 2=mild finding, 3=moderate finding, 4=marked finding, 5=severe finding. C57Bl/6 mice were treated with Listeria-TT and GEM or Saline as described in **Fig 1b** of the manuscript. Two days after the last treatment mice were euthanized and analyzed for potential side effects by a Histopathological board-certified veterinary pathologist. In each group 3 mice were analyzed.

SI Table 1b: The effect of Listeria-TT and Gemcitabine on liver functions in C57Bl/6 mice

Treatment	AST (U/L)	ALT (U/L)
Saline	107	16
Listeria-TT and GEM	137	15
Normal values	50-100	25-60

C57Bl/6 mice were treated with Listeria-TT and GEM or Saline as described in **Fig 1b** of the manuscript. Two days after the last treatment mice were euthanized and analyzed for liver functions such as aspartate aminotransferase (AST) and alanine aminotransferase (ALT). In each group 3 mice were analyzed. The plasma samples were pooled in each group.